

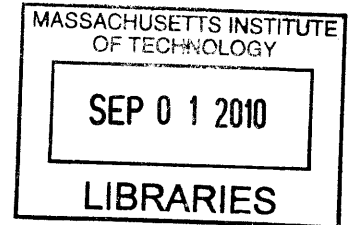
**FEASIBILITY OF LATERAL EMPLACEMENT IN
VERY DEEP BOREHOLE DISPOSAL OF HIGH LEVEL NUCLEAR WASTE**

By
JONATHAN SUTTON GIBBS
B.S. Mechanical Engineering and Mathematical Sciences
United States Military Academy, 2001

Submitted to the
DEPARTMENT OF MECHANICAL ENGINEERING
and the
DEPARTMENT OF NUCLEAR SCIENCE AND ENGINEERING

ARCHIVES

In Partial Fulfillment of the Degrees of
NAVAL ENGINEER
and
NUCLEAR ENGINEER
at the
MASSACHUSETTS INSTITUTE OF TECHNOLOGY
June, 2010



© 2010 Massachusetts Institute of Technology. All rights reserved

Signature of Author: _____
Department of Mechanical Engineering
Department of Nuclear Science and Engineering
May 7, 2010

Certified By: _____
Michael J. Driscoll
Professor Emeritus of Nuclear Science and Engineering
Thesis Co-Supervisor

Certified By: _____
Jacopo Buongiorno
Carl R. Sollerberg Professor of Power Engineering
Associate Professor of Nuclear Science and Engineering
Thesis Co-Supervisor

Certified By: _____
Mark S. Welsh
Professor of the Practice of Naval Construction and Engineering
Thesis Reader

Accepted By: _____
David E. Hardt
Ralph E. and Eloise F. Cross Professor of Mechanical Engineering
Chair, Department Committee on Graduate Students

Accepted By: _____
Jacquelyn C. Yanch
Professor of Nuclear Science and Engineering, and Biological Engineering
Chair, Department Committee on Graduate Students

THE VIEWS EXPRESSED IN THIS THESIS ARE THOSE OF THE AUTHOR
AND DO NOT NECESSARILY REPRESENT THE POSITION OF THE
DEPARTMENT OF DEFENSE OR ANY OF ITS COMPONENTS,
INCLUDING THE DEPARTMENT OF THE NAVY.

FEASIBILITY OF LATERAL EMPLACEMENT IN VERY DEEP BOREHOLE DISPOSAL OF HIGH LEVEL NUCLEAR WASTE

By Jonathan Sutton Gibbs

Submitted to the Departments of Mechanical Engineering and
Nuclear Science and Engineering on 10 May 2010
in Partial Fulfillment of the Requirements for the Degrees
of Naval Engineer and Nuclear Engineer

ABSTRACT

The U.S. Department of Energy recently filed a motion to withdraw the Nuclear Regulatory Commission license application for the High Level Waste Repository at Yucca Mountain in Nevada. As the U.S. has focused exclusively on geologic disposal in shallow mined repositories for the past two decades, an examination of disposal alternatives will be necessary should the Yucca Mountain Project be terminated. This provides an opportunity to study other promising waste disposal technologies. One such technology is the use of very deep boreholes in monolithic granite to permanently segregate high level wastes from the biosphere. While research in this field has focused on vertical emplacement techniques, horizontal emplacement offers the significant advantages of allowing increased emplacement lengths without crushing of the waste package and the use of a single vertical shaft for drilling multiple horizontal shafts. This project examines the application of currently deployed oil and natural gas directional drilling techniques to borehole design. A large trade-space of potential borehole configurations is evaluated and a final design selected using the “V-DeepBoRe” code, a Monte-Carlo simulation based cost model for borehole construction and waste package emplacement. Waste repackaging and reconstitution is evaluated to permit deployment of waste in borehole diameters too small for intact fuel assemblies. A 5 m x 195.26 mm (OD) cylindrical waste package is designed using P-110 drill string steel to meet strength and thermal loading requirements; fuel centerline temperatures are shown to not exceed 190°C by analytical and finite element methods. The total cost of a national borehole repository (including drilling, consolidating and encapsulating the fuel, emplacement, and closure) is shown to fall below \$63/kgHM, well within the capacity of the DOE Commercial Spent Nuclear Fuel Waste Fund.

Thesis Co-Supervisor: Michael J. Driscoll
Title: Professor Emeritus of Nuclear Science and Engineering

Thesis Co-Supervisor: Jacopo Buongiorno
Title: Carl R. Soderberg Professor of Power Engineering and
Associate Professor of Nuclear Science and Engineering

Thesis Reader: Mark S. Welsh
Title: Professor of the Practice of Naval Construction and Engineering

ACKNOWLEDGEMENTS

My great thanks to my wife, Michelle, whose support and understanding have been invaluable in allowing me to complete this work.

Thanks also to the U.S. Navy for fully funding the three years of technical development I have enjoyed at M.I.T. and the professional mentoring and support I received in that same time from Captains Patrick Keenan and Mark Welsh and Commanders Joel Harbour and Trent Gooding.

This project would not have been successful without the great patience, coaching, and guidance of Professors Driscoll and Buongiorno: my sincerest thanks to both.

TABLE OF CONTENTS

ABSTRACT	3
ACKNOWLEDGEMENTS	4
TABLE OF CONTENTS	5
LIST OF FIGURES.....	7
LIST OF TABLES.....	10
1 INTRODUCTION.....	11
1.1 OBJECTIVE OF THE THESIS	11
1.2 TOPIC MOTIVATION	11
1.3 OVERVIEW OF THE DEEP BOREHOLE CONCEPT	12
1.3.1 Nuclear Waste.....	12
1.3.2 Vertical Borehole Studies	14
1.3.3 Site Selection.....	14
1.3.4 Transport Processes and Repository Performance	16
1.3.5 Oil and Natural Gas Directional Drilling Capabilities.....	19
1.4 ARRANGEMENT OF THE THESIS	24
1.4.1 Drilling Cost Model and Repository Configuration Selection.....	24
1.4.2 Waste Package Design and Analysis	24
1.4.3 Rod Consolidation and Package Cost	24
1.4.4 Conclusions and Future Work.....	24
2 DRILLING COST MODEL AND REPOSITORY CONFIGURATION SELECTION.....	25
2.1 MODEL OVERVIEW	25
2.2 MODEL ASSUMPTIONS	26
2.3 MODEL PARAMETERS.....	27
2.3.1 Repository Geometry	28
2.3.2 Handling Speeds	29
2.3.3 Time Parameters.....	30
2.3.4 Cost Parameters	31
2.3.5 Spent Fuel Parameters	32
2.3.6 Drill String Parameters	33
2.4 MODULES.....	35
2.4.1 Waste Mass Calculation	35
2.4.2 Drilling Script.....	37
2.4.3 Output and Plotting	40
2.5 CALIBRATION USING VERTICAL BOREHOLE RESULTS	42
2.6 RESULTS AND REPOSITORY CONFIGURATION SELECTION	44
2.6.1 Complete Trade Space Results	44
2.6.2 Trade Space Results with Crushing Limit Imposed	45
2.6.3 First Narrowing of Trade-space.....	46
2.6.4 Second Narrowing of the Trade-space	47
2.6.5 Final Repository Configuration and Results	48
2.7 MODEL SENSITIVITY ANALYSES AND CURVE FIT OF RESULTS	50
2.8 DRILLING COST MODEL AND REPOSITORY CONFIGURATION SUMMARY	55
3 WASTE PACKAGE DESIGN AND ANALYSIS	56
3.1 WASTE PACKAGE DESIGN	56
3.2 THERMAL ANALYSIS OF WASTE PACKAGE	59
3.2.1 Thermal Study Assumptions.....	60
3.2.2 Effective Conduction Coefficient of Reconstituted Waste.....	61

3.2.2	<i>Package Thermal Power</i>	63
3.2.3	<i>1-D Infinite Medium Temperature Analysis</i>	65
3.2.3.1	PWR Canister Temperature Analysis Results.....	68
3.2.3.2	BWR Canister Temperature Analysis Results	69
3.2.3.3	Canister Temperature Analysis Comparison.....	71
3.2.4	<i>2-D Finite Cell Temperature Analysis</i>	72
3.2.4.1	PWR Canister Temperature Analysis.....	73
3.2.4.2	BWR Canister Thermal Analysis.....	74
3.2.3	<i>3-D Repository Thermal Analysis</i>	76
3.3	MECHANICAL ANALYSIS OF WASTE PACKAGE	82
3.3.1	<i>Tensile Stress</i>	82
3.3.2	<i>Longitudinal Buckling</i>	83
3.3.3	<i>Hydrostatic & Lithostatic Crushing</i>	84
4	ROD CONSOLIDATION AND PACKAGE COST	86
4.1	COST THRESHOLD FOR FEASIBILITY.....	88
4.2	PREVIOUS STUDIES.....	89
4.2.1	<i>Electric Power Research Institute Study</i>	90
4.2.2	<i>Sciencetech Study</i>	92
4.2.3	<i>Cost Comparison</i>	93
4.3	COST ESTIMATION FOR WASTE PACKAGING OF LWR FUEL	94
5	CONCLUSIONS AND FUTURE WORK	96
5.1	SUMMARY OF DESIGN AND RESULTS	96
5.2	RECOMMENDATIONS FOR FUTURE WORK	97
5.3	CONCLUSIONS	98
APPENDIX A: V-DEEPCODE.....		99
A.1	MODEL SCRIPT ORGANIZATION	99
A.2	MODEL SCRIPTS (MATLAB).....	99
A.2.1	<i>Waste Packing Script (wastemass.m)</i>	99
A.2.2	<i>Drilling Cost Realization Script for Lateral Repository (drill_bit_life.m)</i>	103
A.2.3	<i>Lateral Repository Trade Space Study Script (drilling_costs.m)</i>	114
A.2.4	<i>Drilling Cost Realization Script for EGS Borehole (drill_egs.m)</i>	119
A.2.5	<i>EGS Borehole Trial Script (drilling_costs_egs.m)</i>	133
A.3	DRILLING SAMPLE PROBLEM	135
APPENDIX B: THERMAL ANALYSIS CALCULATIONS.....		141
B.1	DECAY HEAT MODELING	141
B.2	SCALING VALIDATION TEST RESULTS.....	146
APPENDIX C: MECHANICAL STRESS CALCULATIONS		148
REFERENCES		151

LIST OF FIGURES

FIGURE 1-1: REPRESENTATIVE PWR FUEL ASSEMBLY	13
FIGURE 1-2: REPRESENTATIVE BWR FUEL ASSEMBLY	13
FIGURE 1-3: SEDIMENTARY OVERBURDEN FOR CONTINENTAL U.S.	14
FIGURE 1-4: MAKEUP OF CANADIAN SHIELD BY AGE	15
FIGURE 1-5: U.S. POPULATION DENSITY BY COUNTY, 2009	15
FIGURE 1-6: HIGH LEVEL WASTE STORAGE SITES IN THE UNITED STATES	16
FIGURE 1-7: HOLDUP PERFORMANCE MAP FOR ADVECTIVE TRANSPORT THROUGH REPOSITORY	18
FIGURE 1-8: EXAMPLES OF COMPLEXITY IN DIRECTIONAL WELLS	19
FIGURE 1-9: RADII OF CURVATURE FOR DIRECTIONAL WELLS	20
FIGURE 1-10: CONFIGURATIONS OF VERTICAL TO LATERAL JUNCTION	21
FIGURE 1-11: "KICKING OFF" TO START A LATERAL	22
FIGURE 1-12: LINING THE LATERAL (LEVEL 3 JOINT)	23
FIGURE 2-1: NOMINAL REPOSITORY CONFIGURATION	26
FIGURE 2-2: MODEL DRILLING RATE PDFS	34
FIGURE 2-3: MODEL BIT LIFE PDFS.....	34
FIGURE 2-4: DRILL BIT REPLACEMENT COSTS CURVE FIT	35
FIGURE 2-5: HEXAGONAL PACKING SCHEME OF RECONSTITUTED PWR & BWR FUEL PINS	36
FIGURE 2-6: OPTIMAL PACKING OF BWR ASSEMBLIES IN WASTE CANISTER	37
FIGURE 2-7: CALCULATION OF MINIMUM REQUIRED RADIUS FOR KICKOFF ARC	38
FIGURE 2-8: SAMPLE OUTPUT (SINGLE TRIAL)	41
FIGURE 2-9: OUTPUT RESULTS FOR VERTICAL BOREHOLE	43
FIGURE 2-10: FULL TRADE-SPACE BY DECLINATION ANGLE (°)	44
FIGURE 2-11: FULL TRADE-SPACE BY EMPLACEMENT LENGTH (M)	44
FIGURE 2-12: FULL TRADE-SPACE BY LATERAL DIAMETER (IN)	44
FIGURE 2-13: FULL TRADE-SPACE BY NUMBER OF LATERALS	44
FIGURE 2-14: TRADE-SPACE WITH CRUSHING LIMIT BY DECLINATION ANGLE (°).....	45
FIGURE 2-15: TRADE-SPACE WITH CRUSHING LIMIT BY EMPLACEMENT LENGTH (M)	45
FIGURE 2-16: TRADE-SPACE WITH CRUSHING LIMIT BY LATERAL DIAMETER (IN)	45
FIGURE 2-17: TRADE-SPACE WITH CRUSHING LIMIT BY NUMBER OF LATERALS	45
FIGURE 2-18: 1ST WINNOWED TRADE-SPACE BY DECLINATION ANGLE (°)	46
FIGURE 2-19: 1ST WINNOWED TRADE-SPACE BY EMPLACEMENT LENGTH (M).....	46
FIGURE 2-20: 1ST WINNOWED TRADE-SPACE BY LATERAL DIAMETER (IN)	46
FIGURE 2-21: 1ST WINNOWED TRADE-SPACE BY NUMBER OF LATERALS	46
FIGURE 2-22: 2ND WINNOWED TRADE-SPACE BY DECLINATION ANGLE (°)	47
FIGURE 2-23: 2ND WINNOWED TRADE-SPACE BY EMPLACEMENT LENGTH (M)	47
FIGURE 2-24: 2ND WINNOWED TRADE-SPACE BY LATERAL DIAMETER (IN)	47
FIGURE 2-25: 2ND WINNOWED TRADE-SPACE BY NUMBER OF LATERALS	47
FIGURE 2-26: SAMPLE REALIZATION OF FINAL REPOSITORY DESIGN	48
FIGURE 2-27: DRILLING COST AND TIME SIMULATIONS OF FINAL REPOSITORY DESIGN	49
FIGURE 2-28: 3-D REPRESENTATION OF MULTIDIRECTIONAL BOREHOLE CONFIGURATION	49
FIGURE 2-29: 3-D REPRESENTATION OF MULTIDIRECTIONAL BOREHOLE CONFIGURATION (HOLE DIAMETERS x500 FOR VISUALIZATION)	49
FIGURE 2-30: 2-D REPRESENTATION OF BIDIRECTIONAL BOREHOLE CONFIGURATION	50
FIGURE 2-31: 3-D REPRESENTATION OF MULTIPLE BIDIRECTIONAL BOREHOLES	50
FIGURE 2-32: EMPLACEMENT LENGTH SENSITIVITY ANALYSIS	50
FIGURE 2-33: CEMENT COST SENSITIVITY ANALYSIS	51
FIGURE 2-34: BILLING RATE SENSITIVITY ANALYSIS	51
FIGURE 2-35: PLUG COST SENSITIVITY ANALYSIS	51
FIGURE 2-36: VITRIFIED WASTE FRACTION OF REPOSITORY SENSITIVITY ANALYSIS	52
FIGURE 2-37: CASING COST SENSITIVITY ANALYSIS	52
FIGURE 2-38: SENSITIVITY RESULTS FOR REPOSITORY MEAN COMPLETION TIME AND RATE	53
FIGURE 2-39: SENSITIVITY RESULTS FOR REPOSITORY MEAN COMPLETION TIME AND RATE (EXPANDED) .	53

FIGURE 2-40: SENSITIVITY RESULTS FOR REPOSITORY STANDARD DEVIATION OF COMPLETION TIME AND RATE	53
FIGURE 3-1: CANISTER ARRANGEMENT- 301 PWR FUEL PINS	57
FIGURE 3-2: CANISTER ARRANGEMENT- 211 BWR FUEL PINS	58
FIGURE 3-3: CANISTER AND LINER CROSS SECTIONS.....	59
FIGURE 3-4: EFFECTIVE HEAT TRANSFER COEFFICIENT ANALYSIS (PWR WASTE PACKAGE).....	62
FIGURE 3-5: EFFECTIVE HEAT TRANSFER COEFFICIENT ANALYSIS (BWR WASTE PACKAGE).....	62
FIGURE 3-6: COMPARISON OF DECAY POWER EMPIRICAL RELATIONS.....	64
FIGURE 3-7: PACKAGE DECAY POWER (M, L, & D CORRELATION)	65
FIGURE 3-8: COMPARISON OF 1-D INTEGRAL SOLUTION AND APPROXIMATION	66
FIGURE 3-9: ROCK TEMPERATURE PROFILES (PWR INFINITE LINE SOURCE).....	68
FIGURE 3-10: PWR CANISTER THERMAL HISTORIES (RADIATION ONLY IN GAPS).....	69
FIGURE 3-11: PWR CANISTER THERMAL HISTORIES (WATER CONDUCTION IN GAPS).....	69
FIGURE 3-12: ROCK TEMPERATURE PROFILES (BWR INFINITE LINE SOURCE).....	70
FIGURE 3-13: BWR CANISTER THERMAL HISTORIES (RADIATION ONLY IN GAPS)	70
FIGURE 3-14: BWR CANISTER THERMAL HISTORIES (WATER CONDUCTION IN GAPS)	71
FIGURE 3-15: TEMPERATURE RISE FROM BOREHOLE WALL TO CANISTER CENTER.....	71
FIGURE 3-16: GRANITE FINITE CELL FOR TRANSIENT THERMAL ANALYSIS	72
FIGURE 3-17: GRANITE FINITE CELL FOR TRANSIENT THERMAL ANALYSIS (ENLARGED TO SHOW BOREHOLE WALL FOR PWR CASE).....	72
FIGURE 3-18: TEMPERATURE DISTRIBUTION IN FINITE CELL (PWR PACKAGE, 200 YR AFTER EMLACEMENT).....	73
FIGURE 3-19: TEMPERATURE DISTRIBUTION IN FINITE CELL (PWR PACKAGE, 2000 YR AFTER EMLACEMENT).....	73
FIGURE 3-20: PWR 2-D FINITE CELL BOREHOLE WALL TEMPERATURE HISTORY	74
FIGURE 3-21: TEMPERATURE DISTRIBUTION IN FINITE CELL (BWR PACKAGE, 200 YR AFTER EMLACEMENT).....	75
FIGURE 3-22: TEMPERATURE DISTRIBUTION IN FINITE CELL (BWR PACKAGE, 2,000 YR AFTER EMLACEMENT).....	75
FIGURE 3-23: BWR 2-D FINITE CELL BOREHOLE WALL TEMPERATURE HISTORY	75
FIGURE 3-24: ONE-TENTH SCALED 3-D ANALYSIS GEOMETRY	76
FIGURE 3-25: 3-D THERMAL ANALYSIS GEOMETRY (ENLARGEMENT OF ONE OF FIVE MODELED LATERALS)	77
FIGURE 3-26: 3-D REPOSITORY MODEL GRANITE TEMPERATURES AT 10.1 YEARS (PEAK BOREHOLE WALL TEMPERATURES).....	79
FIGURE 3-27: 3-D REPOSITORY MODEL GRANITE TEMPERATURES AT 200 YEARS	79
FIGURE 3-28: 3-D REPOSITORY MODEL GRANITE TEMPERATURES AT 2000 YEARS	80
FIGURE 3-29: 3-D REPOSITORY THERMAL RESULTS (PWR WASTE PACKAGE)	80
FIGURE 3-30: CENTERLINE TEMPERATURE RESULTS FOR PWR CANISTER (USING 3-D ANALYSIS ROCK WALL TEMPERATURES).....	81
FIGURE 3-31: CENTERLINE TEMPERATURE RESULTS FOR BWR CANISTER (USING 3-D ANALYSIS ROCK WALL TEMPERATURES).....	81
FIGURE 3-32: CANDU GEOLOGIC DISPOSAL OVER-PACK AND CANISTER DESIGN	85
FIGURE 4-1: ROD CONSOLIDATION CONCEPT ARRANGEMENT	86
FIGURE 4-2: DRY FUEL PIN CONSOLIDATION AT BNFP- 2 CONSOLIDATED PWR ASSEMBLIES (VIEWED END ON)	87
FIGURE 4-3: SHEARING OF NON-FUEL BEARING ASSEMBLY COMPONENTS FOR COMPACTION.....	87
FIGURE 4-4: HOAG WASTE PACKAGE WITH INTACT 17 x 17 PWR FUEL ASSEMBLY	89
FIGURE 4-5: HOAG WASTE PACKAGE WITH CONSOLIDATED PWR FUEL.....	89
FIGURE 4-6: EPRI IN-POOL CONSOLIDATION HANDLING ARRANGEMENT	90
FIGURE 4-7: EPRI PROCESS FOR FUEL ASSEMBLY CONSOLIDATION.....	90
FIGURE A-1: REPOSITORY COST MODEL SCRIPT FLOWCHART	99
FIGURE A-2: SAMPLE PROBLEM OUTPUT	138
FIGURE A-3: TRADE-SPACE BY DECLINATION ANGLE (°).....	140
FIGURE A-4: TRADE-SPACE BY EMLACEMENT LENGTH (M)	140
FIGURE A-5: TRADE-SPACE BY LATERAL INNER DIAMETER (IN).....	140

FIGURE A-6: TRADE-SPACE BY NUMBER OF LATERALS 140
FIGURE B-1: FULL AND SMALL SCALE GEOMETRY 146
FIGURE B-2: TEMPERATURE HISTORY COMPARISON OF SCALED AND UNSCALED GEOMETRIES..... 146
FIGURE B-3: FULL SCALE FINAL TEMPERATURE..... 147
FIGURE B-4: SMALL SCALE FINAL TEMPERATURE..... 147

LIST OF TABLES

TABLE 2-1: REPOSITORY GEOMETRIC PARAMETERS	28
TABLE 2-2: HANDLING SPEED PARAMETERS.....	29
TABLE 2-3: DRILLING TIME PARAMETERS	30
TABLE 2-4: DRILLING COST PARAMETERS	31
TABLE 2-5: SPENT FUEL PARAMETERS.....	32
TABLE 2-6: DRILL STRING PARAMETERS	34
TABLE 2-7: DRILL BIT REPLACEMENT COSTS	35
TABLE 2-8: MINIMUM RADII OF CURVATURE FOR KICKOFF ARCS	38
TABLE 2-9: IMPACT OF KEY PARAMETERS ON REPOSITORY STATISTICS.....	54
TABLE 2-10: MODEL VALUES FOR LINEAR FIT FOR REPOSITORY STATISTICS BASED ON KEY PARAMETERS	54
TABLE 3-1: SUMMARY OF CANISTER DESIGN.....	56
TABLE 3-2: SUMMARY OF THERMAL DESIGN STUDY PROPERTIES AND PARAMETERS	60
TABLE 3-3: EFFECTIVE HEAT TRANSFER COEFFICIENT ANALYSIS RESULTS.....	62
TABLE 4-1: EPRI STUDY RESULTS SUMMARY	91
TABLE 4-2: SCIENTECH PROTOTYPICAL ROD CONSOLIDATION PROJECT COST SUMMARY	92
TABLE 4-3: SCIENTECH PRCP RESULTS SUMMARY	93
TABLE 4-4: EPRI AND SCIENTECH STUDY COST COMPARISON.....	94
TABLE A-1: DRILLING SCRIPT OUTPUT.....	139
TABLE B-1: SCALING PARAMETERS FOR TEST	146

1 INTRODUCTION

1.1 *Objective of the Thesis*

This project examines the application of currently deployed oil and natural gas directional drilling techniques to borehole design for high level nuclear waste disposal. Various drilling configurations are examined and a final repository configuration is selected to minimize drilling costs. Cost modeling for borehole construction and waste package emplacement is developed to evaluate the total costs of a national borehole repository. Disposal of both reconstituted Light Water Reactor (LWR) fuel and high level vitrified reprocessing waste forms is analyzed. A feasible waste package design is developed to meet strength and thermal requirements. Costs for waste repackaging and canister fabrication are also estimated so that the economic feasibility of a lateral borehole repository may be assessed.

1.2 *Topic Motivation*

The U.S. Department of Energy recently filed a motion to withdraw the Nuclear Regulatory Commission license application for the High Level Waste Repository at Yucca Mountain in Nevada. As the U.S. has focused exclusively on shallow mined geologic disposal for the past two decades, an examination of disposal alternatives will be necessary should the Yucca Mountain Project be terminated. This provides an opportunity to study other promising disposal technologies. One such technology is the use of very deep boreholes to permanently segregate the high level wastes from the biosphere.

Boreholes are attractive due to the superior isolation of the waste (mitigating proliferation, terrorist and human intrusion concerns), the impermeability of available geologic formations to radionuclide transport, and the presence, at depth, of reducing environments. While prior MIT research in this field has focused almost exclusively on surface-shaft vertical emplacement techniques (Hoag, 2004)¹, horizontal emplacement offers the significant advantages of allowing increased emplacement lengths and the use of a single vertical shaft for drilling multiple emplacement drifts.

The design philosophy employed in this project is to minimize construction and emplacement costs of the borehole project by using readily fielded commercial oil and natural gas drilling standards and practices. This may be achieved by consolidating spent fuel from intact assemblies (the form as discharged from the reactor) into densely packed arrangements. This permits relaxing the requirement for a large through-bore of the emplacement hole and it is anticipated that the additional costs of repackaging spent nuclear fuel may be recovered through significantly reduced drilling costs. Furthermore, as horizontal emplacement techniques make recovery of wastes impractical and costly, this project will be designed without any particular considerations for future retrieveability. As there will potentially be several different waste forms and spent fuel types loaded into any national repository, this study will examine repackaging of fuel pins from Pressurized Water Reactor (PWR) assemblies and, if made necessary by the geometry of the selected waste package, Boiling Water Reactor (BWR) assemblies.

1.3 Overview of the Deep Borehole Concept

1.3.1 Nuclear Waste

Any national nuclear waste repository must be capable of accommodating a wide variety of high level waste forms from several sources. Among these wastes are:

1. Commercial Spent Nuclear Fuel (CSNF) from light water reactors (LWR)
2. Department of Energy weapons program legacy High Level Waste (HLW: from reprocessing, potentially in vitrified form such as borosilicate glass)
3. Department of Defense spent Naval fuel
4. Long-lived wastes resulting from a (potential future) spent fuel reprocessing regime in the United States

This diverse array of potential loads must be accommodated within the repository design. Rather than design for all of these individually, representative Pressurized Water Reactor (PWR) and Boiling Water Reactor (BWR) CSNF geometries are selected to demonstrate the feasibility of the repository design: schematics of these are shown in Figure 1-1 and Figure 1-2. Similarly, the drilling model developed in this project will consider only a

single, simple vitrified waste form. Defense spent fuel is not specifically evaluated due to classification security requirements.

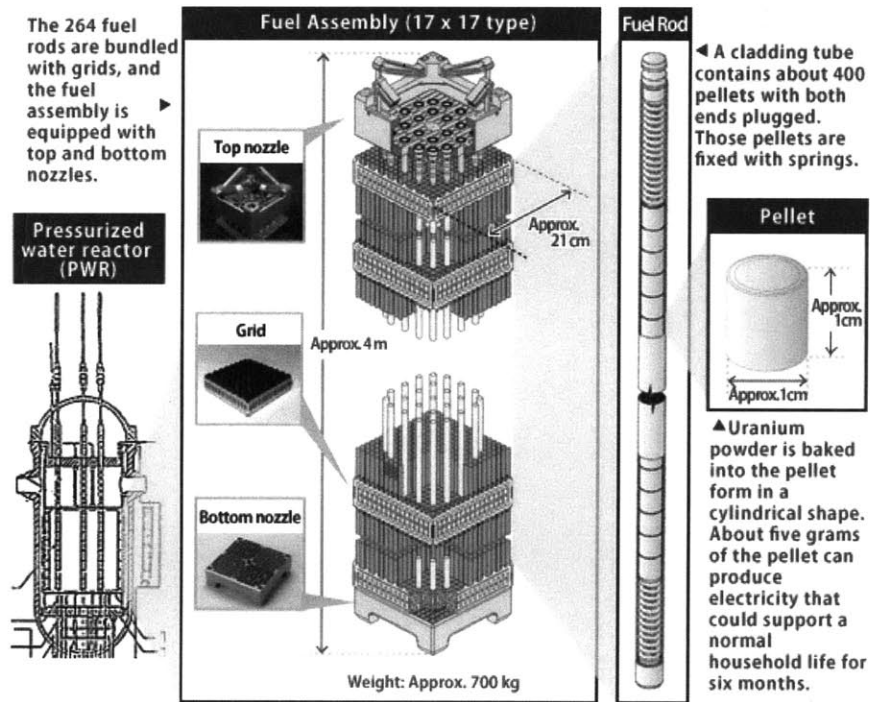


Figure 1-1: Representative PWR fuel Assembly

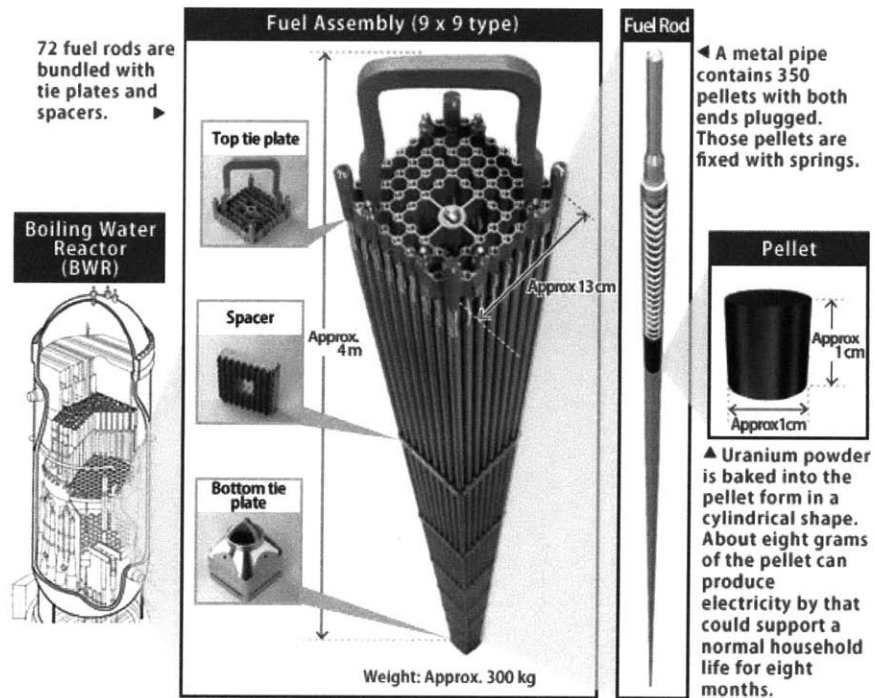


Figure 1-2: Representative BWR Fuel Assembly

(Figure 1-1 and Figure 1-2 Courtesy of Nuclear Fuel Industries)²

1.3.2 Vertical Borehole Studies

MIT^{3 4} and Sandia National Laboratories⁵, as well as others⁶, have conducted extensive studies on the application of very deep borehole technology to waste disposal. While areas of outstanding research and development have been identified, these studies underscore the feasibility of geologic isolation of high level wastes using deep boreholes. The designs examined, however, require that large diameter boreholes be employed to achieve the clearance to permit interment of intact PWR assemblies. Further, the vertical emplacement lengths in these disposal schemes are limited by the self-crushing tendency of a string of massive waste packages. These two drawbacks provide the major motivation for examining lateral emplacement.

1.3.3 Site Selection

Desirable site features for a borehole repository in the contiguous United States:

1. Ready access to high integrity basement crystalline rock (Figure 1-3)

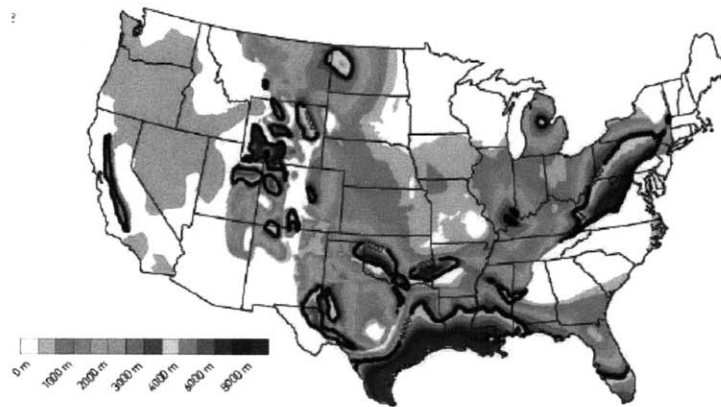


Figure 4.2: Sediment thickness at the surface (Massachusetts Institute of Technology, 2006; AAPG, 1978).

Figure 1-3: Sedimentary Overburden for Continental U.S.
(Courtesy “The Future of Geothermal Energy” by MIT)⁷

2. Age of the granitic formation (Figure 1-4)
3. Proximity to rail, barge, and heavy truck transportation corridors

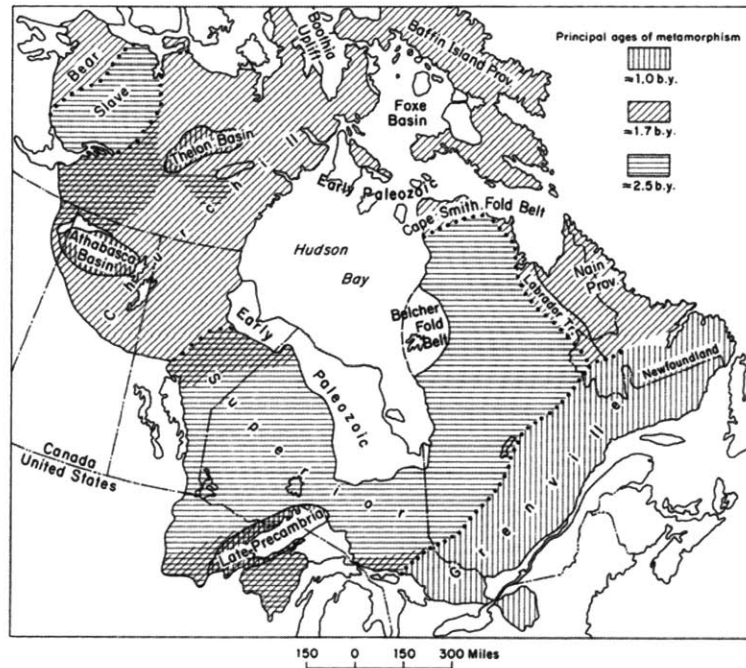


Figure 1-4: Makeup of Canadian Shield by Age

(Courtesy *Natural Regions of the United States and Canada* by Hunt)⁸

4. Isolation from population centers (Figure 1-5)

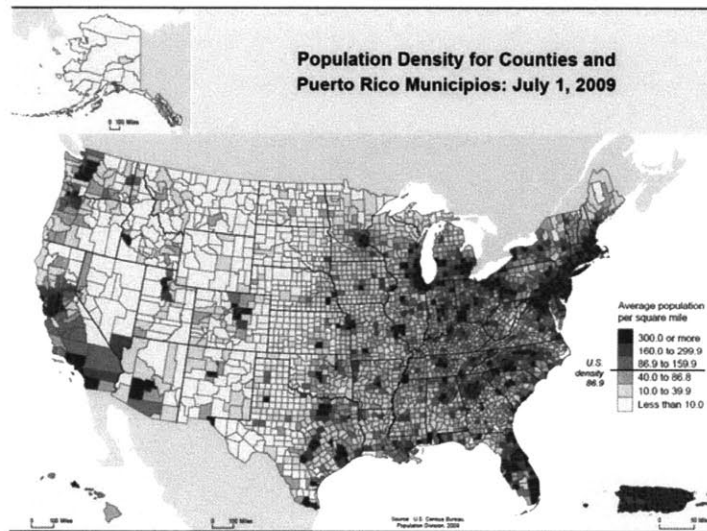


Figure 1-5: U.S. Population Density by County, 2009

(Courtesy U.S. Census Bureau)⁹

5. Proximity to high-level waste storage sites / nuclear utilities to minimize transportation costs and improve likelihood of popular support (Figure 1-6)
6. Distant from regions of significant volcanism and seismic activity

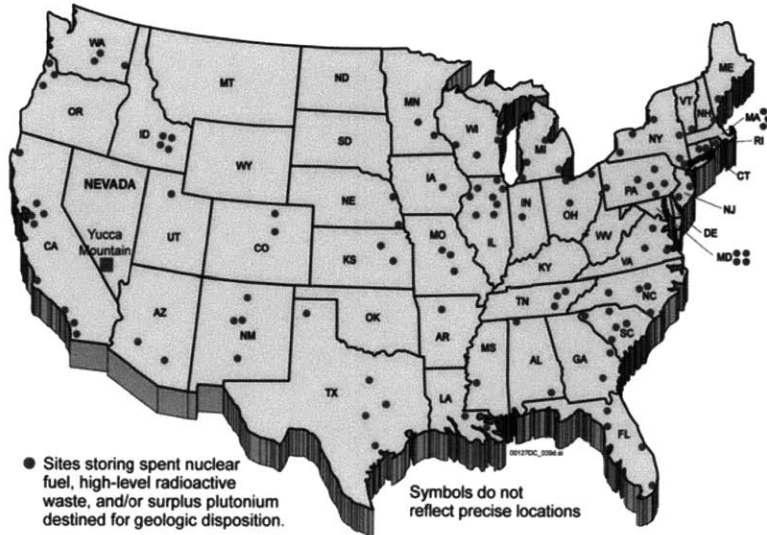


Figure 1-6: High Level Waste Storage Sites in the United States

(Courtesy U.S. DOE Office of Civilian Radioactive Waste Management)¹⁰

As was seen in the development of the Waste Policy Act of 1982 (and as amended in 1987), socio-political considerations will invariably dominate the site selection process. This resulted, for example, in the incorporation of language into the U.S. Code to specifically limit consideration of additional sites:¹¹

TERMINATION OF GRANITE RESEARCH.—Not later than 6 months after December 22, 1987, the Secretary shall phase out in an orderly manner funding for all research programs in existence on December 22, 1987, designed to evaluate the suitability of crystalline rock as a potential repository host medium.

The relative abundance of potentially acceptable deep borehole sites should therefore greatly help to facilitate the political adoption of a new site for a national repository (provided that the law is amended permitting government funded research into granite as a host medium for isolation of high level waste). The upper Midwest and upstate New York state are of particular interest with their access to the ancient and stable Canadian granite shield, but access to suitable formations is found in numerous regions of the U.S.

1.3.4 Transport Processes and Repository Performance

Escape of radioactive species from the repository is primarily driven by transport in groundwater. Should the borehole become flooded (a consideration which cannot be ruled out a priori) water movement will be dominated by advection with limited diffusion possible through the high integrity granite basement rock.

Darcy's Law for groundwater flow may be adapted¹² for advection through a porous rock formation as shown in Equation [1-1]:

$$\frac{\kappa}{\eta R} = \left(\frac{H\varepsilon}{t} \right) \left(\frac{dP}{dz} \right)^{-1} \quad [1-1]$$

Where :

- κ \equiv Medium Permeability, (in darcy)
- η \equiv Dynamic Viscosity of Fluid (in centipoise)
- R \equiv Retardation Factor due to Sorption
- H \equiv Caprock Thickness (cm)
- ε \equiv Rock Porosity
- t \equiv Transit Time (sec)
- $\frac{dP}{dz}$ \equiv Pressure Gradient (bar/cm)

In order for the waste in a borehole repository to be adequately isolated from the biosphere by a 1500 m deep granite formation (granite porosities of less than 0.01 are reasonable), the advective release of radionuclides through the granite is governed by the performance map shown in Figure 1-7. To demonstrate the adequate isolation of the longest-lived species, holdup times in excess of 10^6 years are desired. The theoretical maximum pressure gradient driving advection is approximately $1.5 \cdot 10^{-3}$ bar/cm (the difference between lithostatic and hydrostatic gradients), though actual gradients driving the upward flow through the rock are expected to be significantly lower. Based on this map, identifying repository sites with permeabilities on the order of 0.1 – 1.0 μ darcy will be required unless significant sorption of the radionuclides in the rock formation is demonstrated (experimental values for retardation of sodium range from 1.7 to 30¹³ and for calcium of up to approximately 100 in fractured rock¹⁴). Identifying formations of such quality will not, however be trivial: geothermal researchers in the United Kingdom have identified granite formations with perm abilities of “almost 200 darcies.”¹⁵ Any potential geologic repository will therefore require extensive surveying using pilot boreholes.

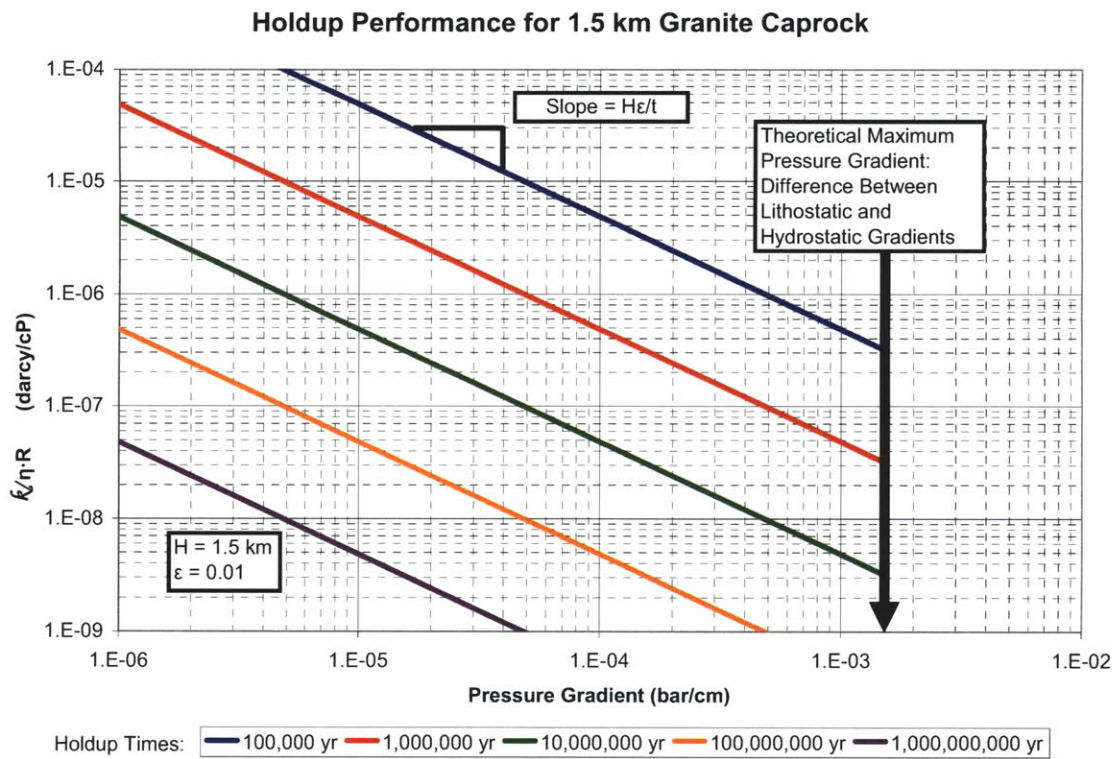


Figure 1-7: Holdup Performance Map for Advective Transport Through Repository

1.3.5 Oil and Natural Gas Directional Drilling Capabilities

Currently deployed oil and natural gas wells frequently make use of directional drilling techniques to significantly improve the production from and access to the formation of interest. Significant advances in measurement-while-drilling (MWD) and well logging permit the real-time control of the drill rig to achieve the desired geometry with high precision. Examples of the complexity of such wells¹⁶ are shown in Figure 1-8.

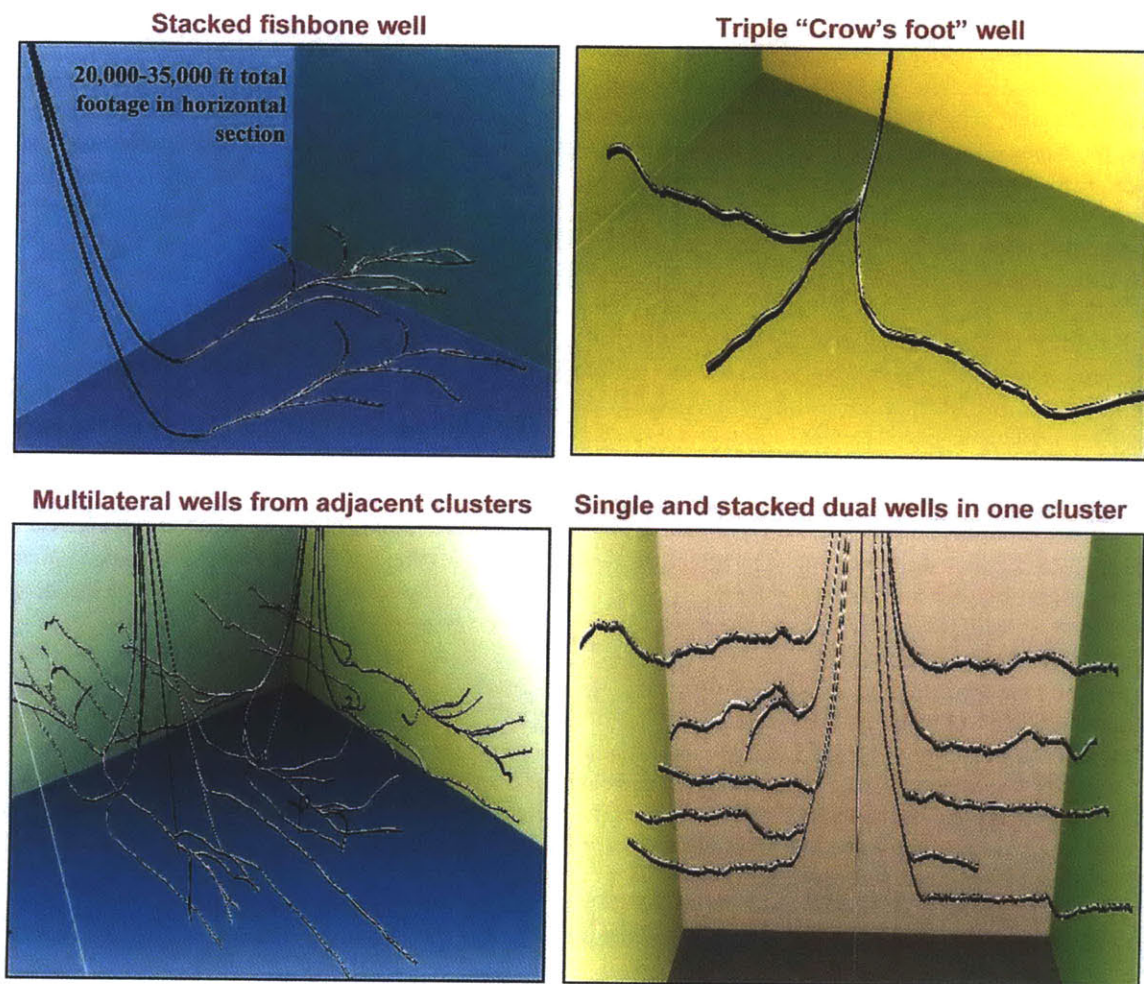


Figure 1-8: Examples of Complexity in Directional Wells

(Courtesy Multilateral Wells, SPE, 2008)

Various radii of curvature are possible in directional drilling. Due to the large lateral lengths of interest, long-radius wells are the focus of this project as seen in Figure 1-9.

The radius of curvature must be sufficiently large to accommodate the waste canister and lateral liner making the turn toward the horizontal.

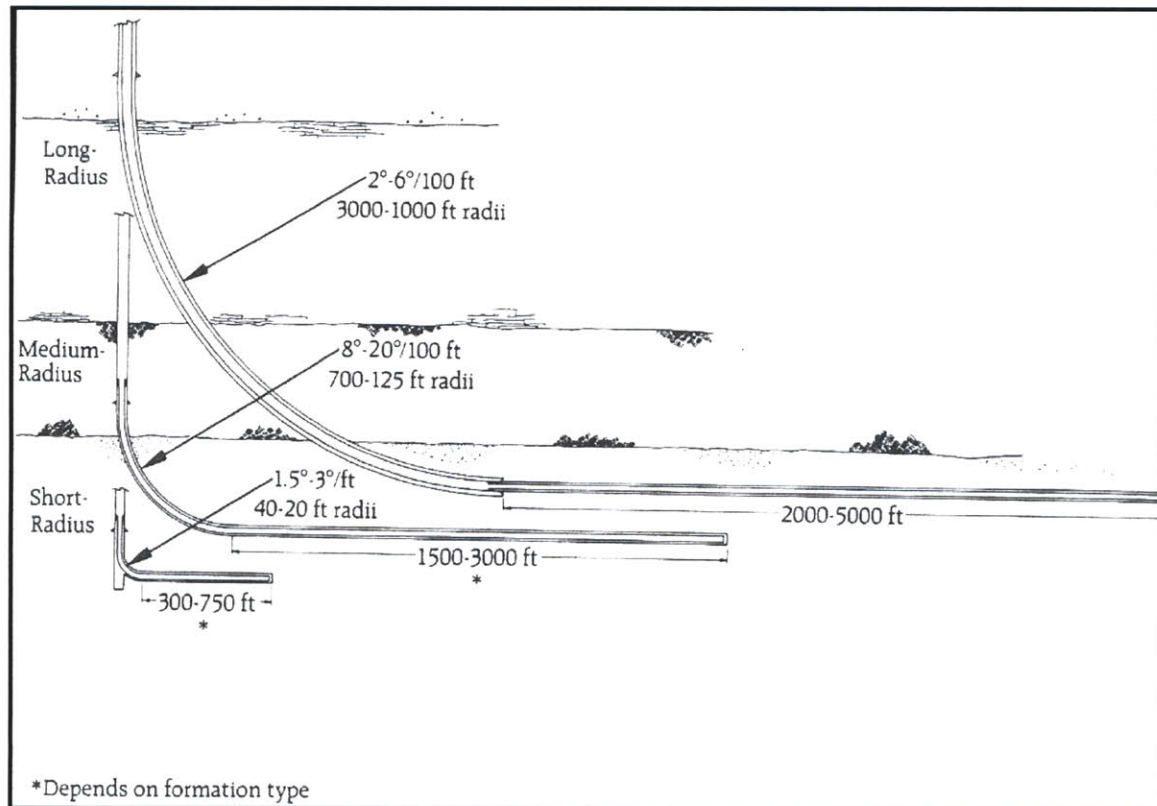
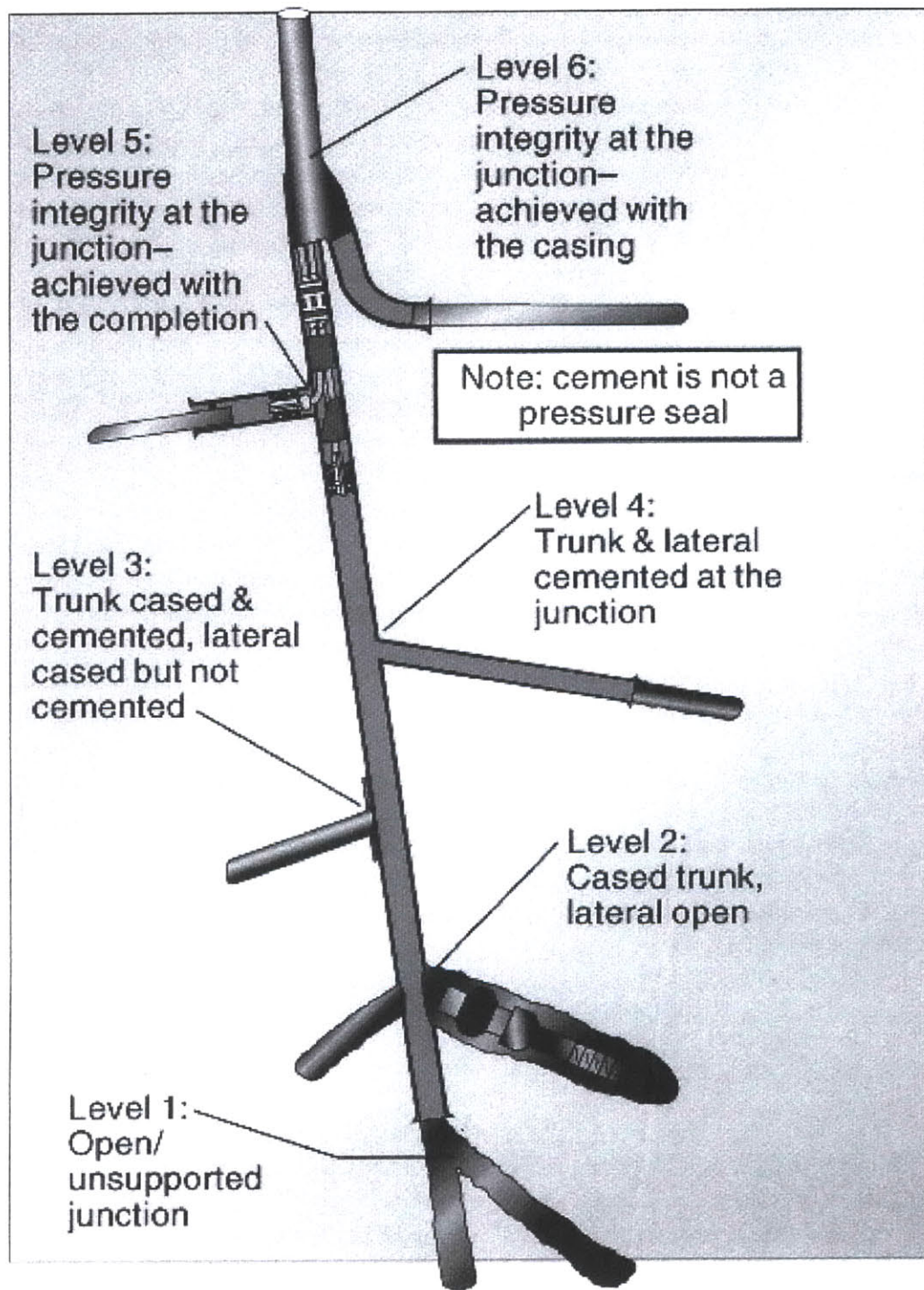


Figure 1-9: Radii of Curvature for Directional Wells
(Courtesy Multilateral Wells, SPE, 2008)

The high integrity of crystalline rock formations should permit drilling longer laterals than is possible in sedimentary formations. According to the required application for the well, the joint between the vertical shaft and the lateral can take several forms (higher level joints are more capable and more costly) shown in Figure 1-10. In the case of waste disposal, Level 3 (lined and cemented vertical borehole and lined but uncemented lateral) should be sufficient.

MULTILATERAL CONFIGURATIONS



OGJ

Figure 1-10: Configurations of Vertical to Lateral Junction
(Courtesy Multilateral Wells, SPE, 2008)

Several different techniques for commencing a lateral branch have been developed in industry. One such method is section milling wherein the vertical casing is milled away to permit the use of a bent drill sub to effect the lateral. As the sub continues through the kickoff, the bit will continue to deflect due to the angle of the sub. This is shown in Figure 1-11.

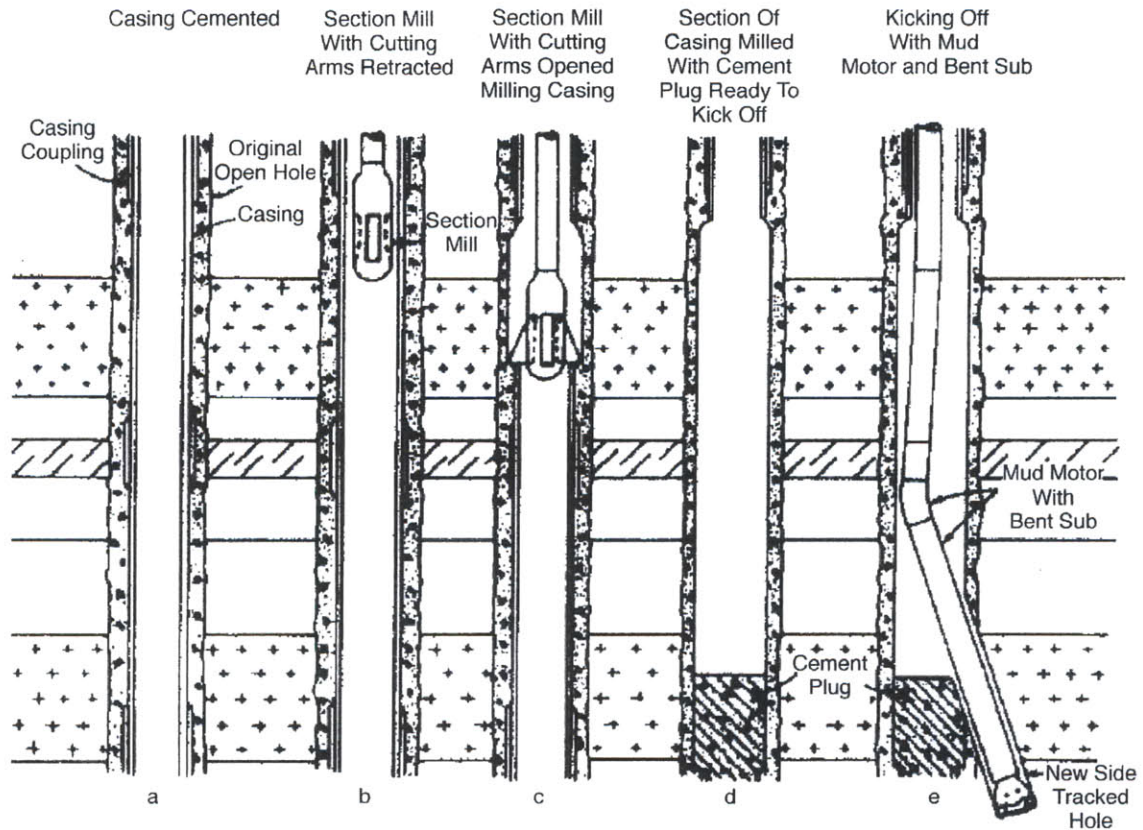


Figure 1-11: "Kicking Off" to Start a Lateral
 (Courtesy Multilateral Wells, SPE, 2008)

Figure 1-12 shows how a level three joint is made up between the vertical and lateral shafts by hanging the liner for the lateral from the main shaft. This completion of the lateral proceeds after drilling the lateral is completed.

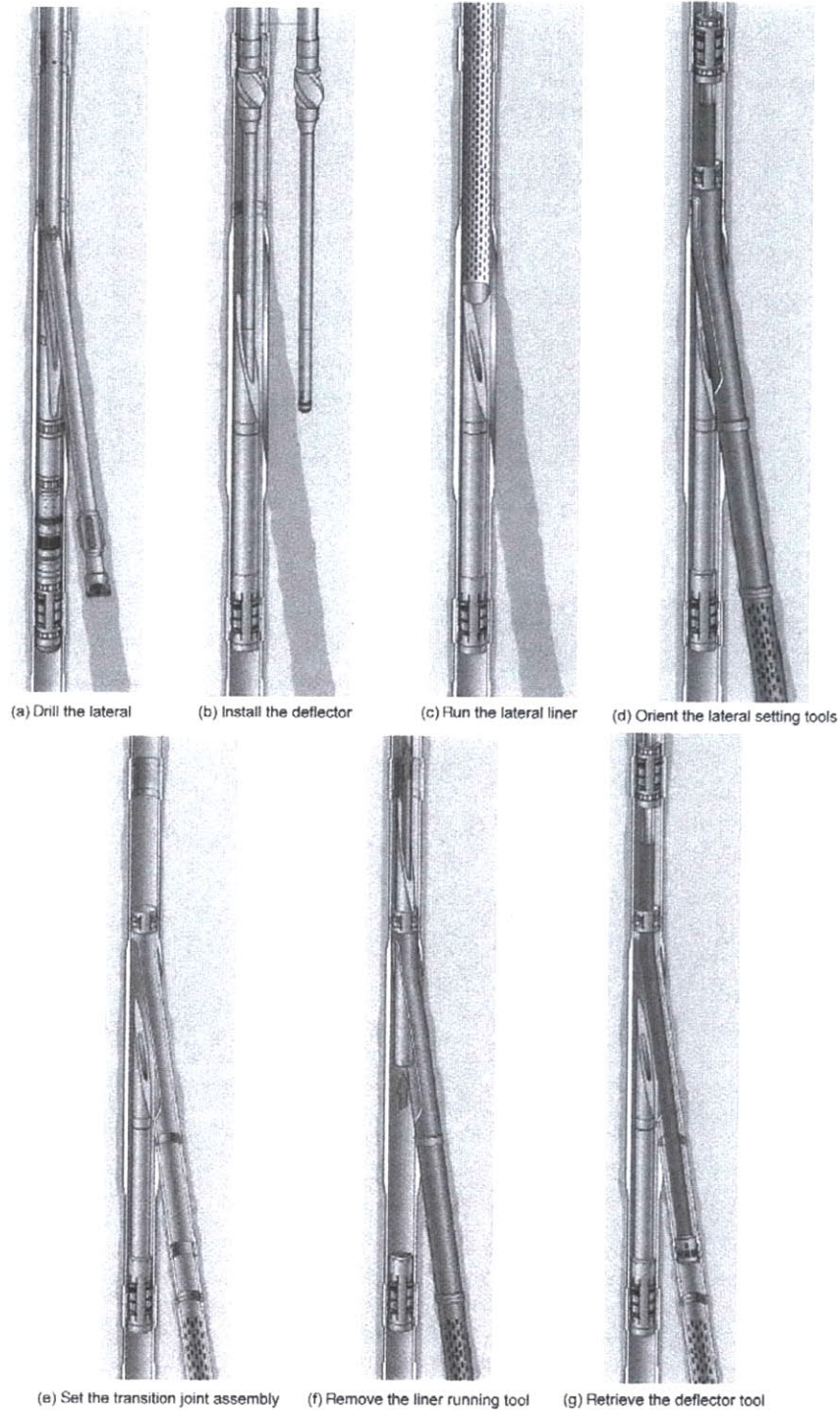


Figure 1-12: Lining the Lateral (Level 3 Joint)
(Courtesy Multilateral Wells, SPE, 2008)

1.4 Arrangement of the Thesis

1.4.1 Drilling Cost Model and Repository Configuration Selection:

Chapter 2

This chapter describes the V-DeepBoRe code and underlying model, critical inputs to the model and how the final design of the borehole repository was selected from over 20,000 potential configurations. With a single configuration selected, a linear model for the expected repository operating time (for an individual vertical shaft and its associated laterals) and the expected overall cost rate are developed based on a sensitivity analysis of key input parameters.

1.4.2 Waste Package Design and Analysis: Chapter 3

With the geometric configuration of the repository selected, design selections for the waste package may be made. This chapter details the characteristics of the final waste package design and the thermal and mechanical analyses and tools used to verify that the repository and canister designs are adequate to meet all suitability requirements. Both analytical and finite element methods are employed in the thermal performance analysis of the repository, while analytical and empirical relations are used to evaluate the mechanical performance of the canister.

1.4.3 Rod Consolidation and Package Cost: Chapter 4

This chapter compares and updates cost estimates for LWR rod consolidation from the 1980s and 90s. In applying these costs to the waste package design, the economic attractiveness of consolidation is examined as applied to deep borehole repositories.

1.4.4 Conclusions and Future Work: Chapter 5

In closing the thesis, the repository design, analyses, and evaluation tools are summarized and recommendations are made for topics of interest to very deep borehole repositories in general and lateral emplacement in particular.

2 DRILLING COST MODEL AND REPOSITORY CONFIGURATION SELECTION

2.1 Model Overview

In order to support the feasibility analysis of lateral emplacement of high level waste in very deep borehole repositories, a repository configuration must be identified. This model will be used to optimize this decision and identify the most attractive repository design. Additionally, it will be useful in identifying the major cost and risk drivers for such a repository as well as the repository design's sensitivity to potential parameters of interest.

The “V-DeepBoRe” model (Very DEEP BOrehole REpository Cost Model) developed for this project combines a deterministic approach with Monte Carlo simulation of the drilling process. Over a large trade space of potential repository designs, the model simulates the drilling of, completion of, emplacing of waste in, and sealing of a finished borehole repository. The solution space spans different emplacement lengths (the lateral portion of the borehole), main shaft depths, different declination angles of the lateral shafts, various piping schedules used, and the number of laterals branching out from a single central shaft.

The general configuration of the borehole repository is shown in Figure 2-1 below. The notional repository site is characterized by the depth of non-crystalline rock, the required depth of surface casing, and the desired size of the plug zone in the granite above the lateral kickoff. In addition, the size of the kickoff radius (which determines the distance traversed to effect the change in drilling direction to the desired lateral declination) impacts the depth at which the waste emplacement zone begins.

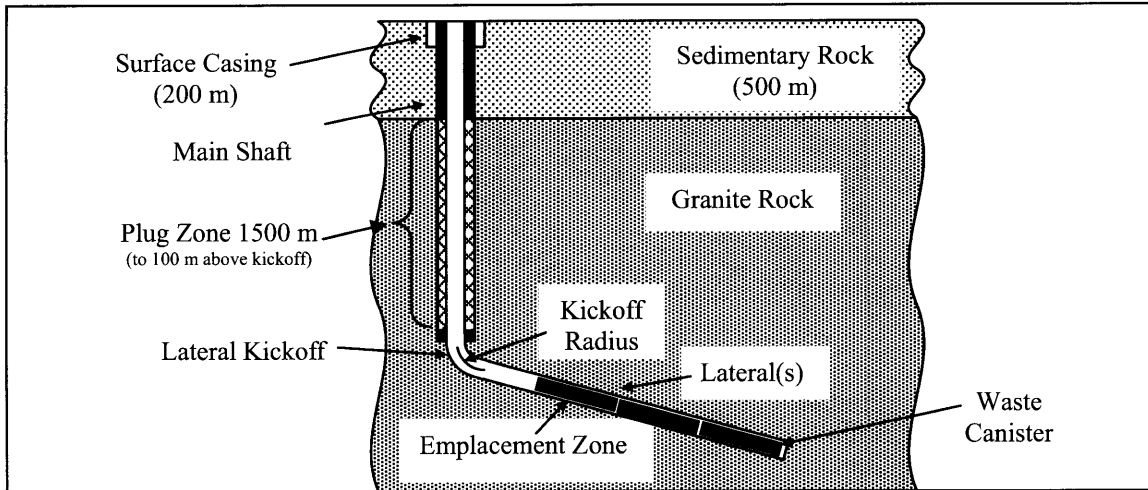


Figure 2-1: Nominal Repository Configuration

V-DeepBoRe incorporates the capacity of the repository (in metric tons of heavy metal in high level waste) to allow meaningful comparison of different repository configurations. This is calculated based on a common canister design that is 5 meters in length (half the standard 10 meter drill string).

2.2 Model Assumptions

V-DeepBoRe was developed using the following assumptions:

- The notional site is characterized by a 500 m sedimentary overburden above an uninterrupted granite basement. The presence of a water table requires the surface string to continue to 200 m below the surface. To permit acceptable continuity in the plug zone adjacent to undisturbed granite, the emplacement zone will start at a depth of 2000 m below the surface.
- Drilling speeds may be effectively modeled using a Gaussian distribution.
- Failures of drill bits (tripping) are independent events and may be effectively modeled by sampling using a probability density function for the expected bit life (in hours).
- Unexpected events are limited to tripping while drilling vertical shafts or laterals. This is to say that all other borehole operations (cementing, emplacing casings, emplacing waste canisters, backhauling equipment etc.) may be treated deterministically.

- The time associated with the pumping of cement depends only on the total volume of cement used (not the depth of the casing to be cemented).
- The main shaft is only cemented below the plug zone. This simplifies the removal of the upper portions of the casing to enhance plug sealing of the borehole. Reuse of this recovered pipestring (and cost savings) is not treated.
- Reconstitution of PWR assemblies is necessitated by the availability of current-practice lateral casing inner diameters.
- Adequate isolation between lateral shafts may be obtained with vertical as well as longitudinal segregation. This will permit as many as 12 lateral shafts to be drilled from a single main shaft, even should main shafts be located as close together as 200 meters.
- Borehole drilling and waste emplacement is conducted in shiftwork to permit around the clock operations.

The model simulates the drilling of the borehole through a Monte Carlo process where drilling speed and bit life are treated probabilistically and all other parameters deterministically. A brief sequence for V-DeepBoRe is shown below:

1. Drill vertical shaft (including several steps of lining the hole, telescoping down in bit diameter, backhauling bits as they wear out, etc.)
2. Drill and complete lateral shaft
3. Emplace waste in lateral, seal lateral
4. Repeat 2 and 3 until all laterals are full
5. Remove vertical liner and plug borehole

The outputs from these steps depend significantly on the parameters described in the next section.

2.3 *Model Parameters*

Tables 2-1 through 2-5, below, list the key parameters used in the V-DeepBoRe code. While many are justified by project work to date and expert input, several represent reasonable estimates (such as waste emplacement speeds and rate impact). Additionally, parameters such as the phase delay, overall billing rate, and borehole closeout costs were

adjusted to calibrate the model output for a 20,000-ft deep borehole to the results of a Sandia Enhanced Geothermal Study (summarized in section 2.5).

2.3.1 Repository Geometry

Table 2-1: Repository Geometric Parameters

Parameter	Value	Basis	Employment in V-DeepBoRe
Required Depth of Surface String	200 m	Assumption of Notional Site	This is the total length of the surface string piping schedule and the starting depth of the main shaft.
Sedimentary Overburden Depth	500 m	Assumption of Notional Site	This is the depth at which drilling speeds and failure rates are adjusted to reflect the ease/difficulty of drilling through different rock formations.
Plug Zone Length	1500 m (w/ 100 m of cemented casing below)	Assumption of Notional Repository (Similar to Other Borehole Proposals)	This is the depth at the start of the lateral waste emplacement zone.
Canister Length	5 m	Hoag Thesis ¹⁷	This is used to determine the number of canisters in an emplacement lateral and factors into the total waste capacity of a repository configuration.
Minimum Vertical Spacing Between Lateral Kickoffs	30 m	John Finger ¹⁸	This value is the estimated vertical separation between starting subsequent laterals from the same vertical borehole shaft.
Turn Radius (kickoff)	Calculated to Conservatively Permit 10m Lateral Liner to Make Curve		This value describes the radius of curvature for the ‘kickoff’ of the lateral (departure from the main shaft to a lateral of given declination). In the model it determines how far above the desired repository minimum depth the kickoff must occur.
Emplacement Depth	Calculated based on Plug Length, Sedimentary Overburden, Declination Angle, Total Number of Laterals per Borehole, and Turn Radius		This value is used in plotting the drilling costs of the repository by depth as the start of the emplacement zone.

2.3.2 Handling Speeds

Table 2-2: Handling Speed Parameters

Parameter	Value	Basis	Employment in V-DeepBoRe
Backhaul Speed (retrieving/tripping)	350 m/hr	John Finger ¹⁹	This is the speed at which drill bits and handling gear is brought up through the borehole (whether for routine retrieval or during a tripping event).
Casing Speed	350 m/hr	John Finger ²⁰	This is the speed at which casing is run into the borehole and is assumed to be constant from the surface all the way to the zone to be cased.
Lowering Speed	350 m/hr	John Finger ²¹	This is the speed at which drill bits are run into the borehole (whether routine for starting a new phase of drilling or after a tripping event).
Waste Speed (Emplacement)	25 m/hr (5 cans/hr) Once waste is >100m below drill rig, shifts to ½ of casing speed.		This is the speed at which waste canisters are connected together to form a drill string at the surface of the borehole and then run into the hole. This speed is assumed to be constant from the surface all the way into the lateral emplacement zone.
Cementing Speed	10 m ³ /hr		This is the volumetric flow rate of pumping cement into the borehole when required for cementing string casing in place.

2.3.3 Time Parameters

Table 2-3: Drilling Time Parameters

Parameter	Value	Basis	Employment in V-DeepBoRe
Phase Delay	192 hours	Fit to Match Sandia EGS ²² Well Cost Lite Results	This is the fixed delay assumed during the completion of each drilling phase, also used in this model during the completion of the lateral. Principally this serves as added conservatism in the time and cost projections of the model.
Cement Cure Time	48 hr		This time represents the delay after pumping cement into the borehole to hold casing in place before the next phase of the borehole completion may begin. This allows for the cement to appropriately set.
Time to Cement for New Kickoff and Mill Through Vertical Casing	48 hrs		This is a delay time to represent preparation of the base of the main borehole shaft to permit kicking off for a new lateral. A cement base is poured allowing for a (new) off-center kickoff.
Time to Plug Lateral	72 hrs		This is a delay time associated with the plugging of the lateral. This plug is merely intended to isolate the waste string from drilling operations for the other laterals and will not be designed to act as a barrier to the long term transport of radionuclides.
Borehole Plugging Time	240 hr		This is a delay time to capture the extensive effort involved in plugging the main shaft of the borehole with sufficient integrity to mitigate release of radionuclides to the environment. This is approximately 5 times slower than the pumping speed of cement assumed and is extremely conservative.

2.3.4 Cost Parameters

Table 2-4: Drilling Cost Parameters

Parameter	Value	Basis	Employment in V-DeepBoRe
Drill Bit Replacement Cost (tripping)	Various, by Bit Size	John Finger ²³	This cost represents the cost of repairing/replacing damaged drilling equipment as a result of a tripping event. This is in addition to the cost of delayed operations at the borehole (captured through the billing rate).
Cement Material Cost	\$90.36/m ³	Survey of Supplier Prices ²⁴	This is the material cost associated with the specialized cement used in the completion of the borehole.
Casing Material Cost	\$6/kg	Survey of Supplier Prices ²⁵	This is the material cost associated with the drill casing used in the completion of the borehole.
Billing Rate (Non-Emplacement)	\$4200/hr	Fit to Match EGS ²⁶ Well Cost Lite Model Results	This billing rate represents the principle operating costs at the drilling site regardless of the phase of borehole development (with the exception of emplacement of the waste canisters).
Billing Rate (Emplacement)	2.5x Billing Rate (until waste is >100m below rig) 1.15x Billing Rate (thereafter)		This billing rate represents the elevated operating costs at the drilling site when waste canisters are being assembled into drill strings and run into the borehole. While radiation workers will need to remain on site to supervise the waste emplacement, once the waste is shielded in the borehole, remote handling of string is no longer required. It is also intended that with multiple boreholes being constructed and filled at the same time, that the work load for radiological personnel can be level-loaded across the entire repository.
Plugging Cost (Main Shaft)	\$1,000,000		This cost represents the material and specialized labor costs that result from sealing the main shaft of the borehole with an impermeable plug zone.
Borehole Closeout Cost	\$2,000,000	Fit to Match EGS ²⁷ Well Cost Lite Model Results	This parameter captures the costs associated with final completion of a drilling site and the breakdown of the rig and other equipment (those costs not captured elsewhere)

2.3.5 Spent Fuel Parameters

Table 2-5: Spent Fuel Parameters

Parameter	Value	Basis	Employment in V-DeepBoRe
Vitrified Waste Fraction (of Canisters)	20%		This fraction is used to determine the relative composition of the waste sent to the repository.
Waste Loading of Borosilicate Glass	25 weight % (Heavy Metal)		The weight loading of waste species into vitrified waste forms permits the calculation of the total capacity of the repository in MTHM.
PWR Fraction of Canisters	64% (of LWR Canisters)	Nuclear Engineering International ²⁸	This fraction is used to determine the relative composition of the waste sent to the repository. Specifically, this is used to determine the number of canisters used for disposal of PWR and BWR spent fuel assemblies.
Ratio of Usable Waste Diameter to Casing Inner Diameter	0.9		This parameter describes how much of the available inner diameter of the cased lateral may be occupied by waste in the waste canister. This permits the comparison of different repository designs without having to design canisters for each.
BWR Assembly Width	13.4 cm	Nuclear Engineering International ²⁹	This geometric factor will determine if intact BWR assemblies can be used in the repository design or if the small size of the final inner diameter of the lateral emplacement casing will require consolidation of BWR fuel pins.
PWR Pin Outer Diameter	0.95 cm	Nuclear Engineering International ³⁰	This factor will determine how densely PWR fuel pins may be packed together into the waste canister and, ultimately, what mass of waste may be placed in a canister.
BWR Pin Outer Diameter	1.1 cm	Nuclear Engineering International ³¹	This factor will determine how densely BWR fuel pins may be packed together into the waste canister and, ultimately, what mass of waste may be placed in a canister (if fuel consolidation is necessary).
Pins/Assy (PWR)	264	Nuclear Engineering International ³²	This factor is used to compare the number of fuel pins in a canister to that of an intact fuel assembly so that the mass of waste in the canister can be determined from the mass in an intact PWR assembly.

Table 2-5: Spent Fuel Parameters (Continued)

Parameter	Value	Basis	Employment in V-DeepBoRe
Pins/Assy (BWR)	72	Nuclear Engineering International ³³	This factor is used to compare the number of fuel pins in a canister to that of an intact fuel assembly so that the mass of waste in the canister can be determined from the mass in an intact BWR assembly.
Mass of HM/Assy (PWR)	0.50 MTHM	Nuclear Engineering International ³⁴	This factor is used to compare the number of fuel pins in a canister to that of an intact fuel assembly so that the mass of waste in the canister can be determined from the mass in an intact PWR assembly.
Mass of HM/Assy (BWR)	0.19 MTHM	Nuclear Engineering International ³⁵	This factor is used to compare the number of fuel pins in a canister to that of an intact fuel assembly so that the mass of waste in the canister can be determined from the mass in an intact BWR assembly.

2.3.6 Drill String Parameters

Table 2-6, below, depicts the ‘menu’ of 14 standard drill bit sizes and associated casing sizes employed in the model (as well as the 48” and 36” diameter holes used in the EGS comparison calculations). The model examines the impact of the various drill bit sizes on the overall cost and time to drill the repository by using 69 potential piping schedules (one size for the surface shaft/casing, one for the main shaft, and one for the lateral). These 69 combinations ensure reasonable telescoping of casing to the subsequent drill bit while permitting a finished lateral casing interior diameter of at least 4 inches.

Drill Bit/Hole Size (inches)	Casing Pipe Size (Nominal)	Casing Pipe Schedule	OD (in)	ID (in)	Wall Thickness (in)	Weight (lbs/ft)	Casing Mass (kg/m)	Replacement Bit Cost (\$2009)
48	40	STD	40	39.125	0.237	184.86	275.10	\$158,300
36	30	STD	30	29.125	0.237	138.13	205.57	\$109,800
26	20	STD	20	19.25	0.375	78.6	116.97	\$72,000
24	18	STD	18	17.25	0.375	70.59	105.05	\$64,800
20	16	STD	16	15.25	0.375	62.48	92.98	\$50,600
17.5	14	STD	14	13.25	0.375	54.57	81.21	\$41,900
17	12	STD	12.75	12	0.375	49.56	73.75	\$40,200
15.5	11	STD	11.75	11	0.375	45.56	67.80	\$35,100
14.5	10	STD	10.75	10.02	0.365	40.48	60.24	\$31,700
12.25	9	STD	9.625	8.941	0.342	33.91	50.46	\$24,200
11.625	8	STD	8.625	7.981	0.322	28.55	42.49	\$22,100
10.75	7	STD	7.625	7.023	0.301	23.54	35.03	\$19,200
9	6	STD	6.625	6.065	0.28	18.97	28.23	\$13,500
8.75	5	STD	5.563	5.047	0.258	14.62	21.76	\$12,700
7.875	5	STD	5	4.506	0.247	12.54	18.66	\$9,900
6.25	4	STD	4.5	4.026	0.237	10.79	16.06	\$4,700

Table 2-6: Drill String Parameters
(Drill and Casing Sizes and Weights Courtesy of WoodCo USA³⁶)

For each drilling/casing size, drilling parameters are identified in yellow. As part of the Monte Carlo simulation of the drilling of the repository, each drill bit has a Gaussian drilling speed distribution characterized by a mean and standard deviation as shown in Figure 2-2, as well as a logarithmically distributed failure probability, to model bit failure events as shown in Figure 2-3.

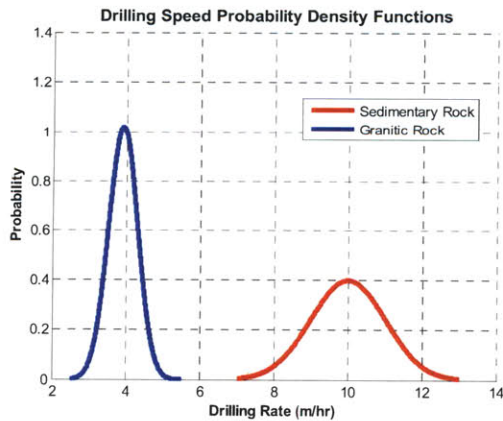


Figure 2-2: Model Drilling Rate PDFs

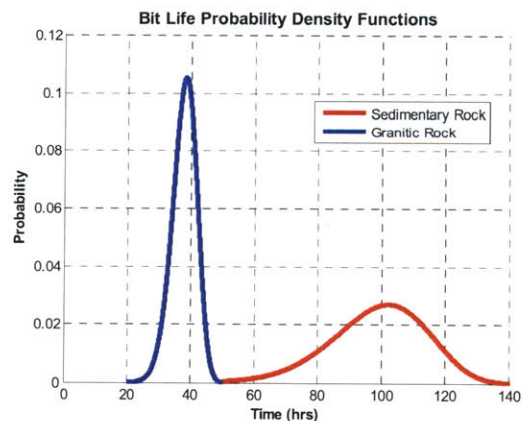


Figure 2-3: Model Bit Life PDFs

The model further breaks down these speeds and failure probabilities between the sedimentary overburden zone (more similar to conventional oil and natural gas drilling

experience) and the crystalline granite basement rock (similar to enhanced geothermal applications). The nature of these distributions is based largely on the input of Mr. John Finger, formerly of Sandia National Laboratory³⁷.

One of the key costs employed in the model is the cost of replacing a drill bit after it is no longer effective. Based on input from John Finger³⁸, Table 2-7 reflects the estimated replacement cost for several Drill Bits in 2009-year dollars.

Table 2-7: Drill Bit Replacement Costs

Drill Bit Size	Replacement Cost Estimate (\$2009)
26"	\$72,000
17.5"	\$42,000
12.25"	\$24,000
8.5"	\$12,000

By plotting these costs by bit size, the replacement costs appear to obey a very weak quadratic relation (highly linear). Using the regression in Figure 2-4, an empirical relation is used to obtain the replacement cost for each drill bit; this is shown in Table 2-6.

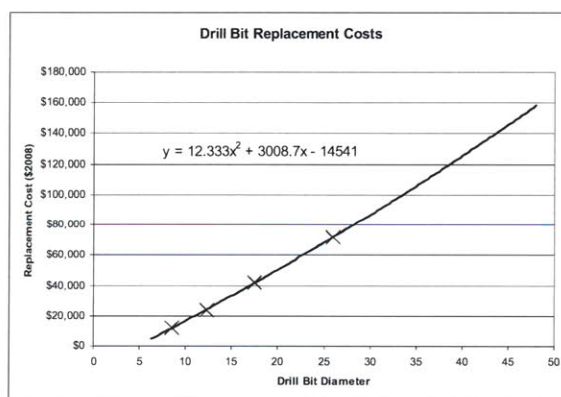


Figure 2-4: Drill Bit Replacement Costs Curve Fit

2.4 Modules

2.4.1 Waste Mass Calculation

To permit the comparison of different sizes of repositories, each candidate repository is scored based on the mass of nuclear waste that it can accommodate in the emplacement

zone. Using the spent fuel parameters identified above, 90% of the inner diameter of the lateral casing is used as an upper limit on the diameter of the fueled portion of the waste canister. As PWR assemblies are larger than the lateral casings we are examining, reconstitution of PWR fuel assemblies is assumed. This is to say that the PWR assemblies will be disassembled at a facility near the repository to be repacked into the borehole waste canisters. Assembly compaction of this type is a well proven procedure (EPRI Fuel Consolidation Demonstration Program, EPRI NP-6892, June 1990); (Sciencetech Prototypical Consolidation Demonstration Project, BW1/22066, March 1998) and will be discussed further in Chapter 4. Figure 2-5 shows the hexagonal packing of fuel pins into the waste canister. For many ratios of canister diameter to fuel pin diameter, additional pins could be packed within the required diameter outside of the hexagonal array. For simplicity this is not considered in the trade-space produced by the model but is reflected in the canister design selected in Chapter 3.

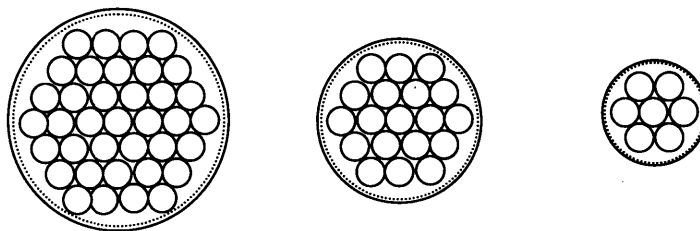


Figure 2-5: Hexagonal Packing Scheme of Reconstituted PWR & BWR Fuel Pins

With the number of fuel pins in a canister so identified, the total mass of waste in a PWR canister is found by multiplying the number of pins by the mass of waste in a PWR assembly and dividing by the total number of pins in a PWR assembly.

A similar approach is used for consolidated BWR fuel pins, provided that intact assemblies cannot fit within the required diameter. To check this, V-DeepBoRe compares the available diameter to that required for various packing configurations of the square BWR assemblies. A sample of these configurations is shown in Figure 2-6.

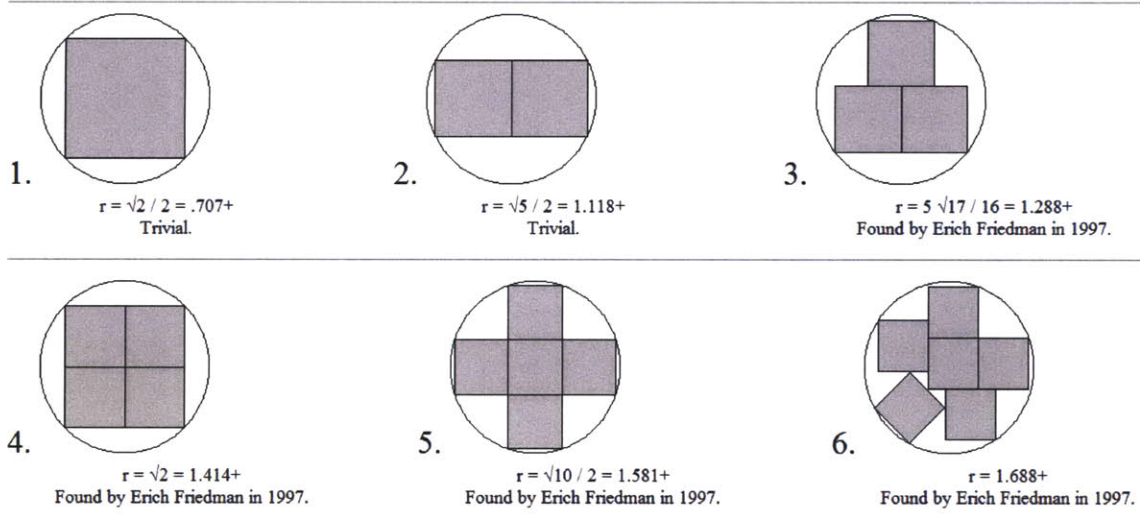


Figure 2-6: Optimal Packing of BWR Assemblies in Waste Canister
(courtesy Erich Friedman of Stetson University³⁹)

Generally BWR fuel consolidation is avoided due to its increased handling costs.

Additional credit is given to that fraction of the waste canisters containing vitrified wastes. A wasteform weight density, an input parameter, yields a volumetric density of waste in borosilicate glass based on the relative densities of the glass and the waste species (assumed here to be natural uranium). By using the volume available to the waste canister (based on the 5 meter length and inner diameter available from the lateral casing), the total mass of waste from the vitrified canisters is calculated. Taken together, the total capacity of the repository is identified by summing up the mass contributions of PWR, BWR, and vitrified waste canisters according to the fractions identified in the key parameters section.

2.4.2 Drilling Script

The drilling model evaluates each combination of the trade space variables over a series of realizations (to account for the probabilistic nature of the drilling operations themselves). Within each realization, the entire borehole is drilled and completed, waste canisters are emplaced, and the vertical shaft is sealed using a 1500 meter plug zone. At each step, the current depth of the hole, the total time since drilling began, and the total cost of the borehole are retained in a history file. The MATLAB scripts for the drilling model are reproduced in Appendix A. The sequence below describes how these scripts

evaluate each drilling simulation (parameters of interest are called out and explained in section 2.3, above):

1. Calculate Minimum Required Radius of Curvature for Kickoff Arc per Figure 2-7 such that the gap is not less than 1/3 of the difference between hole inner diameter and casing/canister outer diameter (the limit imposed by the 10 m lateral casing liner sections is significantly more restrictive than emplacing 5 m waste canisters)

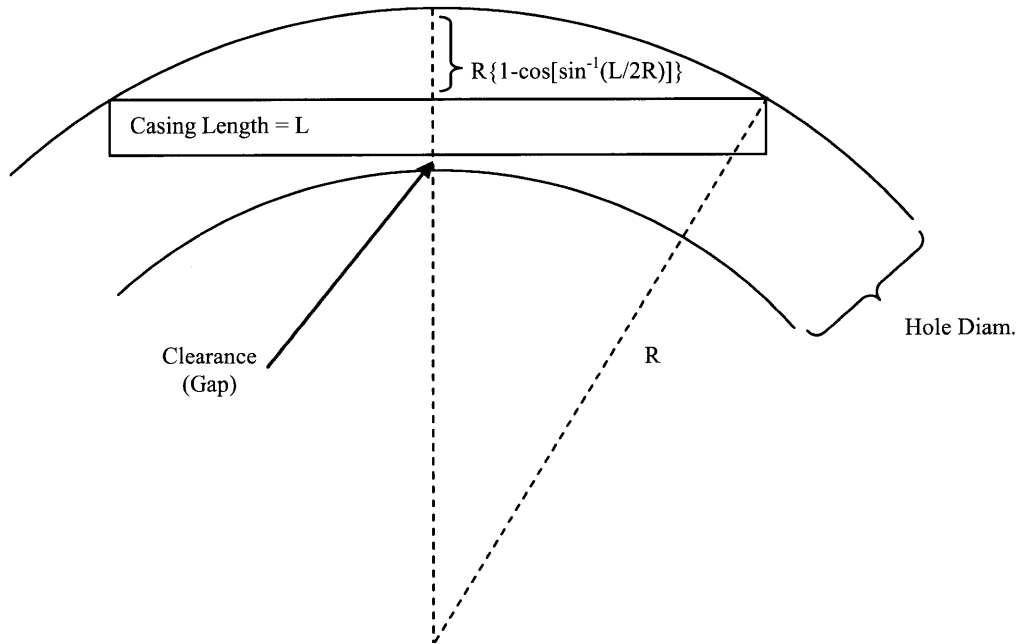


Figure 2-7: Calculation of Minimum Required Radius for Kickoff Arc

Table 2-8 lists the resulting minimum radii for the 8 potential lateral drill bit sizes:

Table 2-8: Minimum Radii of Curvature for Kickoff Arcs

Lateral Hole ID (in)	Lateral Casing OD (in)	Minimum Radius (m)
12.250	9.625	270.69
11.625	8.625	242.41
10.750	7.625	234.51
9.000	6.625	305.65
8.750	5.563	230.59
7.875	6.000	250.31
6.250	4.500	392.05

2. Drill the Surface Shaft
 - a. Sample Drilling Speed (For Overburden Normal Distribution Figure 2-2)
 - b. Determine Time to Complete to 200m

- c. Determine if Bit Failure Occurs (Logarithmic Distribution Figure 2-3)
 - d. Calculate Total Time and Costs
- 3. Back out Surface Drill String
- 4. Emplace Surface String Casing (Update the Total Casing Mass Used)
- 5. Cement Surface Casing
 - a. Calculate Annular Volume Between Liner and Hole
 - b. Calculate Total Time and Costs
- 6. Lower Main Shaft Drill String
- 7. Drill Main Vertical Shaft
 - a. Sample Drilling Speed (For Overburden Normal Distribution Figure 2-2)
 - b. Determine Time to 500 m
 - c. Determine if Bit Failure Occurs in Overburden (Logarithmic Distribution Figure 2-3)
 - d. Calculate Total Time and Costs to Reach 500 m (Granite Formation)
 - e. Sample Drilling Speed (For Granite Normal Distribution Figure 2-2)
 - f. Determine Time to Reach Kickoff Depth
 - g. Determine if Bit Failure Occurs in Granite (Logarithmic Distribution Figure 2-3)
 - h. Calculate Total Time and Costs to Kickoff Depth
- 8. Back Out Main Drill String
- 9. Emplace Main String Casing (Update Total Casing Mass Used)
- 10. Cement Main Casing (100 m Below Plug Zone)
 - a. Calculate Annular Volume and Update Cement Volume
 - b. Calculate Total Time and Costs
- 11. Lateral Operations (Repeat for Each Lateral in Repository)
 - a. Cement for Kickoff (Update Time and Cost)
 - b. Lower Lateral Drill String
 - c. Drill Through to Lateral Declination
 - i. Sample Drilling Speed (For Granite Normal Distribution Figure 2-2)
 - ii. Divide Speed by 2 (Accounts for Difficulty in Kicking Off)

- iii. Determine Time to Drill Radial
- iv. Determine if Bit Failure Occurs in Radial (Logarithmic Distribution Figure 2-3)
- v. Calculate Total Time and Costs to Lateral Declination
- d. Drill Lateral
 - i. Multiply Previous Speed by 2 (Restores Original Sampled Value)
 - ii. Determine Time to Drill Lateral
 - iii. Determine if Bit Failure Occurs in Lateral (Logarithmic Distribution Figure 2-3)
 - iv. Calculate Total Time and Costs to Lateral Declination
- e. Back out Lateral Drill String
- f. Emplace Lateral Casing (Update Total Casing Mass Used)
- g. Emplace Waste Canisters (Use Updated Speed and Rate Once Waste is >100m Below the Surface)
- h. Seal Lateral
- i. Update Total Time and Costs
- 12. Remove Main String Casing (Up to 100m Below Plug Zone – this region of the casing was never cemented and will be cut or unscrewed)
- 13. Seal Borehole with Plug (Update Cost and Time)
- 14. “Score” Repository Using Waste Mass Calculations and Generate Outputs

2.4.3 Output and Plotting

Figure 2-8, below, depicts a sample realization of V-DeepBoRe evaluating the time and cost to drill a 4 lateral repository with 2000 meter lateral emplacement lengths. The stepped nature of the drilling lines indicates the influence of bit failure on drilling a given shaft or lateral. The horizontal breaks in the top two plots reflect the times when active drilling is not going on (such as while waste is being emplaced or other drilling delays occur).

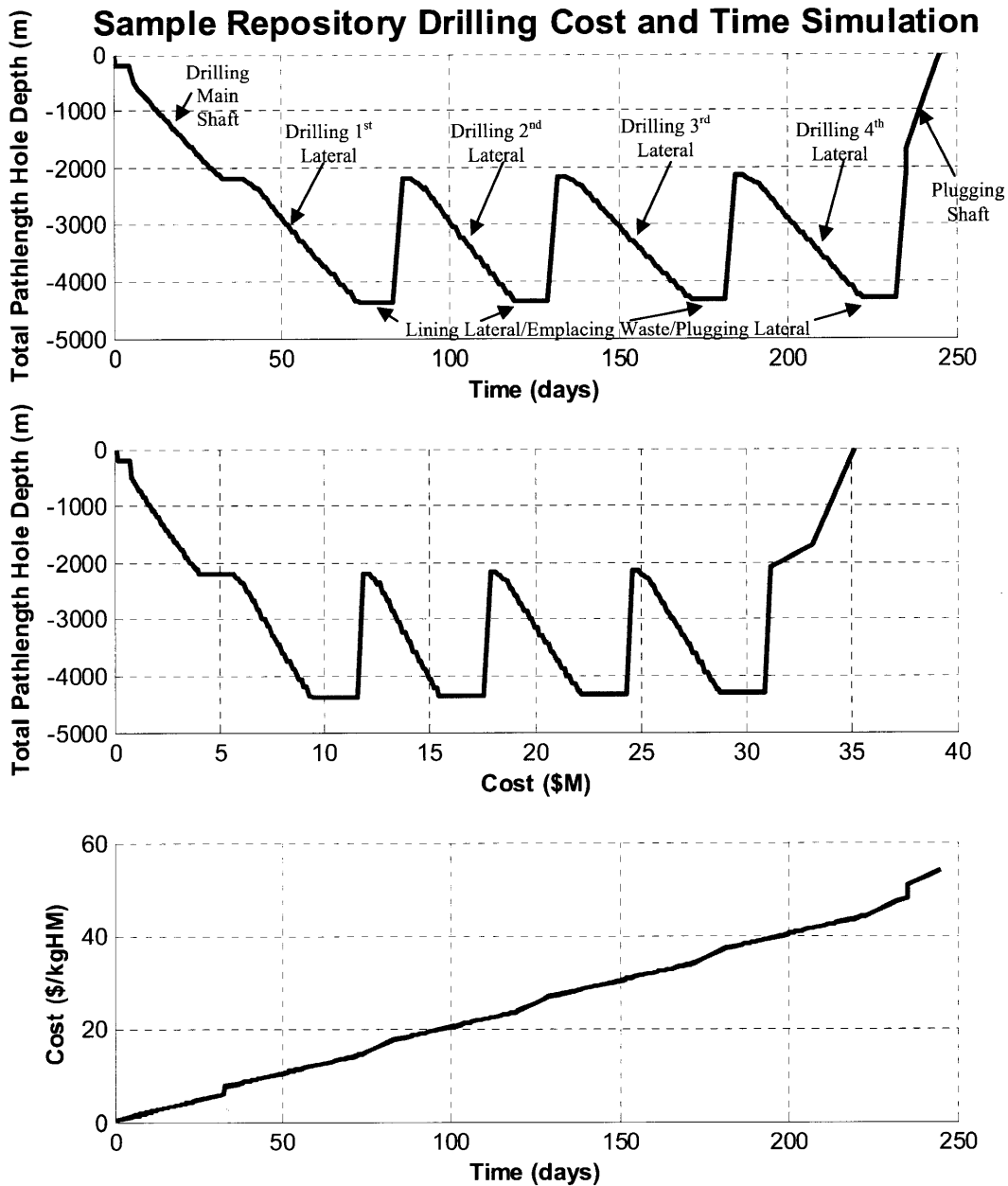


Figure 2-8: Sample Output (Single Trial)

Based on the input parameters currently in use, the model appears to be very sensitive to the diameter of the lateral and the length of the emplacement and less so to the number of laterals used and the declination angle of the lateral emplacement. Revising the input parameters, however, is likely to change these results.

As currently configured, the drilling model also outputs several key results from the simulation. These are listed below [note, a trial represents a unique repository configuration (number of laterals, length of laterals, declination angle of laterals, and pipe-schedule to be used), whereas a realization is the simulation of drilling, completing, filling, and closing/plugging a borehole; thus multiple realizations should be employed to capture the variability of a particular configuration].

1. Total Time for Repository Completion (From Surface String Through Plugging)
[days/MTHM]
2. Total Cost for Repository Completion (From Surface String Through Plugging)
[\$/MTHM]
3. Total Volume of Cement Used [m³]
4. Total Mass of Drill String Casing Used [kg]
5. Total Capacity of Repository [MTHM]
6. If BWR Fuel was Consolidated
7. Number of PWR Pins per Canister
8. Number of BWR Assemblies per Canister (0 if Pins are Consolidated)
9. Number of BWR Pins per Canister (0 if Assemblies are Left Intact)
10. Emplacement Length of Each Trial / Realization
11. Emplacement Declination Angle of Each Trial / Realization
12. Number of Laterals Used in Each Trial / Realization
13. Piping Schedule Used in Each Trail / Realization

2.5 Calibration Using Vertical Borehole Results

To help demonstrate the acceptability of the parameters input into this drilling script, a simple simulation was developed for comparison with work to date on vertical boreholes. Figure 2-9 shows the results from 100 realizations of this simulation wherein a drill bit schedule of 48", 36", 26", 17 ½", 12 ¼" and 8 ¾" diameters were used for the conductor string, surface string, intermediate shaft, and three production phases respectively (to an ultimate depth of 20,000 ft [6096 m]). The drilling parameters were otherwise the same as those used for the lateral emplacement simulation (those parameters called out in sections

2.3.3-2.3.4 were calibrated to match these data). The EGS data are from Enhanced Geothermal Systems Well Construction Technology Evaluation Report (Sandia Report 2008-7866, December 2008)⁴⁰.

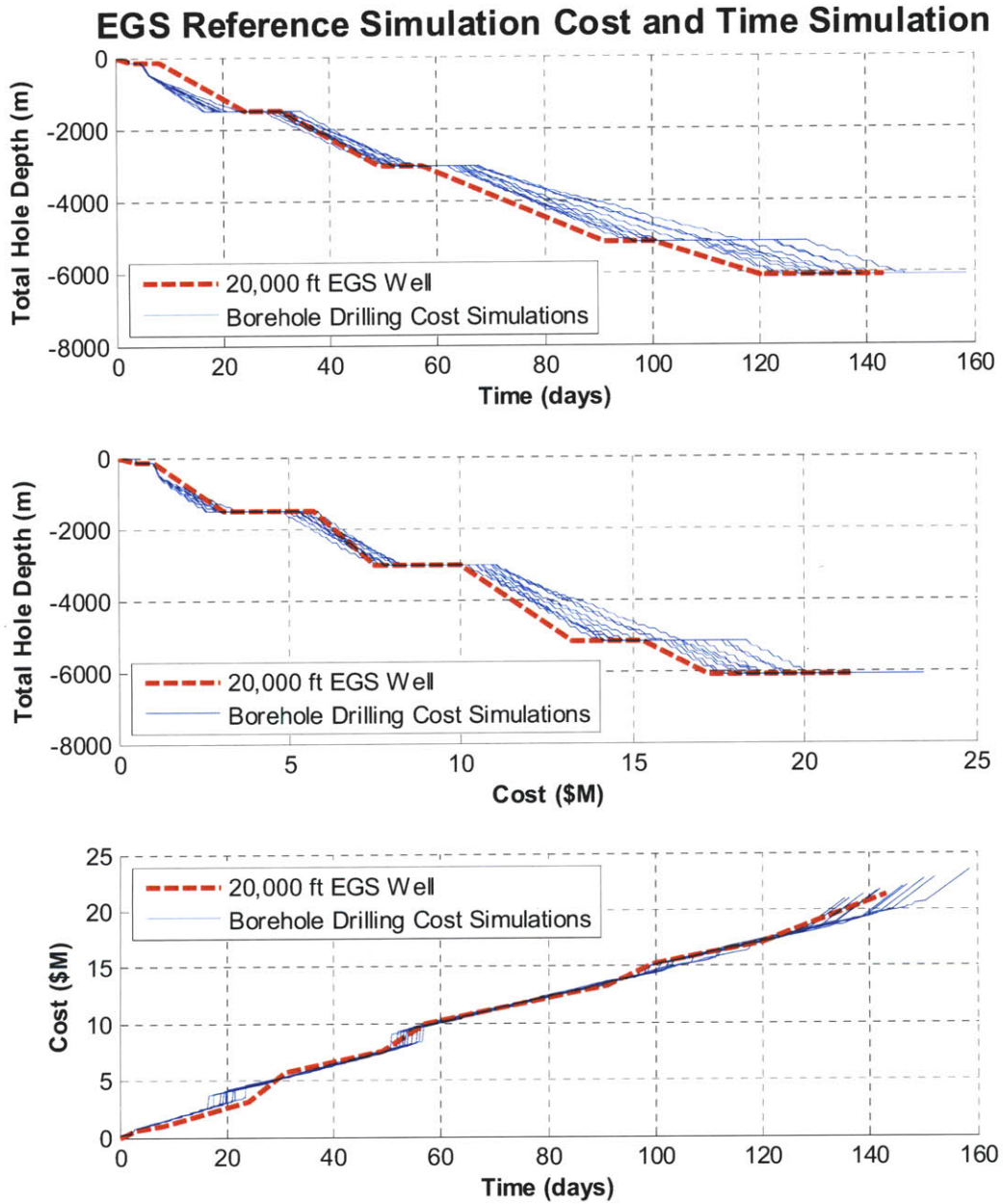


Figure 2-9: Output Results for Vertical Borehole

The output values for this simulation were made to effectively correlate with reference Sandia borehole data.

2.6 Results and Repository Configuration Selection

Figure 2-10 through Figure 2-25 depict the results from a trade space study of several thousand repository configurations. In order to parse out key cost and time drivers, each plot breaks apart the trade-space by applying colors according to the various parameters employed.

2.6.1 Complete Trade Space Results

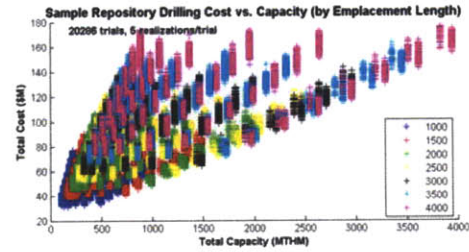
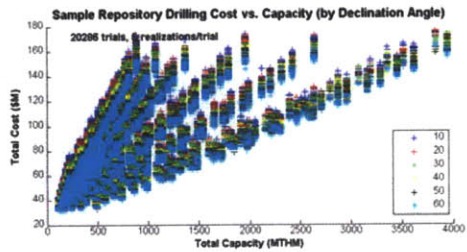
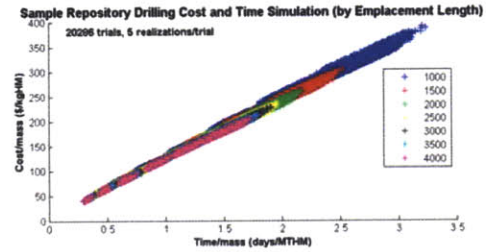
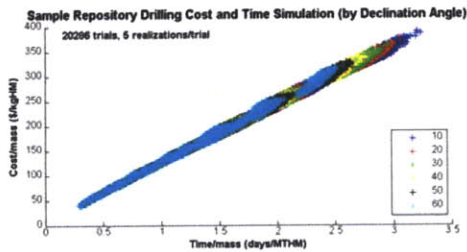


Figure 2-10: Full Trade-space by Declination Angle ($^{\circ}$)

Figure 2-11: Full Trade-space by Emplacement Length (m)

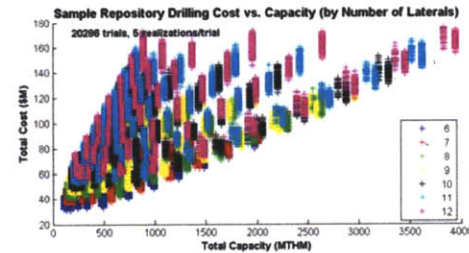
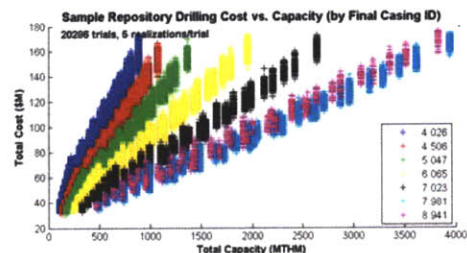
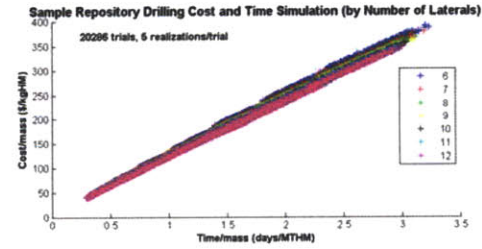
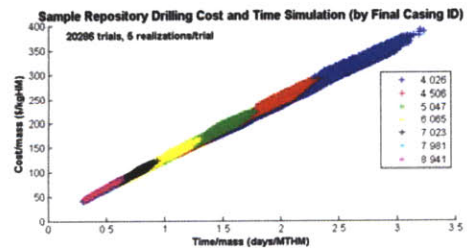


Figure 2-12: Full Trade-space by Lateral Diameter (in)

Figure 2-13: Full Trade-space by Number of Laterals

2.6.2 Trade Space Results with Crushing Limit Imposed

The first down-selection of the trade-space was achieved by removing those combinations of declination angle and emplacement length that produced a lateral with a total vertical height of 800 m or more. This was done to mitigate the hydrostatic crushing weight on the bottommost canister and, as a result, ensures that horizontal (i.e. significantly departed from standard, vertical boreholes) geometry was explored.

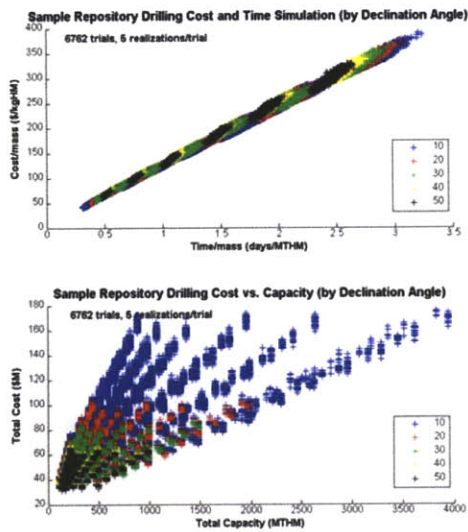


Figure 2-14: Trade-space with Crushing Limit by Declination Angle ($^{\circ}$)

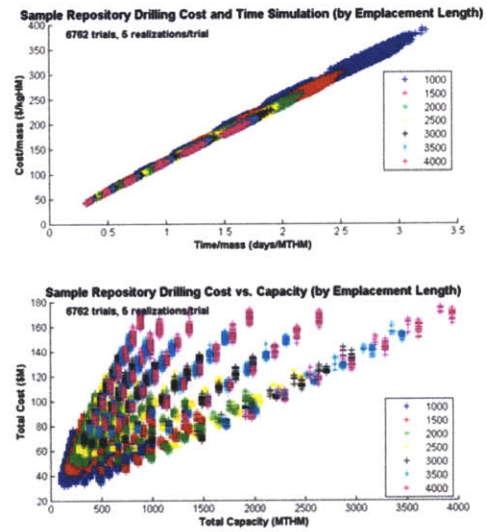


Figure 2-15: Trade-space with Crushing Limit by Emplacement Length (m)

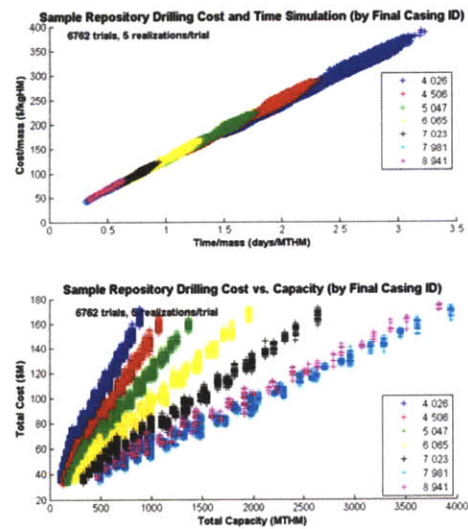


Figure 2-16: Trade-space with Crushing Limit by Lateral Diameter (in)

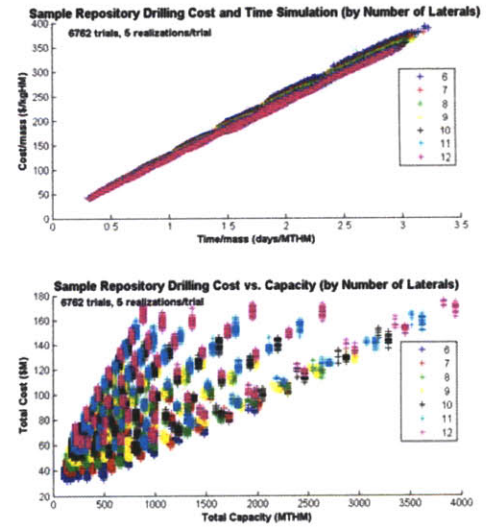


Figure 2-17: Trade-space with Crushing Limit by Number of Laterals

2.6.3 First Narrowing of Trade-space

To ensure an economically feasible design cost per mass was used to eliminate several potential repository configurations. This was achieved by eliminating configurations with fewer than 10 laterals (more laterals allows the spreading of the “sunk” vertical shaft costs over more waste canisters) and the elimination of pipe-schedules with final lateral hole (drill bit) diameters of less than 10”.

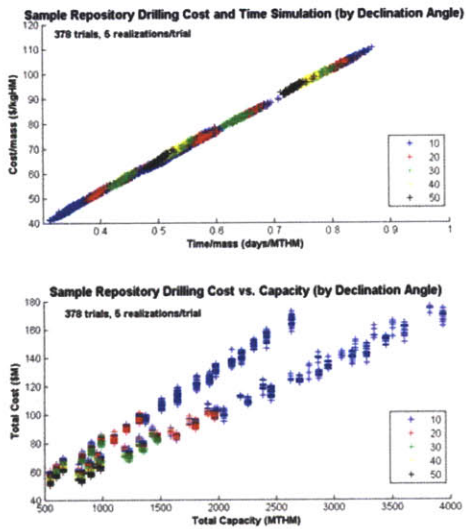


Figure 2-18: 1st Winnowed Trade-space by Declination Angle (°)

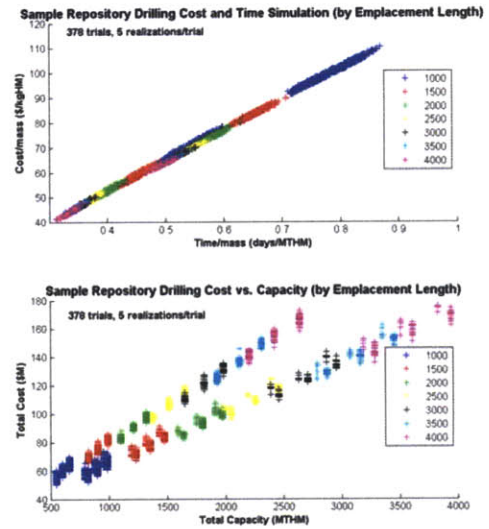


Figure 2-19: 1st Winnowed Trade-space by Emplacement Length (m)

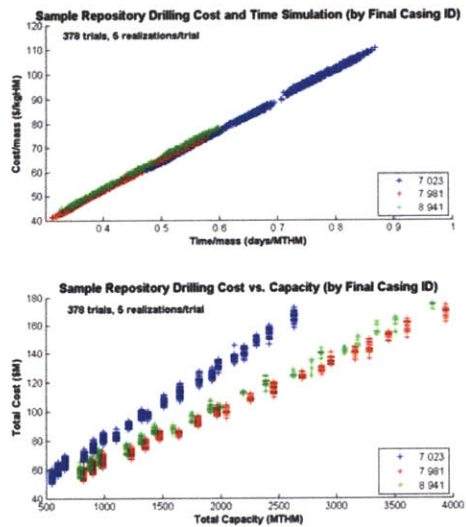


Figure 2-20: 1st Winnowed Trade-space by Lateral Diameter (in)

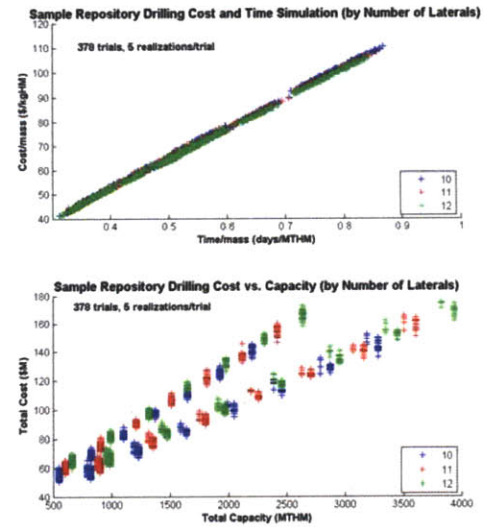


Figure 2-21: 1st Winnowed Trade-space by Number of Laterals

2.6.4 Second Narrowing of the Trade-space

Further inspecting the pared-down trade-space results suggested further limiting the scope of study to laterals of length 1500 – 2500 m, lateral declinations of 10 – 30 degrees, and final lateral drill bit diameter of 11.625.”

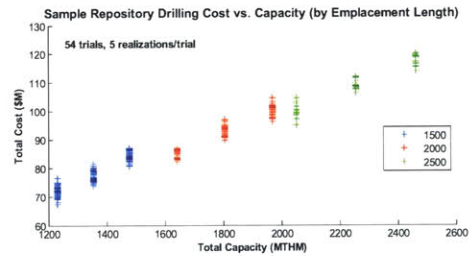
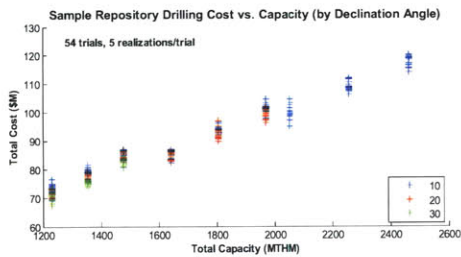
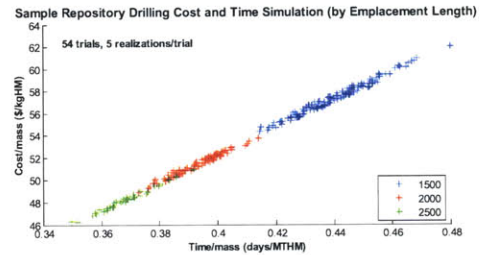
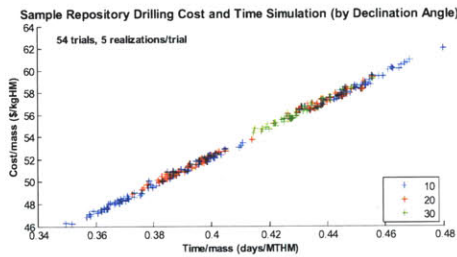


Figure 2-22: 2nd Winnowed Trade-space by Declination Angle (°)

Figure 2-23: 2nd Winnowed Trade-space by Emplacement Length (m)

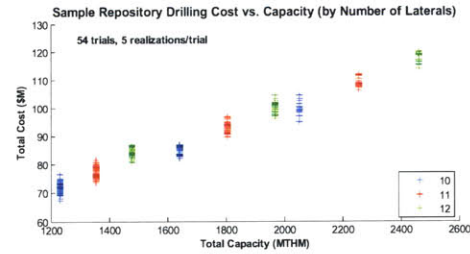
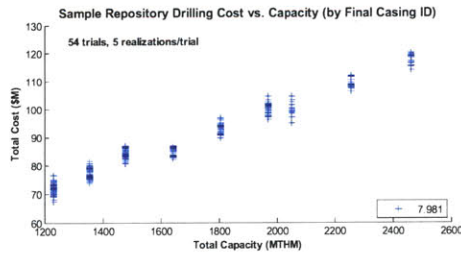
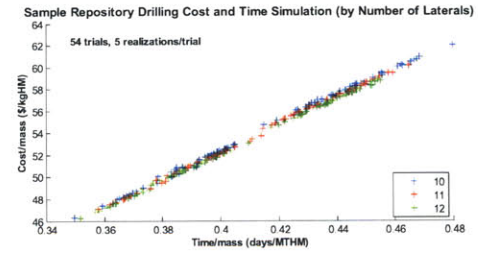
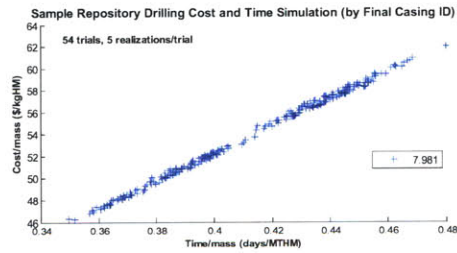


Figure 2-24: 2nd Winnowed Trade-space by Lateral Diameter (in)

Figure 2-25: 2nd Winnowed Trade-space by Number of Laterals

2.6.5 Final Repository Configuration and Results

Having almost completely refined the trade-space, the final repository design was selected (not necessarily as the most cost-optimal of the remaining choices):

- Ten 2000-m emplacement laterals from a single vertical shaft at a declination of 20 degrees
- Pipe Schedule: 26", 17 1/2", 11 5/8"

A sample time history for this configuration is shown below in Figure 2-26:

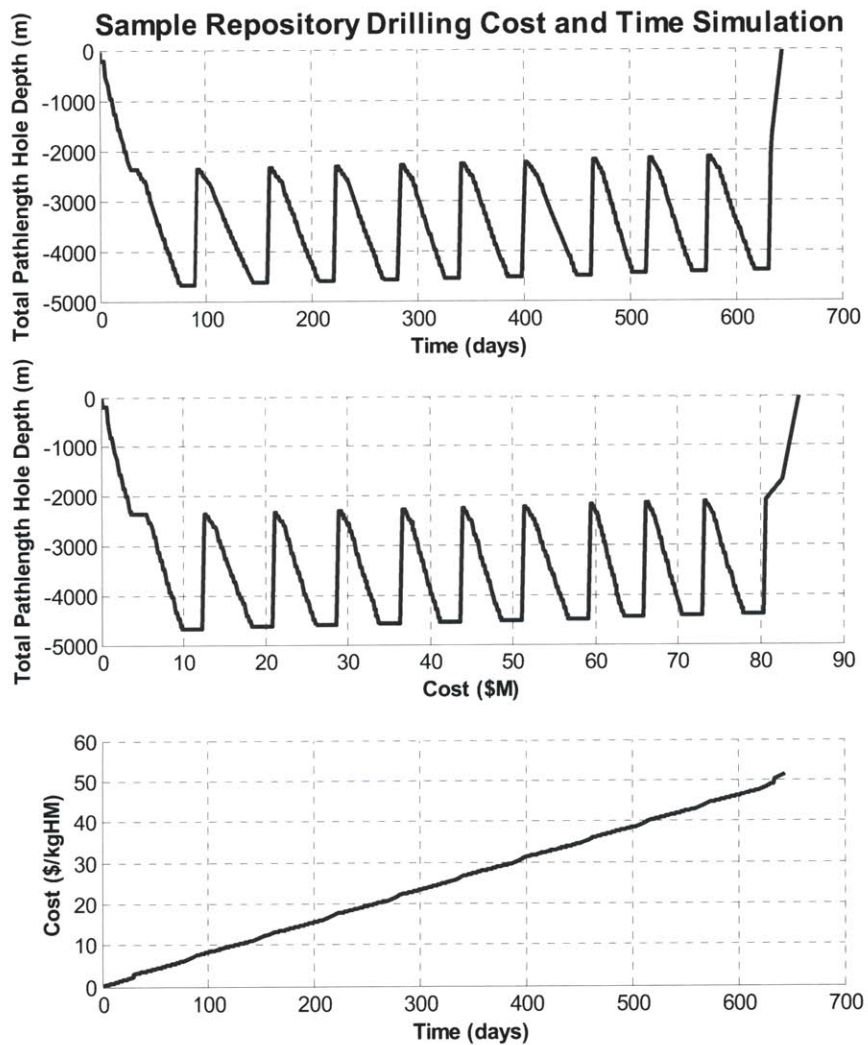
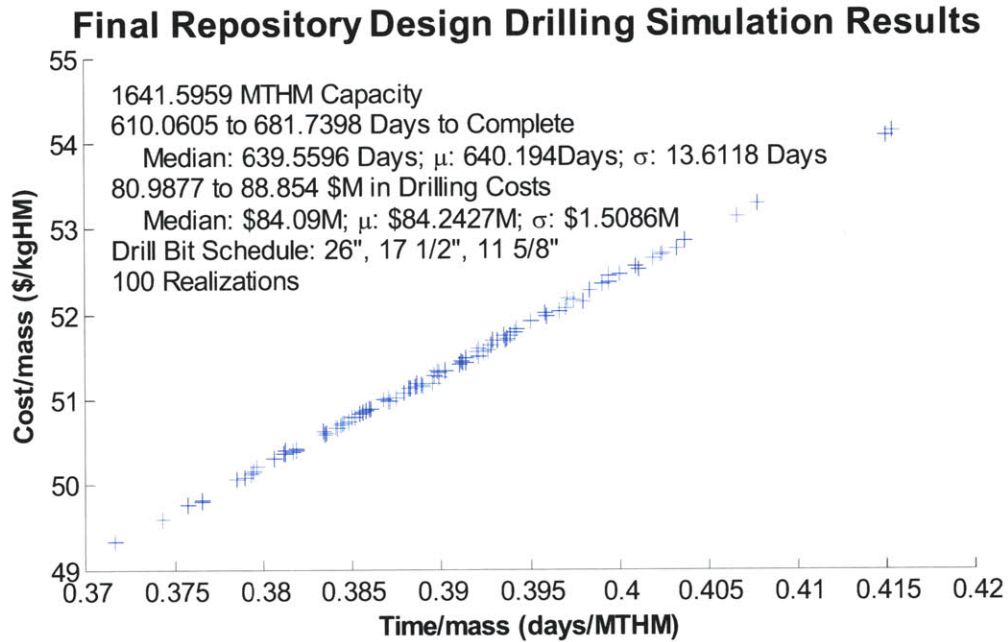


Figure 2-26: Sample Realization of Final Repository Design

Figure 2-27 displays 100 realizations of the Final Repository Design. As shown, total repository cost is \$80-90 Million and the total time to drill, fill, and close each vertical repository shaft varies between approximately 610 and 680 days.



The following Figures depict potential geometric arrangements of the borehole design (radial versus bidirectional shafts).

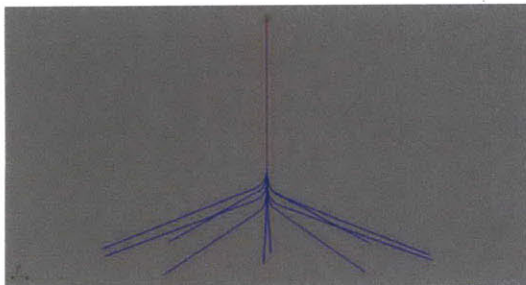


Figure 2-28: 3-D Representation of Multidirectional Borehole Configuration

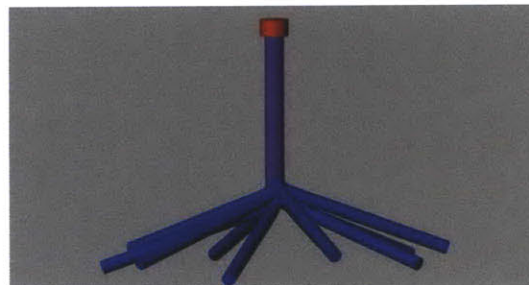


Figure 2-29: 3-D Representation of Multidirectional Borehole Configuration (Hole Diameters x500 for Visualization)

A multidirectional radial configuration such as is shown in Figure 2-28 and Figure 2-29 would be desirable to maximize the spacing between laterals should a single vertical shaft be needed (such as for small regional repositories). While directional drilling and vertical staggering techniques could well accommodate a closely packed array of such

multidirectional boreholes, it is significantly more difficult than accommodating bidirectional-configured boreholes.

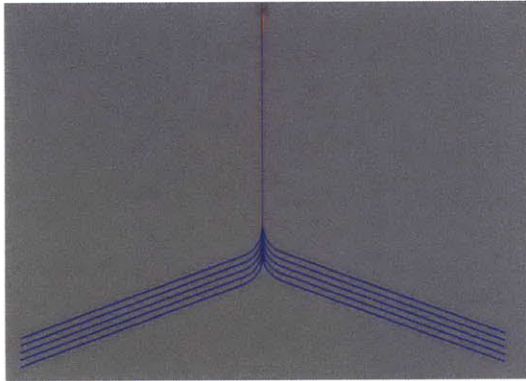


Figure 2-30: 2-D Representation of Bidirectional Borehole Configuration

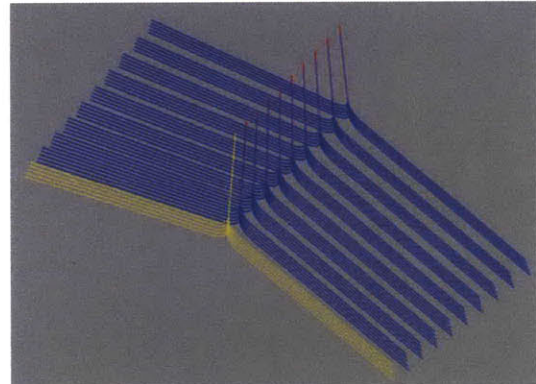


Figure 2-31: 3-D Representation of Multiple Bidirectional Boreholes

Figure 2-30 and Figure 2-31 show how a close array of boreholes can be accommodated using 200 meter spacing between adjacent sets of laterals.

2.7 Model Sensitivity Analyses and Curve Fit of Results

In evaluating the robustness of the V-DeepBoRe model, it is helpful to identify those input parameters which most heavily impact the resulting completion cost and time for the repository. Figure 2-32 through Figure 2-37 show how the selected repository unit costs and time vary with the length of the borehole plug, cost of cement, overall billing rate, cost of the borehole plug, vitrified waste fraction, and material costs of the liners. In each case, 100 realizations of each scenario are plotted for comparison purposes.

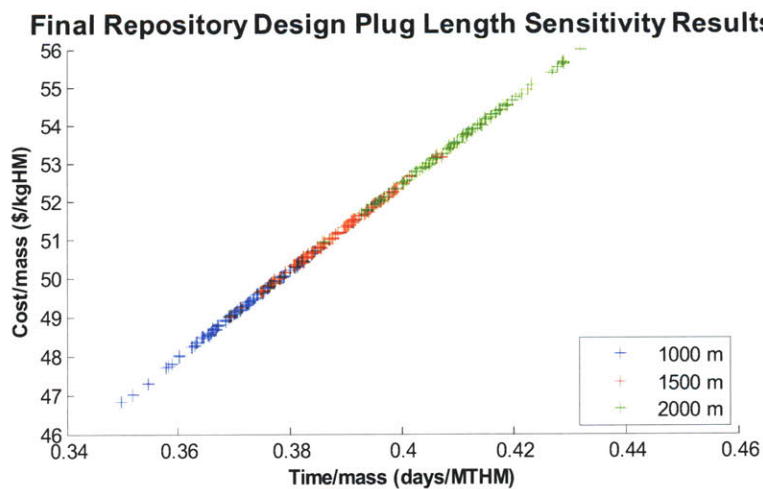


Figure 2-32: Emplacement Length Sensitivity Analysis

Final Repository Design Cement Cost Sensitivity Results

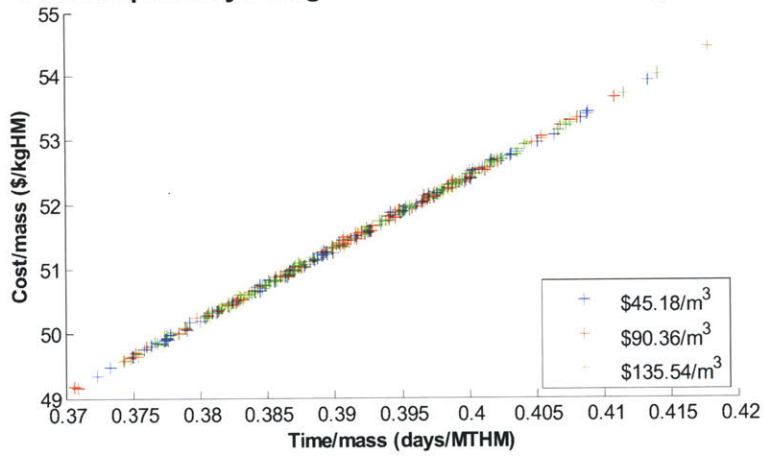


Figure 2-33: Cement Cost Sensitivity Analysis

Final Repository Design Billing Rate Sensitivity Results

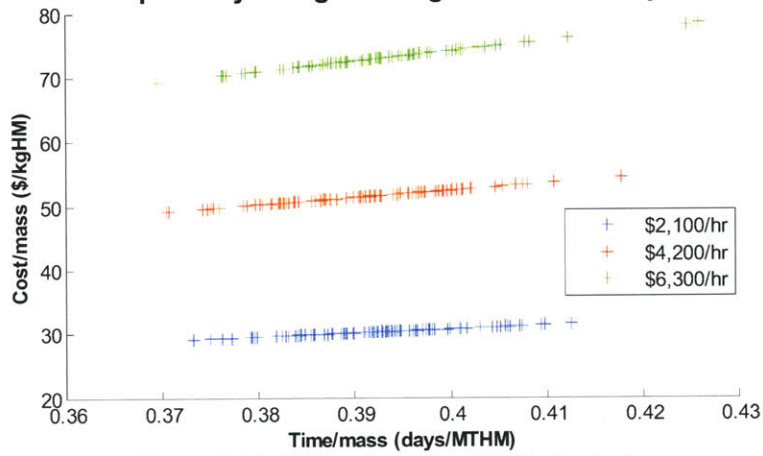


Figure 2-34: Billing Rate Sensitivity Analysis

Final Repository Design Plug Cost Sensitivity Results

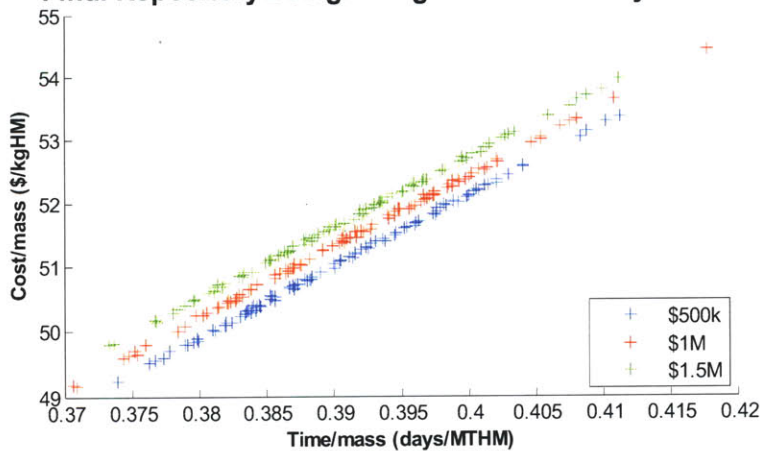


Figure 2-35: Plug Cost Sensitivity Analysis

Final Repository Design Vitrified Waste Fraction Sensitivity Results

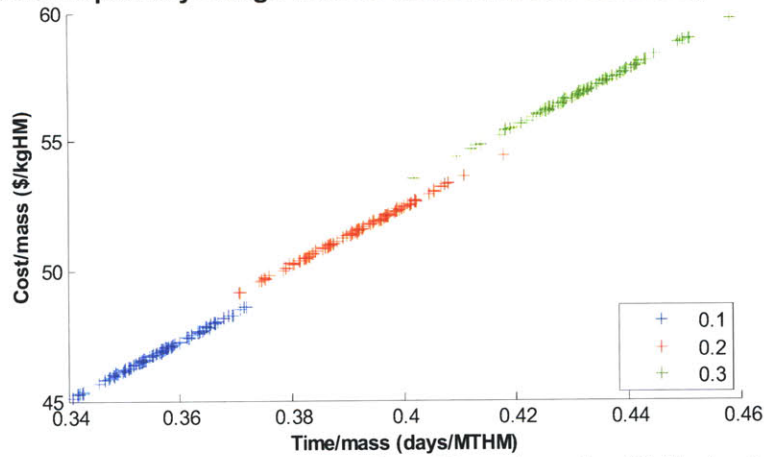


Figure 2-36: Vitrified Waste Fraction of Repository Sensitivity Analysis

Final Repository Design Casing Cost Sensitivity Results

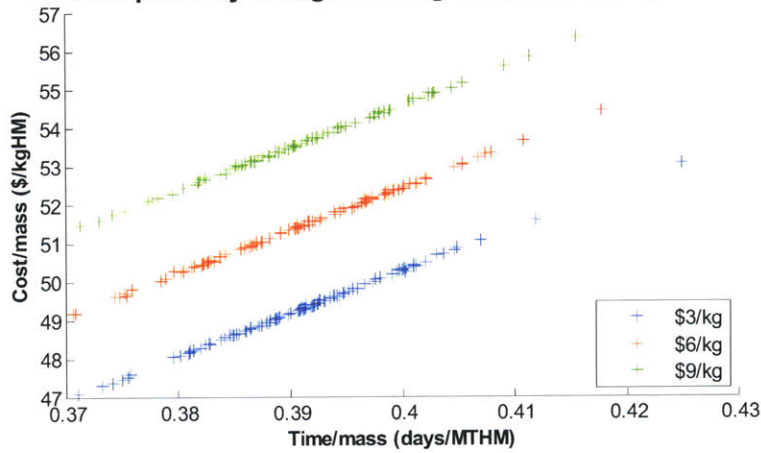


Figure 2-37: Casing Cost Sensitivity Analysis

From these sensitivity runs, a stochastic model for the repository time and total cost is based on these 6 input parameters. Figure 2-38 through Figure 2-40 graphically plot the impact of each parameter on the overall repository completion time and effective cost rate.

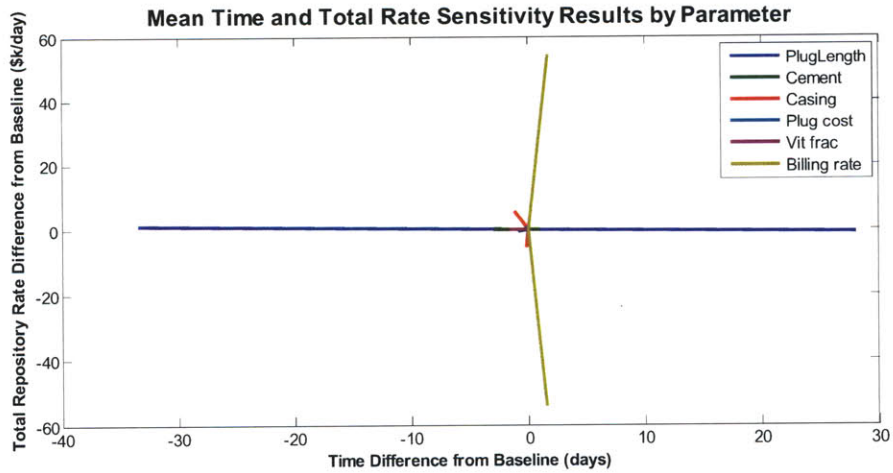


Figure 2-38: Sensitivity Results for Repository Mean Completion Time and Rate

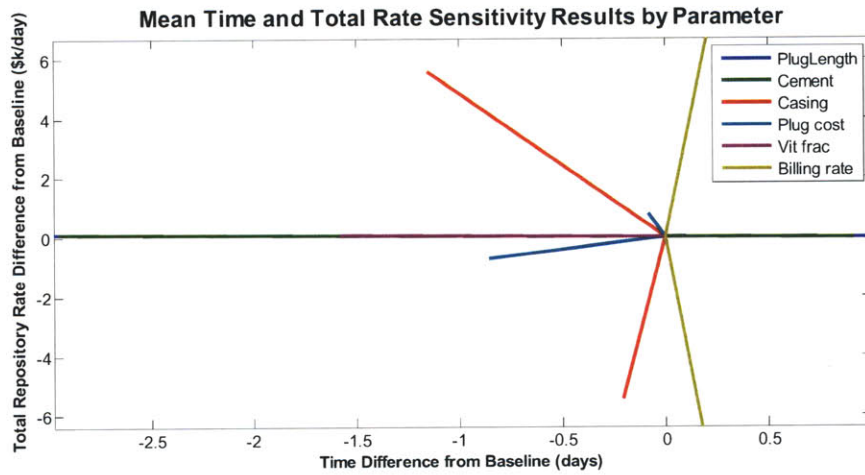


Figure 2-39: Sensitivity Results for Repository Mean Completion Time and Rate (Expanded)

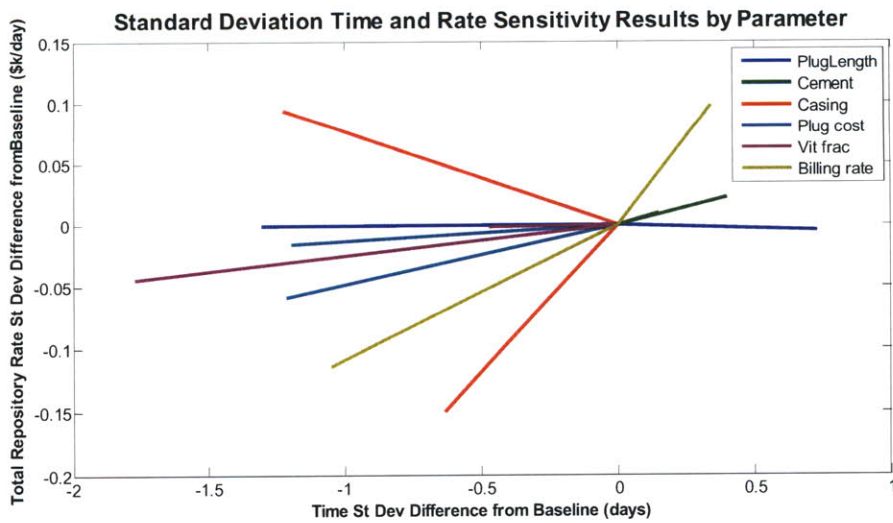


Figure 2-40: Sensitivity Results for Repository Standard Deviation of Completion Time and Rate

The major and minor factors are summarized in Table 2-9.

Table 2-9: Impact of Key Parameters on Repository Statistics

	Mean		Stdev		Repository
	Rate	Time	Rate	Time	Capacity
Plug Length		Major		Major	
Cement	Statistically Insignificant				
Casing	Minor		Minor		
Plug Cost	Minor				
Vit Frac					Major
Billing Rate	Major		Major		

Having identified the major contributions of each parameter, a linear regression is performed for each effect. The regression model values are shown in Table 2-10.

Table 2-10: Model Values for Linear Fit for Repository Statistics Based on Key Parameters

Input	Slope	Intercept	Output
Vit Frac	-1.8965E+03	2.2646E+03	repository size (MTHM)
Casing Cost	1.8415E+00	1.0237E+01	mean rate (\$k/Day)
Plug Cost	1.5292E+00		
Billing Rate	2.5889E-02		
Plug Length	6.1418E-02	5.4810E+02	mean time (Days)
Casing Cost	4.0748E-02	4.0387E-03	stdev rate (\$k/Day)
Billing Rate	5.0635E-05		
Plug Length	2.0355E-03	1.1773E+01	stdev time (Days)

Equations [2-1] through [2-5] summarize these linear relations

$$S_r = (f_{vit}) \cdot (-1896.5) + 2264.6 \quad [2-1]$$

$$\mu_{rate} = [C_{casing} \cdot 1.8415 + C_{plug} \cdot 1.5292 + R_{bill} \cdot 2.5889 \cdot 10^{-2} + 10.237] \cdot 10^3 \quad [2-2]$$

$$\mu_{time} = L_{plug} \cdot 6.1218 \cdot 10^{-2} + 548.171 \quad [2-3]$$

$$\sigma_{rate} = [C_{casing} \cdot 4.0748 \cdot 10^{-2} + R_{bill} \cdot 5.0635 \cdot 10^{-5} + 4.0387 \cdot 10^{-3}] \cdot 10^3 \quad [2-4]$$

$$\sigma_{time} = L_{plug} \cdot 2.0355 \cdot 10^{-3} + 11.773 \quad [2-5]$$

Where

- S_r \equiv Total Capacity of Repository (MTHM)
- f_{vit} \equiv Fraction of Repository Canisters that are vitrified waste
- μ_{rate} \equiv Mean Repository Cost Rate (\$/Day)
- c_{casing} \equiv Specific Casing Cost (\$/kg)
- C_{plug} \equiv Total Plug Cost (\$M)
- R_{bill} \equiv Overall Repository Billing Rate (\$/hr)
- μ_{time} \equiv Mean Repository Completion Time (Days)
- L_{plug} \equiv Vertical Plug Length (m)
- σ_{rate} \equiv Standard Deviation of Repository Cost Rate (\$/Day)
- σ_{time} \equiv Standard Deviation of Repository Completion Time (Days)

Note that equation [2-1] reflects the additional waste mass in the repository associated with consolidating 301 PWR and 211 BWR fuel pins into a canister (as opposed to the 271 and 175, respectively, calculated based on strictly hexagonal packing as is assumed in the drilling script).

2.8 Drilling Cost Model and Repository Configuration Summary

The V-DeepBoRe model demonstrates the economical feasibility of using lateral emplacement of high level nuclear waste in very deep boreholes. Drilling, emplacement, and sealing costs for the borehole are estimated at less than \$48/kg of heavy metal. The model is extremely sensitive to the overall billing rate of drilling operations and, to a lesser extent, to the cost of the drill casing. Additional data are required to further refine and validate the model and verify the modeling assumptions used.

Study of the trade-space of repository configurations produced a final repository design featuring a telescoping pipe-schedule of 26", 17 1/2", and 11 5/8" diameters, lateral emplacement lengths of 2 km, angled 20° declined from horizontal, and 10 laterals per vertical borehole. With the repository geometry so prescribed, design of the waste package could then proceed.

3 WASTE PACKAGE DESIGN AND ANALYSIS

Having completed the design of the repository, a waste canister design is developed given the geometric constraints of the selected lateral. This chapter will detail the package design selection, the expected thermal performance of the loaded waste canisters once emplaced in the repository, and the mechanical performance of the waste canister under repository conditions.

3.1 Waste Package Design

The final waste canister design selection is summarized in Table 3-1. This waste package accommodates vitrified waste (i.e. borosilicate glass waste-form) as well as reconstituted Light Water Reactor (LWR) fuel pins that have been removed from their assemblies to be consolidated and compacted in a close-packed arrangement.

Table 3-1: Summary of Canister Design

Canister Properties		
	Metric	English
Canister Material	P-110 Casing Steel	
Minimum Tensile Strength	861.84 MPa	125000 psi
Canister Inner Diameter	180.98 mm	7 1/8 in
Canister Outer Diameter	195.26 mm	7 11/16 in
Canister Length	5000.00 mm	196.85 in
Interior Volume	128616.61 cm ³	7848.67 in ³
Steel Mass	169.11 kg	372.82 lbm
PWR Waste Canister Properties		
	Metric	English
Fill Volume PWR	38639.83 cm ³	2357.95 in ³
Fill Mass PWR (SiC)	77.86 kg	171.65 lbm
Waste Mass PWR	729.07 kg	1607.32 lbm
Heavy Metal Mass PWR	568.59 kg	1253.53 lbm
Total PWR Canister Mass	976.04 kg	2151.79 lbm
BWR Waste Canister Properties		
	Metric	English
Fill Volume BWR	46035.89 cm ³	2809.28 in ³
Fill Mass BWR (SiC)	92.76 kg	204.51 lbm
Waste Mass BWR	711.15 kg	1567.81 lbm
Heavy Metal Mass BWR	561.79 kg	1238.53 lbm
Total BWR Canister Mass	973.02 kg	2145.14 lbm

The canister material of P-110 drill string steel ensures adequate tensile strength for the waste string as it is lowered into the borehole. The choice for fill material of SiC

particles is expected to enhance hydrostatic crushing resistance while permitting adequate conduction of decay heat outward from the package while only moderately contributing to the overall mass of the package. Other potential fill materials such as SiO₂ (silica sand) or crushed granite should provide similar crushing resistance and adequate conduction of heat from the waste to the borehole wall at moderately reduced cost, but have not been analyzed in this project. The final canister inner diameter permits the encapsulation of 301 PWR spent fuel pins or 211 BWR spent fuel pins; this exceeds the initial estimate used in the waste-mass subroutine of the V-DeepBoRe model from Chapter 2 (from purely hexagonal packing) of 271 PWR pins and 176 BWR pins. Figure 3-1 and Figure 3-2 show the cross-sectional arrangement of the PWR pins and BWR pins respectively.

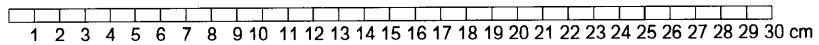
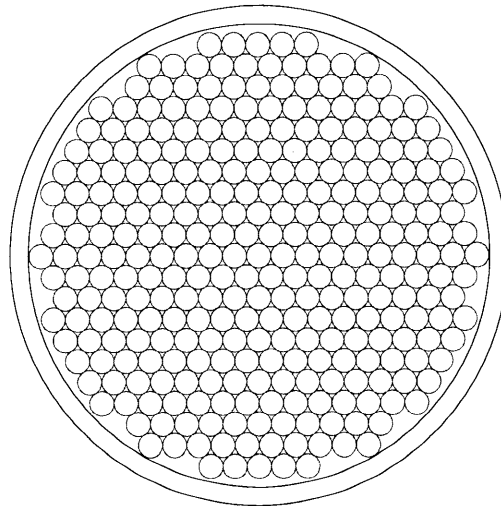


Figure 3-1: Canister Arrangement- 301 PWR Fuel Pins

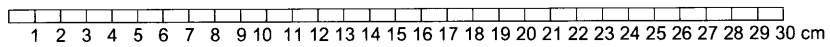
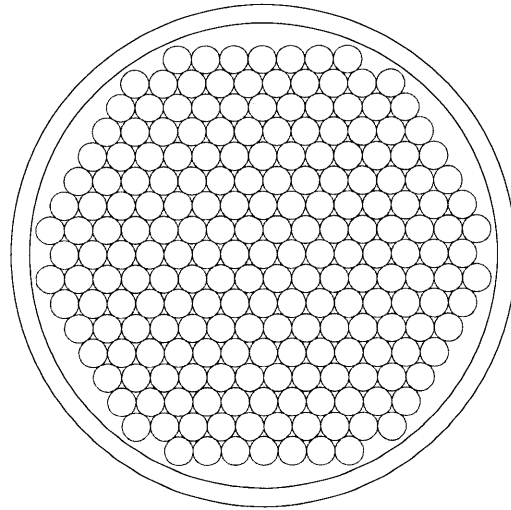


Figure 3-2: Canister Arrangement- 211 BWR Fuel Pins

Figure 3-3 illustrates the waste package and liner as configured in the lined lateral. The two gaps in this diagram will be analyzed for both a vacuum (conservatively assuming radiation only between the rock wall and the liner and between the liner and the waste package) and a water-flooded (assuming conduction only in water between the rock wall and the liner and between the liner and the waste package) thermal case study.

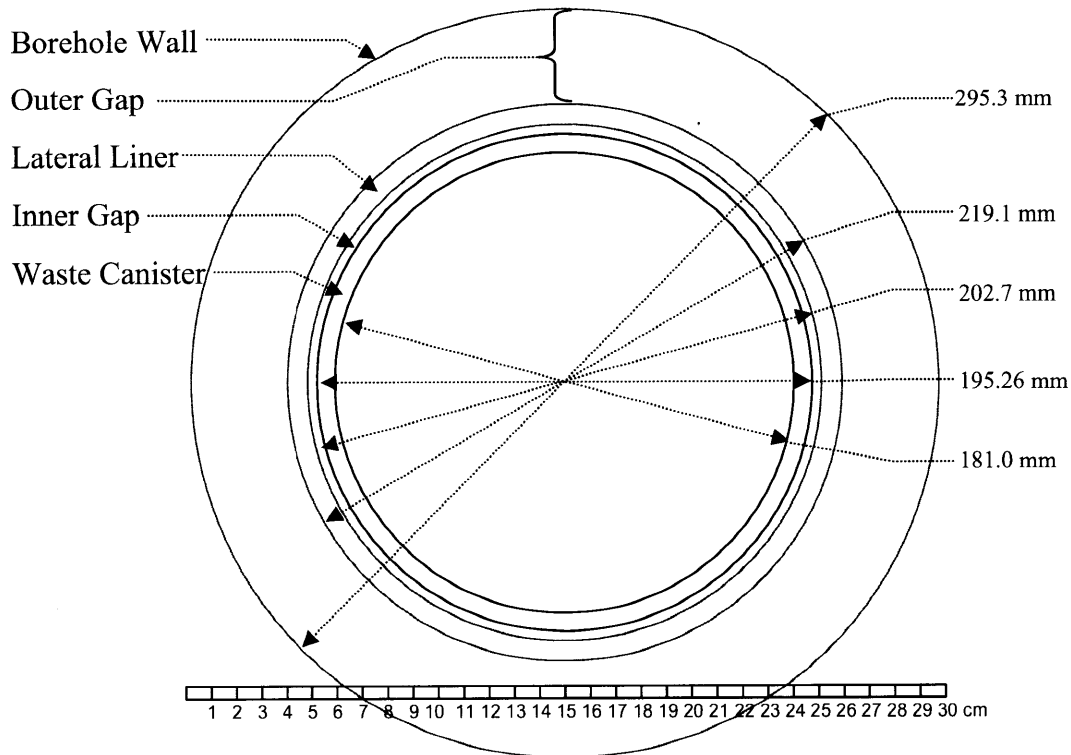


Figure 3-3: Canister and Liner Cross Sections

3.2 Thermal Analysis of Waste Package

The thermal performance assessment of the canister design is conducted in three separate analyses. In the most basic of these, the lateral of waste is modeled as an infinite line source in an infinite, homogenous granite slab. This reduces to a one-dimensional problem where temperature varies with time and distance from the line source only. A more refined model is the two-dimensional heating of an adiabatically bounded finite cell surrounding the lateral in the repository (this will account for the influence of neighboring laterals). Further refined still is a three-dimensional analysis using a scaled model of the laterals in the repository and the application of fixed temperature boundary conditions replicating the thermal gradient in the earth's crust (accounting for the diffusion of heat vertically which is not modeled in the two-dimensional study). All three of these analyses demonstrate the feasibility of the canister design selected.

3.2.1 Thermal Study Assumptions

Table 3-2 calls out the thermal properties and parameters used in the waste package performance analysis. The waste package, as modeled in these analyses is assumed to remain concentrically centered within the lateral, as is the liner, despite the inclination of the lateral 70° from vertical. Further, convection is conservatively ignored as is conduction through air for the case of a non-flooded borehole. Further conservatism is achieved by modeling the 2000m lateral string of waste packages with the same linear power as the fueled regions of the canister. This is to say that while only 82% or 84% of the canister length is generating heat, the entire 5 meter length is assumed to be fueled. Also, to observe the worst case thermal power for a given package, it is assumed that there are no material defects or irregularities in the fuel pins that would prevent full compacting to 301 PWR and 211 BWR pins per canister. As fuel pin packages are anticipated to present a higher thermal load than vitrified wastes, the entire repository is assumed to contain LWR fuel packages only.

Table 3-2: Summary of Thermal Design Study Properties and Parameters

Granite Material Properties		Ref
Thermal Conductivity, k	2.2 W/m·K	41
Density, ρ	2500 kg/m ³	42
Emissivity, ϵ	0.45	43
Specific Heat Capacity, C_p	790 J/kg·K	44

Repository Properties		Ref
Surface Temperature	25 °C	
Subterranean Thermal Gradient	24 °C/km	45
Cooling Time Before Emplacement, t_c	40 years	
Irradiation Time (for ANS Std Decay Heat), τ_s	3.53 years	
Lateral Radius, r	0.14764 m	
BWR Fueled Length	4.1 m	
PWR Fueled Length	4.2 m	
Borehole Shaft Spacing (Pitch)	200 m	
Borehole Shaft Spacing (Back Pitch)	5 km	

Table 3-2: Summary of Thermal Design Study Properties and Parameters (Continued)

Canister, Waste, and Fill Thermal Properties		Ref
Steel Thermal Conductivity, k	50.2 W/m·K	46
Steel (Oxidized) Emissivity, ε	0.79	47
SiC Carbon Bed Volumetric Packing Factor	0.65	48
SiC Particle Density, ρ	3100 kg/m ³	49
SiC Bed Thermal Conductivity, k	0.33 W/m·K	50
PWR & BWR Fuel Pin Thermal Conductivity, k _{eff}	1.87 W/m·K	51

For simplicity, the PWR effective thermal conductivity calculation performed by Hoag (2006) is applied to the BWR fuel pins, despite minor distinctions in geometry. In each of the long term thermal studies, the waste package is assumed to be in quasi-steady state while transient conditions may exist in the surrounding granite. This is justified by the relatively low thermal capacity of the waste package with respect to the surrounding granitic rock.

3.2.2 Effective Conduction Coefficient of Reconstituted Waste

As a survey of the literature did not identify any relations for the effective conductivity of close packed arrays of spent fuel pins in a matrix, an effective homogenization of the fuel pin and fill interior of the waste package is developed using finite element analysis with the *Solidworks Simulation* code (assuming conduction only and no contact resistance between fill and fuel). The effective homogenized conduction coefficient, $k_{hom\ eff}$, is calculated using Equation [3-1]⁵²:

$$k_{hom\ eff} = \frac{q'}{4\pi} (T_{CL} - T_{Edge})^{-1} \quad [3-1]$$

Where $q' \equiv$ Linear Thermal Power Modeled in the Study
 $T_{Edge} \equiv$ Boundary Condition Fixed Temperature
 $T_{CL} \equiv$ Canister Centerline Temperature Produced in the Study

The thermal power and boundary temperature may be chosen arbitrarily as the material properties used in the study are taken to be constant as a function of the temperature of the material, and the T_{CL} observed will vary accordingly. For both the PWR and BWR canister configurations, a 30° section of the canister, 5 cm in thickness, is modeled. An appropriate linear power q' is applied and a fixed edge temperature of 150 °C is applied.

Figure 3-4 and Figure 3-5 show the temperature profiles of the 30° wedge for each of the PWR canister and BWR canister as modeled in *Solidworks*.

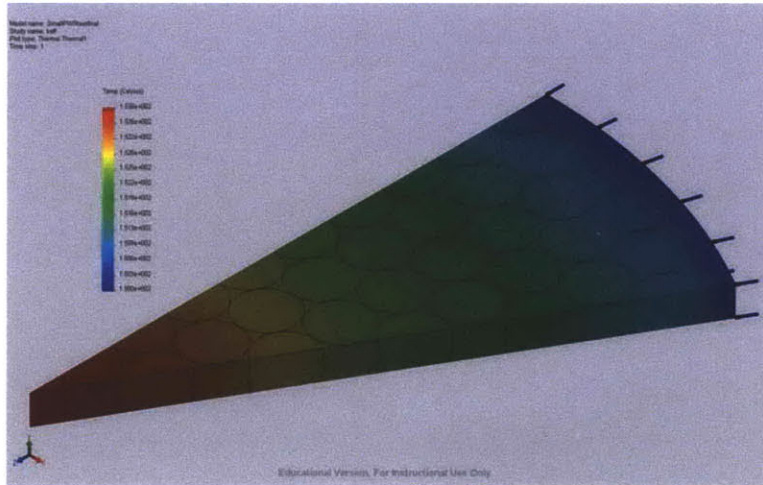


Figure 3-4: Effective Heat Transfer Coefficient Analysis (PWR Waste Package)

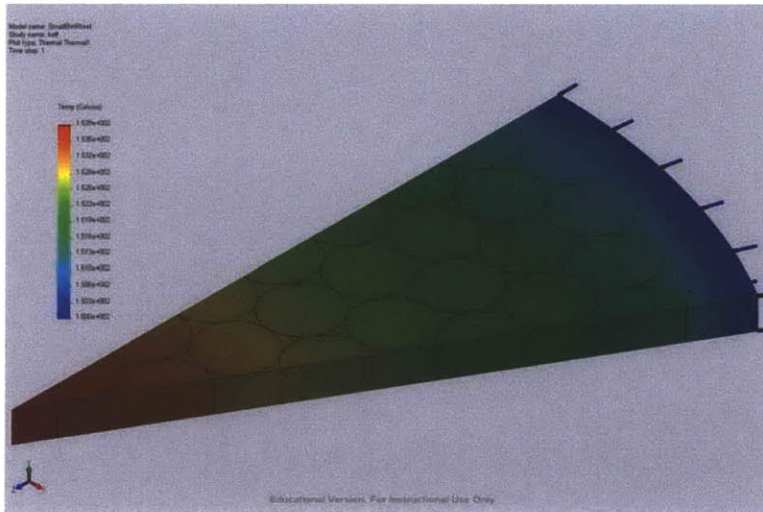


Figure 3-5: Effective Heat Transfer Coefficient Analysis (BWR Waste Package)

Table 3-3 summarizes the results from the effective homogenized conduction coefficient studies: the $k_{hom\ eff}$ is highlighted in green.

Table 3-3: Effective Heat Transfer Coefficient Analysis Results

	Angle Modeled (°)	k_{pin} W/(m·K)	k_{fill} W/(m·K)	Power in Wedge (W)	Thickness (m)	B.C. Temp (C)	Peak CL Temp (C)	k_{eff} W/(m·K)	Canister Inner Radius (m)	No. Pins	Metal Area Ratio
PWR Waste	30	1.87	0.33	0.015587917	0.005	150	153.794	0.7847	0.0904875	301	82.94%
BWR Waste	30	1.87	0.33	0.01297375	0.005	150	153.853	0.6431	0.0904875	211	77.95%

The resulting values of 0.7847 W/m·K and 0.6431 W/m·K for the PWR and BWR packages, respectively, are used in the thermal conduction analysis for the rest of this section.

3.2.2 Package Thermal Power

In order to model the long term temperatures in the waste package and in the repository, an appropriate model must be employed for the decay power of the entombed waste.

Equation [3-2] shows the ANS Standard Decay Power (times in seconds)⁵³

$$\frac{Q(t_e)}{Q_0} = 0.066 \left[(t_e + t_c)^{-0.2} - (t_e + t_c + \tau_s)^{-0.2} \right] \quad [3-2]$$

Where: $t_e \equiv$ Time Since Emplacement (sec)

$t_c \equiv$ Cooling Time Between Irradiation and Emplacement (sec)

$\tau_s \equiv$ Total Time of Irradiation (sec)

$Q(t_e) \equiv$ Decay Power at Time t_e (W)

$Q_0 \equiv$ Thermal Power of Fuel During Irradiation (W)

While this empirical correlation is appropriate for time scales of up to 10^9 seconds (~32 years), the long term performance of the repository will require an empirical form that is applicable for several thousand years. Malbrain, Lester, and Deutch develop the thermal power of spent Light Water Reactor fuel in Equation [3-3]⁵⁴

$$q(t_e) = \begin{cases} C_1 \cdot e^{\frac{1}{[C_2 + C_3 \cdot (t_e + t_c)]}} & \text{for } t_e + t_c < 30 \text{ years} \\ D_1 \cdot (t_e + t_c)^{-\beta} & \text{for } 30 \text{ years} \leq t_e + t_c < 100,000 \text{ years} \end{cases} \quad [3-3]$$

Where: $q(t_e) \equiv$ Decay Power (W/MTHM)

$t_e \equiv$ Time Since Emplacement (years)

$t_c \equiv$ Cooling Time Between Irradiation and Emplacement (years)

$C_1 \equiv 550$

$C_2 \equiv 0.223$

$C_3 \equiv 0.117$

$D_1 \equiv 9.41 \cdot 10^3$

$\beta \equiv 0.749$

Figure 3-6 graphically depicts the decay power variation between these two empirical relations. Note that the duration of irradiation for the ANS Standard Decay Heat relation was adjusted to 3.53 years in order that the two relations have equivalent initial decay powers. Additional decay power calculations are shown in the Appendices in section B.1.

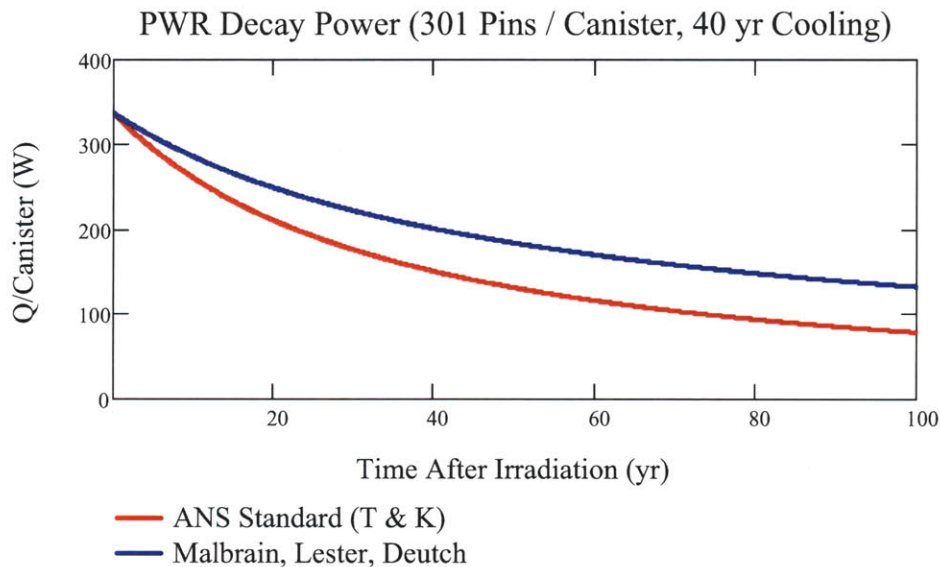


Figure 3-6: Comparison of Decay Power Empirical Relations

From a desire to conservatively estimate the decay power of the waste package and to ensure the long-term accuracy of the analyses, decay power based on Equation [3-3] is used for the remaining studies with the following modification: Malbrain, Lester, and Deutch assume a burnup of 33,000 GWd/MTHM for their light water reactor fuel. To better reflect the higher burnup of current LWR fuel discharges, the decay power is scaled up linearly with the burnup, assuming a 57,000 GWd/MTHM irradiation for the repository fuel. This decay power relation is very similar to one used in a recent thermal FEA at Hongik University in South Korea⁵⁵. Figure 3-7 depicts the decay heat power of the reconstituted PWR and BWR waste packages (of 301 and 211 pins respectively). While nearly identical in loading, the PWR package produces a slightly higher thermal power, as later analyses will underscore.

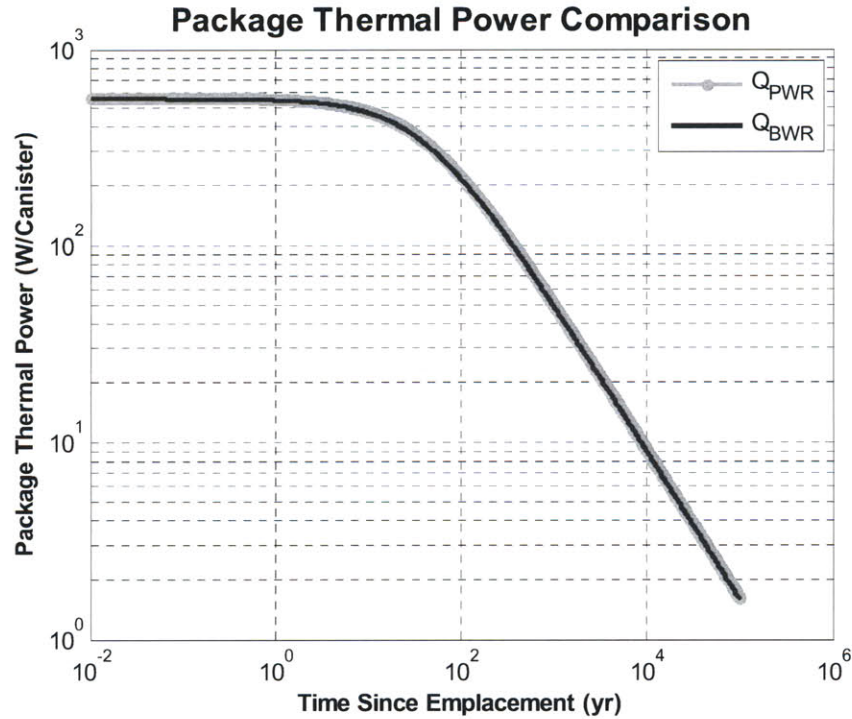


Figure 3-7: Package Decay Power (M, L, & D Correlation)

3.2.3 1-D Infinite Medium Temperature Analysis

The first thermal analysis performed was for a simple one-dimensional problem. The general solution for the radial temperature profile resulting from an infinite line source in an infinite, homogeneous medium is given in Equation [3-4]⁵⁶

$$T(r,t) = T_0 + \int_0^t \frac{q'(\tau) e^{-\frac{r^2}{4\alpha(t-\tau)}}}{4\pi \cdot k \cdot (t-\tau)} d\tau \quad [3-4]$$

Where : $T(r,t) \equiv$ Temperature

$T_0 \equiv$ Initial (Uniform) Temperature

$t \equiv$ Time (sec)

$r \equiv$ Distance from Line Source (m)

$q' \equiv$ Linear Thermal Power (W/m)

$k \equiv$ Thermal Conductivity of Medium (W/m \cdot °C)

$\alpha \equiv$ Thermal Diffusivity of Medium (m²/sec)

$$= \frac{k}{\rho \cdot C_p}$$

$\tau \equiv$ Dummy Integration Variable

While this integral may be calculated numerically, it is appropriate to check the results from computer tools using a simplified calculation. By assuming that the linear power is of the form

$$q'(t) = q'_0 \frac{t_c}{t_c + t} \quad [3-5]$$

Where: $t \equiv$ Time After Emplacement (sec)

$t_c \equiv$ Cooling Time Between Irradiation and Emplacement (sec)

$q'_0 \equiv$ Initial Linear Thermal Power (W/m)

the integral form simplifies to:

$$T(r,t) = T_0 + \frac{q'_0}{4\pi \cdot k} \frac{t_c}{t_c + t} \left[\ln\left(\frac{4\alpha \cdot t}{r^2}\right) - 0.5772 \right] \quad \text{for } \frac{r^2}{4\alpha \cdot t} \ll 1 \text{ and } t \ll t_c \quad [3-6]$$

A comparison of the results of Equation [3-6] and the numerical integration using the source from [3-3] are shown in Figure 3-8 (this case is for the PWR consolidated waste package linear decay power). Even with moderately different forms of the source term, the approximation to the integral solution validates the numerical integration and generates peak times within a few years and the peak temperatures within a few degrees Celsius of the integral method.

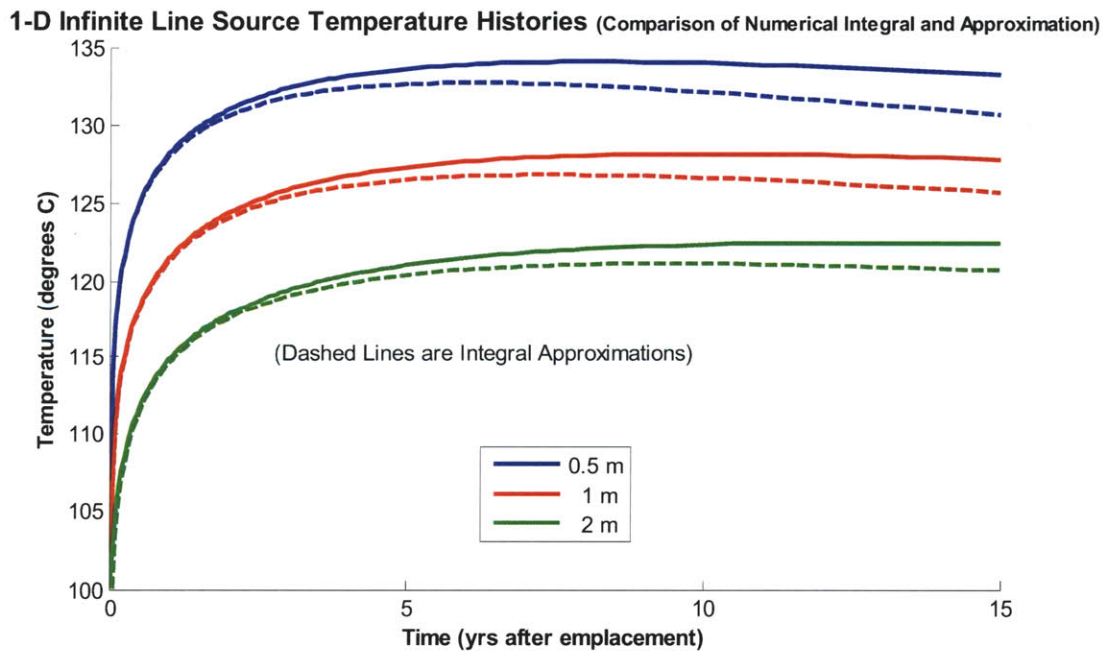


Figure 3-8: Comparison of 1-D Integral Solution and Approximation

The temperature for steady state conduction in cylindrical coordinates is shown in Equation [3-7]⁵⁷

$$T_{inner} = T_{outer} + q' \cdot R_{cond} = T_{outer} + \frac{q' \cdot \ln\left(\frac{r_{outer}}{r_{inner}}\right)}{2\pi \cdot k} \quad [3-7]$$

Where: T_{inner} \equiv Temperature on Inner Surface

T_{outer} \equiv Temperature on Outer Surface

q' \equiv Linear Thermal Power (W/m)

R_{cond} \equiv Conductive Thermal Resistance (m · K/W)

k \equiv Thermal Conductivity of Medium (W/m · K)

r_{inner} \equiv Inner Surface Radius

r_{outer} \equiv Outer Surface Radius

Radiation in a vacuum in cylindrical coordinates is shown in Equation [3-8]⁵⁸

$$h_{rad} = \frac{\sigma}{\frac{1}{\epsilon_{inner}} + \left(\frac{r_{inner}}{r_{outer}}\right)\left(\frac{1}{\epsilon_{outer}} - 1\right)} \left(\frac{T_{inner}^4 - T_{outer}^4}{T_{inner} - T_{outer}}\right) \quad [3-8]$$

Where: h_{rad} \equiv Heat Transfer Coefficient of Medium (W/m² · K)

σ \equiv Stefan – Boltzmann Constant $\left(5.6704 \cdot 10^{-8} \frac{W}{m^2 K^4}\right)$

ϵ_{inner} \equiv Emissivity of Inner Surface

ϵ_{outer} \equiv Emissivity of Outer Surface

And therefore, the effective conductive coefficient may be found using Equation [3-9]:

$$k_{rad\ eff} = h_{rad} \cdot r_{inner} \cdot \ln\left(\frac{r_{outer}}{r_{inner}}\right) \quad [3-9]$$

Where: $k_{rad\ eff}$ \equiv Effective Conductive Coefficient for Radiation (W/m · K)

In evaluating the peak centerline temperature of the waste package, an appropriate thermal limit is needed. Manteufel (1994)⁵⁹ suggests using the transportation canister peak fuel centerline thermal limit of 380 °C. This limit appears on the temperature history plots of this chapter as a heavy red dashed line.

The one-dimensional analysis begins by solving [3-3] (assuming an ambient granite temperature of 100.15 °C at a depth of 3007m) for the temperature history at a set of distances from the line source (to include the borehole wall at a radius of 0.14764m). Using the temperature history at 1 meter from the line source, a thermal circuit for each material is evaluated to calculate the temperature at progressively smaller radii, until the centerline temperature of the package is developed. The 1 meter boundary condition is used as this is sufficiently distant from the borehole (radius of 0.148 m) that approximating the package thermal power as a concentrated line source and neglecting the thermal capacity difference between the canister and the surrounding granite are accurate modeling assumptions.

3.2.3.1 PWR Canister Temperature Analysis Results

Figure 3-9 shows the resulting rock temperature profiles at several distances from the lateral centerline.

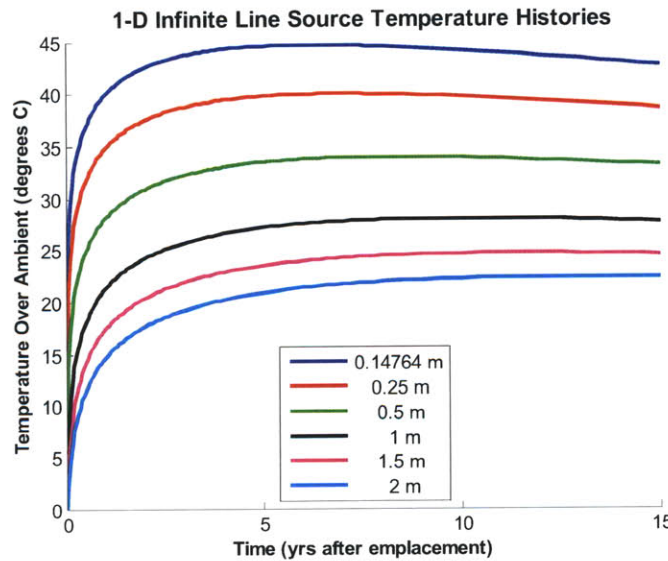


Figure 3-9: Rock Temperature Profiles (PWR Infinite Line Source)

Figure 3-10 and Figure 3-11 show the resulting temperatures of the surfaces of the waste package under the conditions of vacuum gaps and gaps flooded with water, respectively. In the water flooded gaps, convective effects are conservatively neglected and water conductivity is modeled as 0.606 W/m·K.

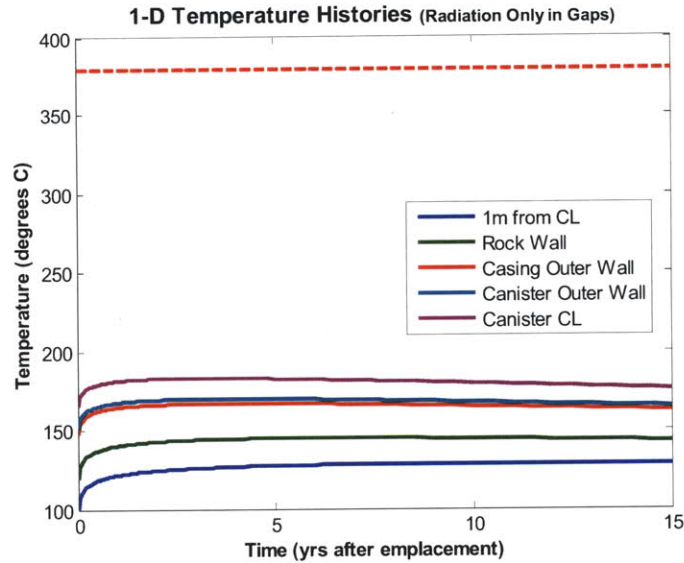


Figure 3-10: PWR Canister Thermal Histories (Radiation Only in Gaps)

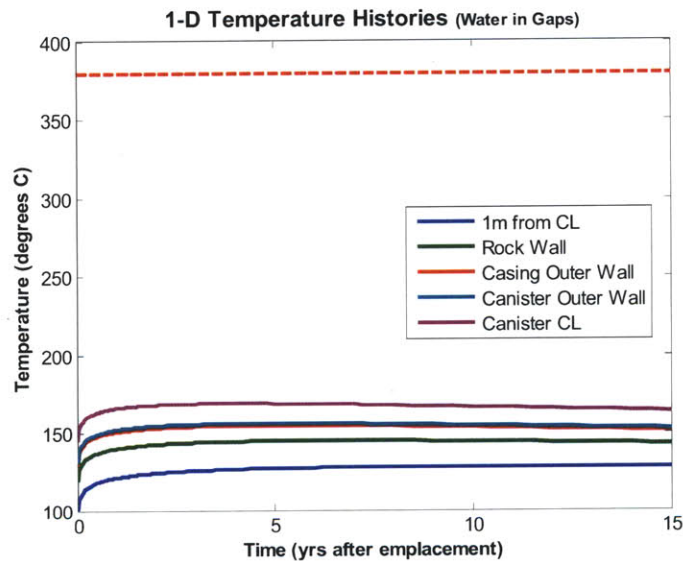


Figure 3-11: PWR Canister Thermal Histories (Water Conduction in Gaps)

The analyses predict a peak PWR centerline temperature of 182.98 °C at 3.0 years for the radiation only case and 168.74 °C at 3.8 years for water-flooded gaps case.

3.2.3.2 BWR Canister Temperature Analysis Results

Figure 3-12 shows the resulting rock temperature profiles at several distances from the lateral centerline.

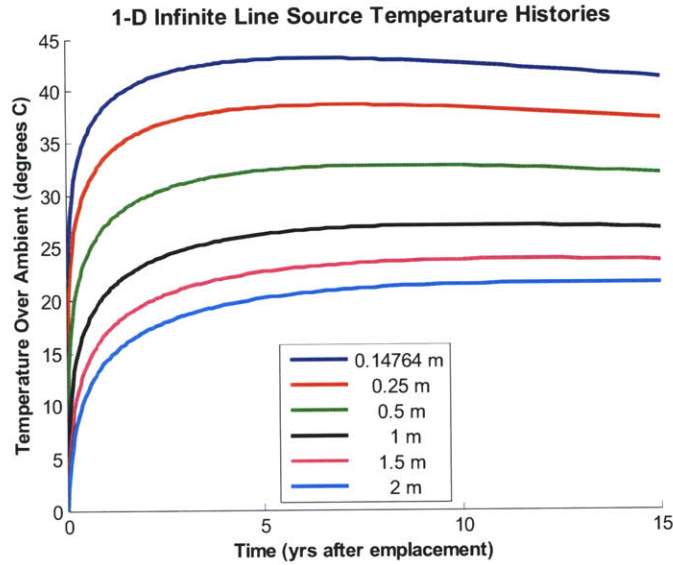


Figure 3-12: Rock Temperature Profiles (BWR Infinite Line Source)

Figure 3-13 and Figure 3-14 show the resulting temperatures of the surfaces of the waste package under the conditions of vacuum gaps and gaps flooded with water, respectively.

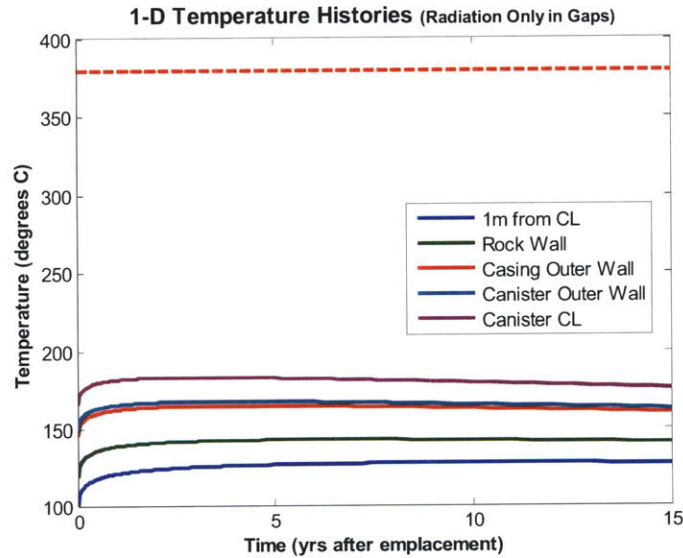


Figure 3-13: BWR Canister Thermal Histories (Radiation Only in Gaps)

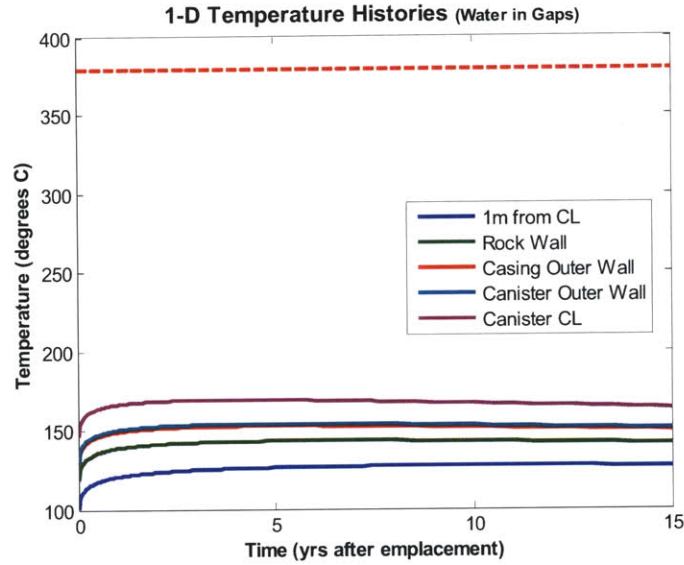


Figure 3-14: BWR Canister Thermal Histories (Water Conduction in Gaps)

The analyses predict a peak BWR centerline temperature of 183.16 °C at 2.9 years for the radiation only case and 169.04 °C at 3.9 years for the water-flooded gaps case.

3.2.3.3 Canister Temperature Analysis Comparison

The temperature rise across the borehole-canister circuit is shown in Figure 3-15 for PWR and BWR waste packages where the gaps are either vacuum or water-flooded.

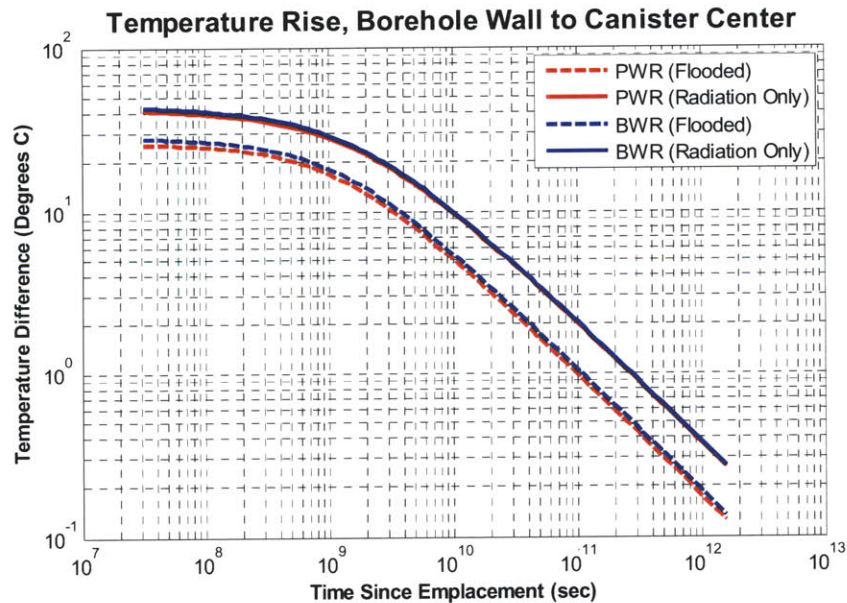


Figure 3-15: Temperature Rise from Borehole Wall to Canister Center

3.2.4 2-D Finite Cell Temperature Analysis

The second thermal analysis conducted is a two-dimensional study. The geometry of this study represents $\frac{1}{4}$ of the unit cell of granite surrounding a single canister of waste. This geometry is shown below in Figure 3-16 and Figure 3-17. The rock wall of the lateral modeled is highlighted in green

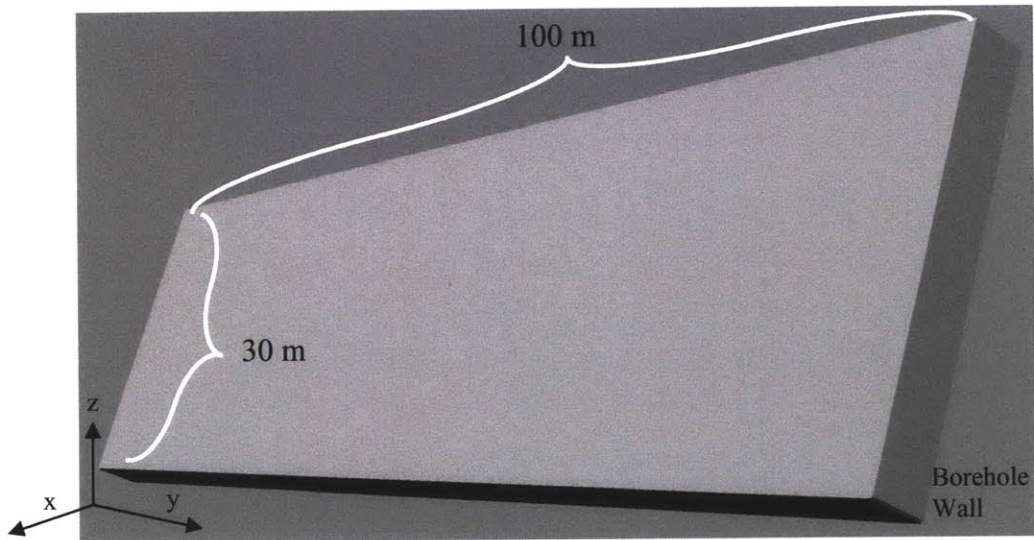


Figure 3-16: Granite Finite Cell for Transient Thermal Analysis

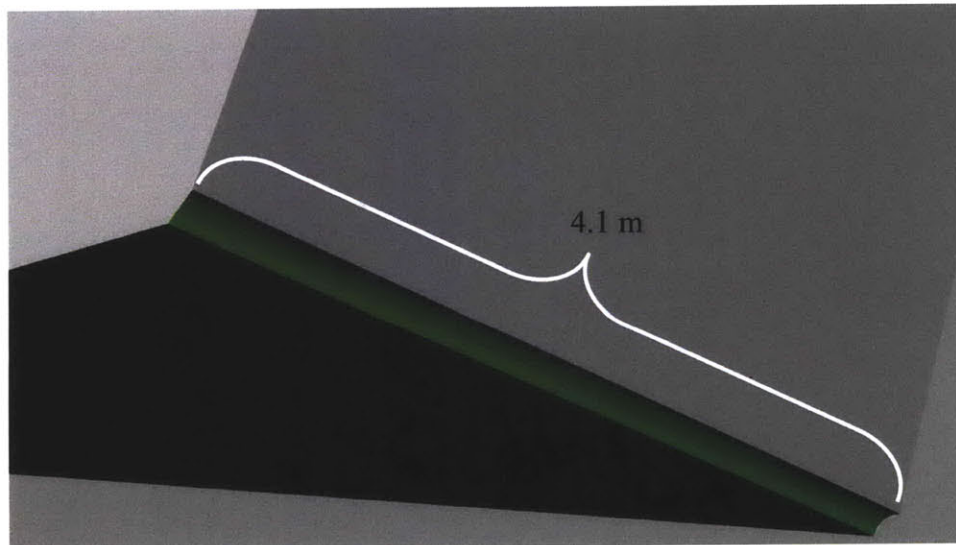


Figure 3-17: Granite Finite Cell for Transient Thermal Analysis
(Enlarged to Show Borehole Wall for PWR case)

The unit cell extends half of the distance to the next lateral above and below the modeled borehole and half the distance to the next vertical borehole in the array. This leads to a 30 m by 100 m slab with thickness the same as the LWR assembly studied (4.1 m for

PWR and 4.2 m for BWR). The boundary conditions imposed on the slab are adiabatic on all faces with the exception of the heat flux onto the borehole wall.

3.2.4.1 PWR Canister Temperature Analysis

Running the transient analyses for the PWR waste package produces the results shown in Figure 3-18, Figure 3-19, and Figure 3-20. In performing the analyses in *Solidworks*, two time regimes were used: a 200 year simulation with timesteps of 1 year and a 2000 year simulation with timesteps of 20 years; this is why Figure 3-20 and Figure 3-23 show a short term and long term wall temperature series.

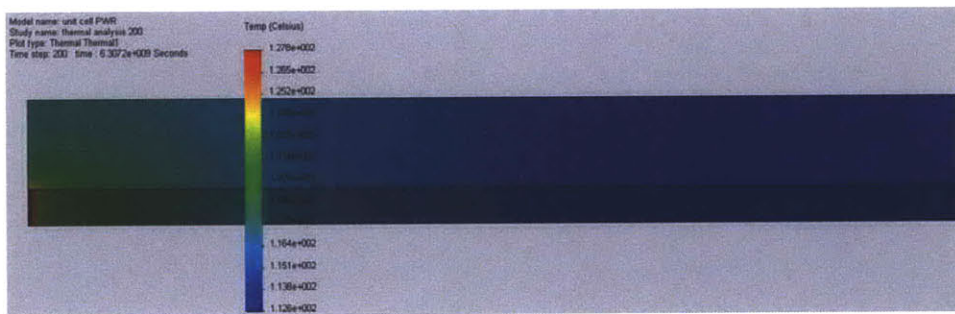


**Figure 3-18: Temperature Distribution in Finite Cell
(PWR Package, 200 yr after Emplacement)**

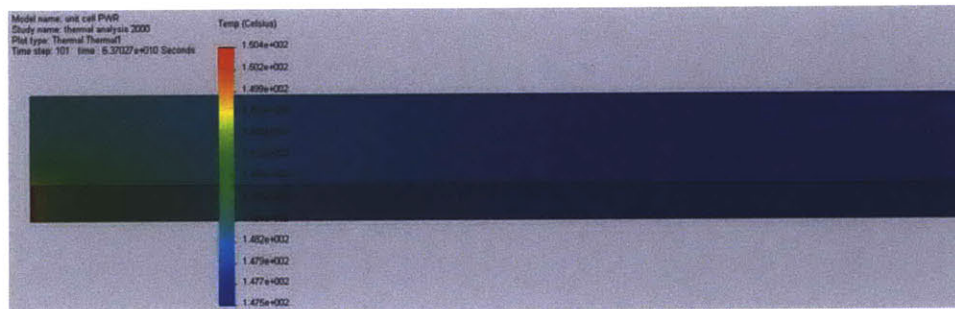


**Figure 3-19: Temperature Distribution in Finite Cell
(PWR Package, 2000 yr after Emplacement)**

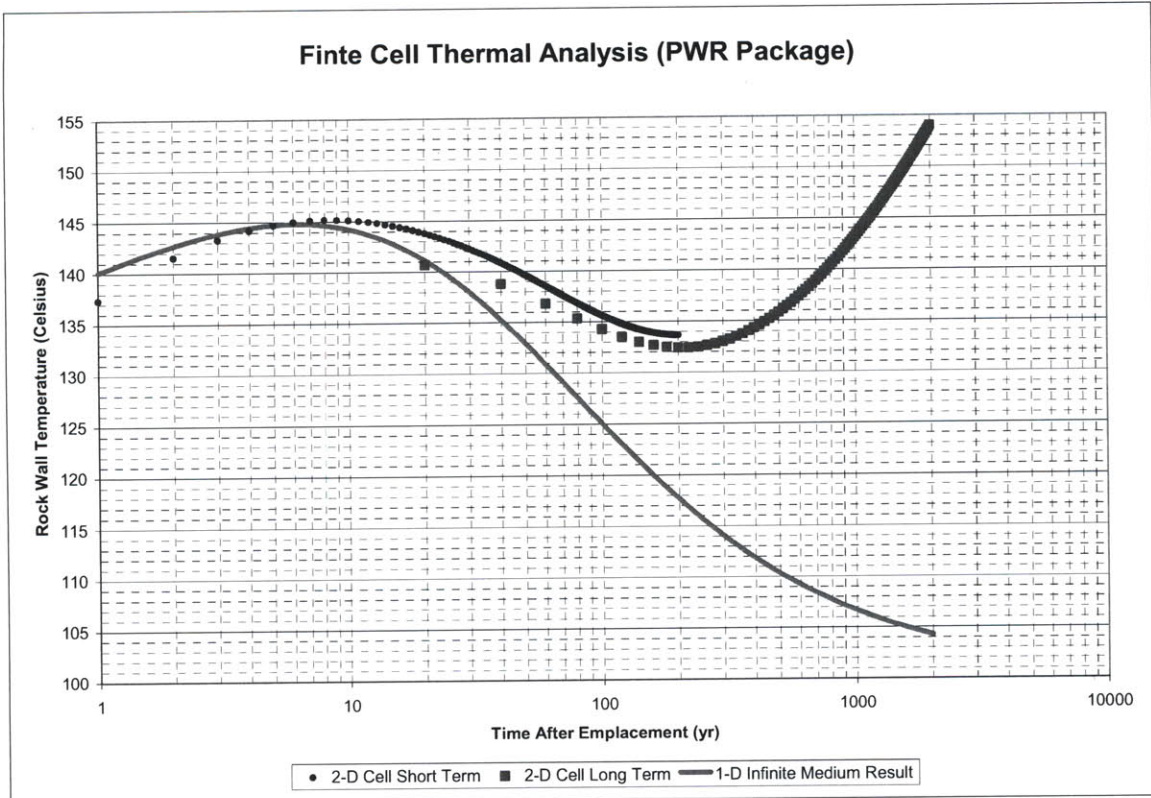
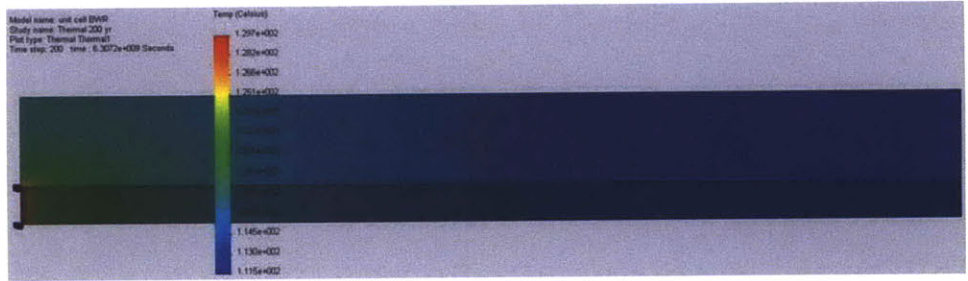


Figure 3-20: PWR 2-D Finite Cell Borehole Wall Temperature History

The PWR waste case produces a local short-term peak wall temperature at approximately 10 years after emplacement. The peak observed agrees well with the 1-D model, demonstrating that the 1-D line source accurately models the short term behavior. The 2-D analysis, however, indicates the potential for a second peak: depending on how rapidly the decay power falls off as compared with the rate that heat is diffused through the granite, a second (local) maxima is possible. Over the long duration of the study the utility of the 2-D analysis breaks down: once the thermal pulse has traveled from one corner of the slab to the opposite corner, the entire slab is then heated steadily to higher and higher temperatures due to the purely adiabatic boundary conditions. In the real repository, heat is still free to flow vertically toward the surface. This limitation motivated the three-dimensional study in the next section.

3.2.4.2 BWR Canister Thermal Analysis

Running the transient analyses for the BWR waste package produces the results shown in Figure 3-21 and Figure 3-22. Similar to the PWR results, the long term results show a run-away thermal transient.



**Figure 3-21: Temperature Distribution in Finite Cell
(BWR Package, 200 yr after Emplacement)**

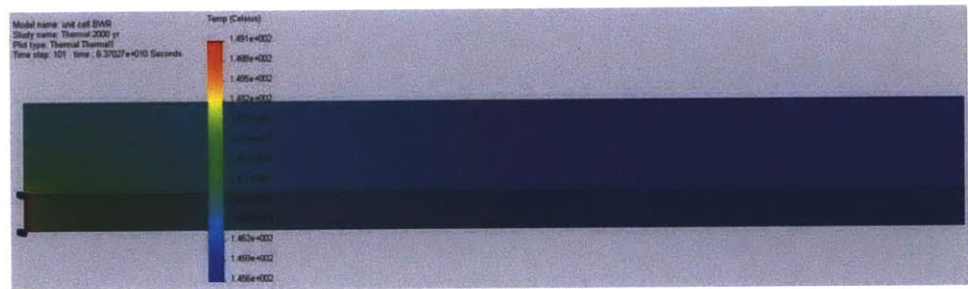


**Figure 3-22: Temperature Distribution in Finite Cell
(BWR Package, 2,000 yr after Emplacement)**

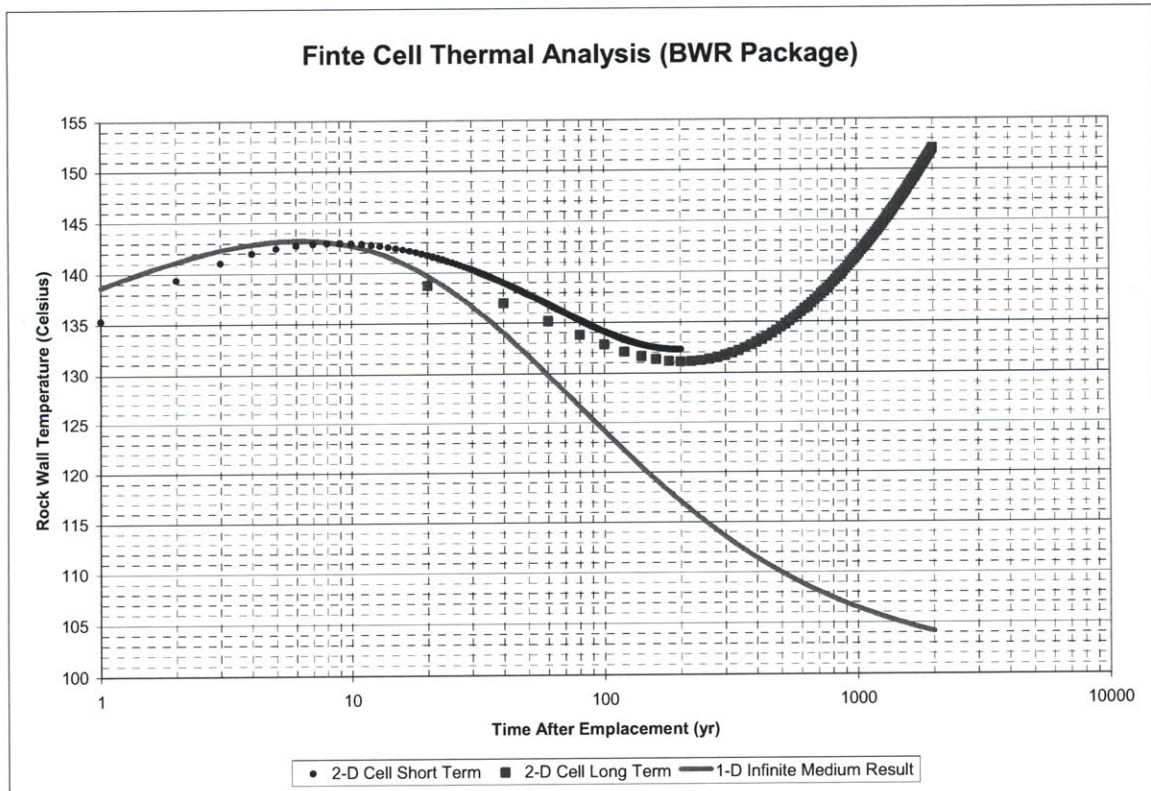


Figure 3-23: BWR 2-D Finite Cell Borehole Wall Temperature History

3.2.3 3-D Repository Thermal Analysis

To further refine the thermal analysis of the repository performance and be able to fully model vertical diffusion of heat through the repository, a three-dimensional model of the repository laterals is employed. Due to the limitations of *Solidworks Simulation*, a full scale analysis was not possible. Accordingly, a 1/10 scale slab of the repository is modeled and analyzed. Figure 3-24 and Figure 3-25 show the geometry of the rescaled repository model. The analysis applies fixed heat flux boundary conditions on the borehole lateral rock walls, fixed temperature boundary conditions at the top and bottom of the repository (25 °C at the surface and 109 °C at a depth of 3500m), and adiabatic boundary conditions at all other faces. The vertical slab geometry represents 200 m spacing between adjacent vertical boreholes, and 5 km spacing between subsequent arrays of boreholes. This geometry is shown in Figure 3-24 and Figure 3-25.

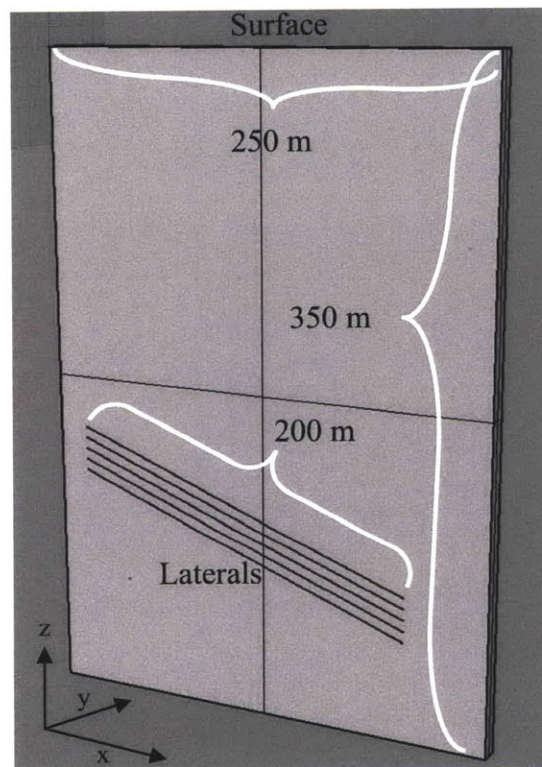
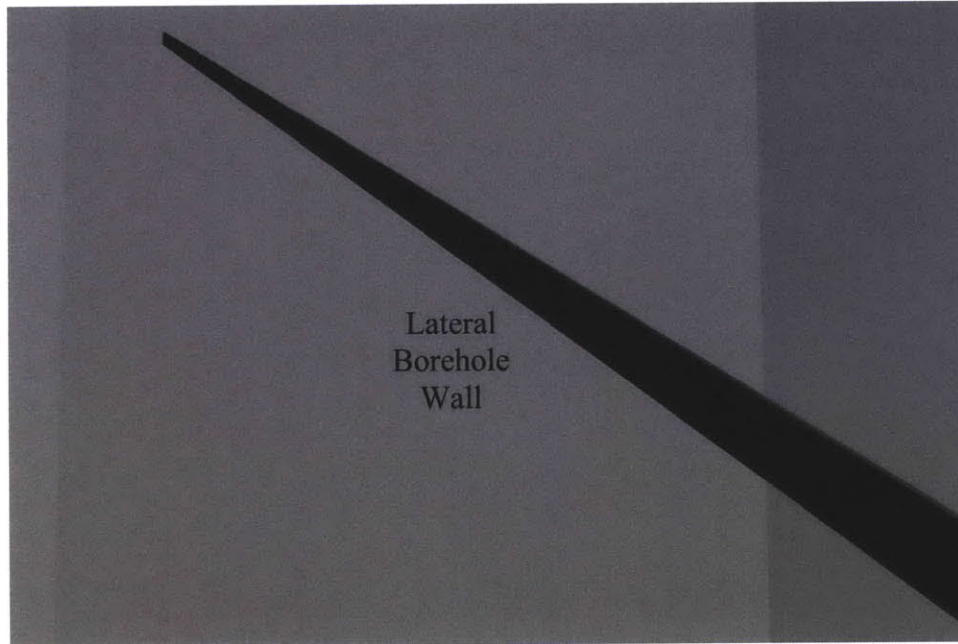


Figure 3-24: One-Tenth Scaled 3-D Analysis Geometry



**Figure 3-25: 3-D Thermal Analysis Geometry
(Enlargement of One of Five Modeled Laterals)**

In creating the small scale repository model in *Solidworks Simulation*, similitude requires that the Fourier number be preserved (to maintain results at the same times as the full scale problem):

$$Fo_{Model} = Fo_{Repository} \quad [3-10]$$

$$\frac{\alpha_{Model} \cdot \tau_{Model}}{R_{Model}^2} = \frac{\alpha_{Repository} \cdot \tau_{Repository}}{R_{Repository}^2}$$

Where : $\alpha \equiv$ Thermal Diffusivity (m^2/s)
 $\tau \equiv$ Characteristic Time
 $R \equiv$ Characteristic Length

Thus, in order to scale down the repository characteristic length by a factor of ten while maintaining the same characteristic time, the thermal diffusivity of the granite must be decreased by a factor of 100 (this is achieved by modeling the granite in the scaled repository with a density of $250,000 \text{ kg/m}^3$ vice $2,500 \text{ kg/m}^3$ for the full scale repository). Furthermore, in order for the temperature values to be the same between the model and the full scale problem, the non-dimensional temperature, θ , must be maintained between the two cases.

$$\theta_{Model} = \frac{T_{Model}}{\left(\frac{q''_{Model} R_{Model}}{k_{Model}} \right)} = \theta_{Repository} = \frac{T_{Repository}}{\left(\frac{q''_{Repository} R_{Repository}}{k_{Repository}} \right)} \quad [3-11]$$

Where : $q'' \equiv$ Heat Flux ($W/m^2 \cdot K$)

$\theta \equiv$ Non - Dimensionalized Temperature

T \equiv Temperature Result from Analysis

Having adjusted the thermal diffusivity, α , by modifying density, ρ , k is left the same for the model as for the full repository. This only leaves modifying the heat flux, q'' , to maintain similarity between the model and full-scale temperatures. As the length scale is reduced by a factor of 10, q'' must be increased by a factor of 10. Put another way, this preserves energy continuity between the heat removed from the waste and the heat deposited in the granite. The energy relationship maintained is:

$$\begin{aligned} Q_{waste} \cdot \tau &\propto \rho \cdot V_{slab} \cdot C_p \cdot \Delta T \\ q'' \cdot A_{wall} \cdot \tau &\propto \rho \cdot V_{slab} \cdot C_p \cdot \Delta T \end{aligned} \quad [3-12]$$

Where : $Q_{waste} \equiv$ Total Heat Generation Rate in Waste Canister

$A_{wall} \equiv$ Area of the Heated Wall

$V_{slab} \equiv$ Volume of Granite Slab

$C_p \equiv$ Granite Specific Heat Capacity (Constant Pressure)

$\tau \equiv$ Characteristic Time

$\Delta T \equiv$ Characteristic Temperature Rise

For the small scale geometry, wall area is reduced by 10^2 , heat flux increased by 10, slab volume decreased by 10^3 , so density must increase by 10^2 to balance [3-12] and keep the characteristic time and temperature rise consistent with the full scale problem. Section B.2 in Appendix B also features a validation of this methodology by running a similar FEA thermal problem on two scales, both of which were modeled in *Solidworks* with identical results.

Figure 3-26 through Figure 3-29 show the short term and long term impact on wall temperatures of the borehole that result from the three-dimensional analysis. Peak borehole wall temperatures observed occur at approximately 10 years after emplacement and are on the order of 145 °C. This wall temperature is significantly consistent with the 1-D and 2-D analysis, as seen in Figure 3-29.

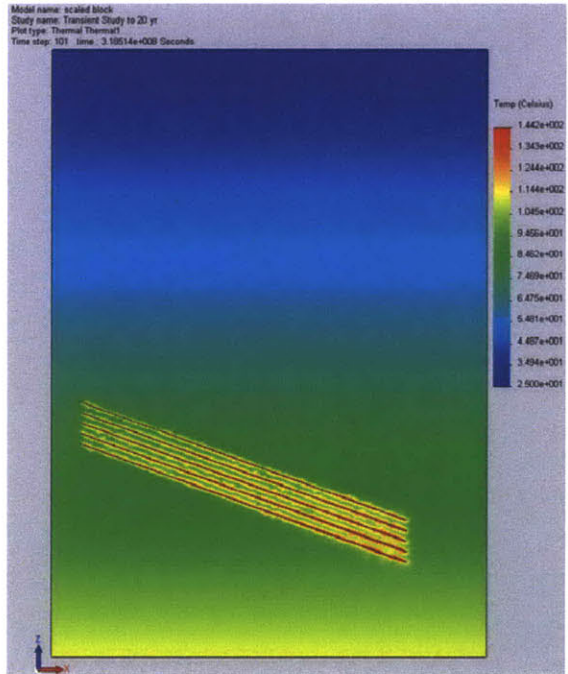


**Figure 3-26: 3-D Repository Model Granite Temperatures at 10.1 Years
 (Peak Borehole Wall Temperatures)**

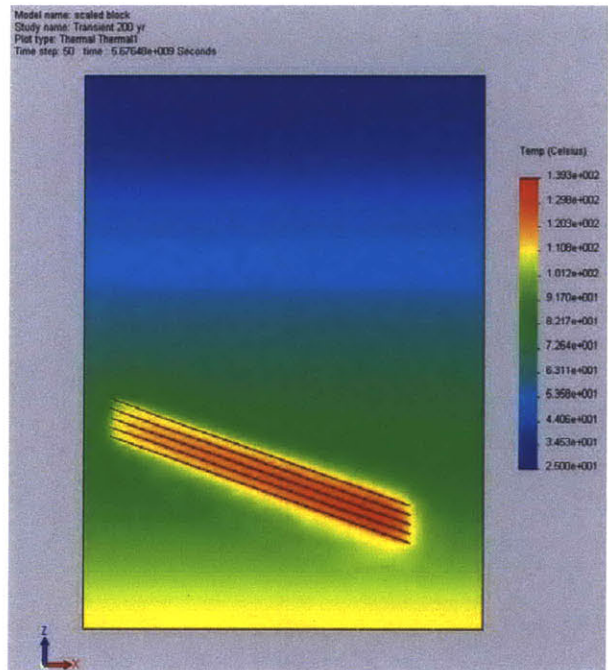


Figure 3-27: 3-D Repository Model Granite Temperatures at 200 Years

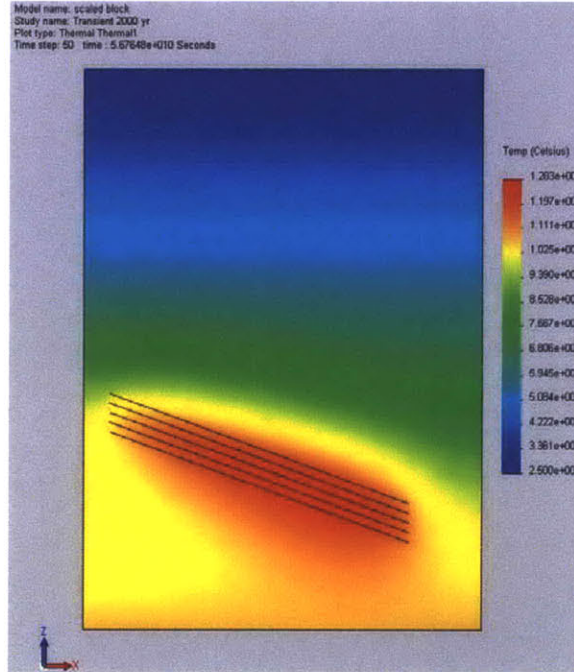


Figure 3-28: 3-D Repository Model Granite Temperatures at 2000 Years

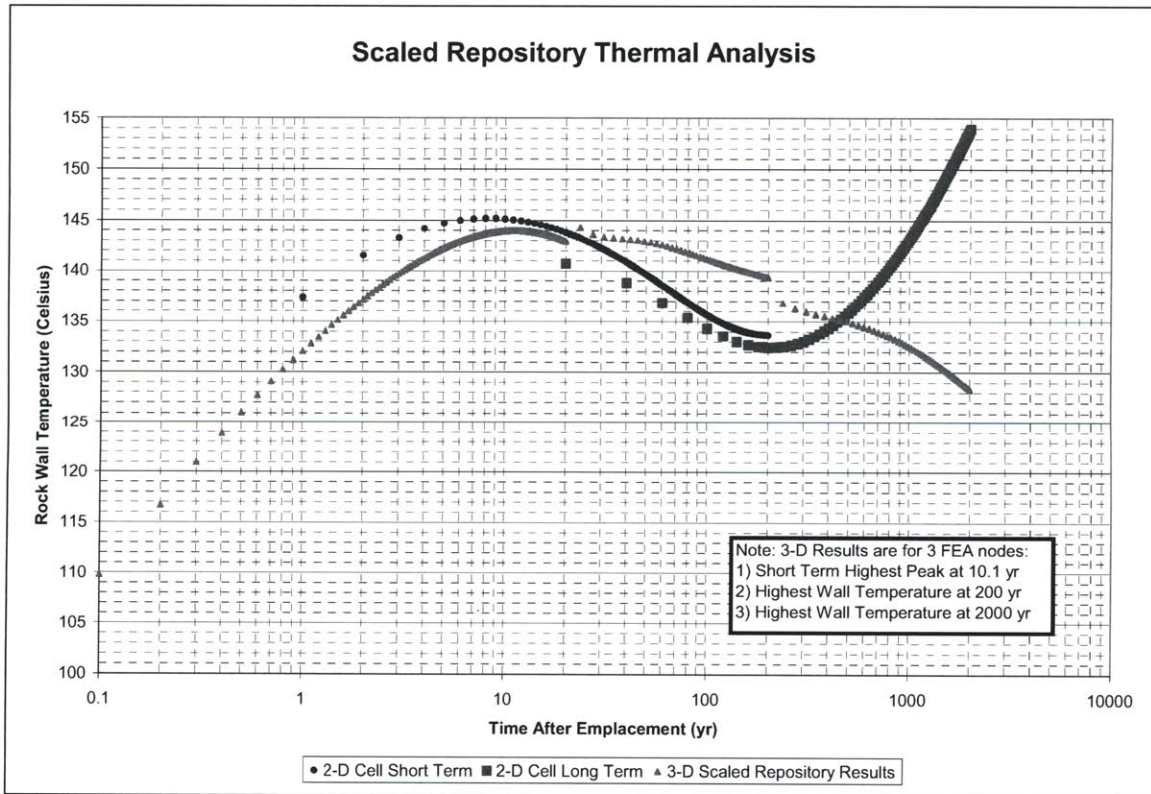
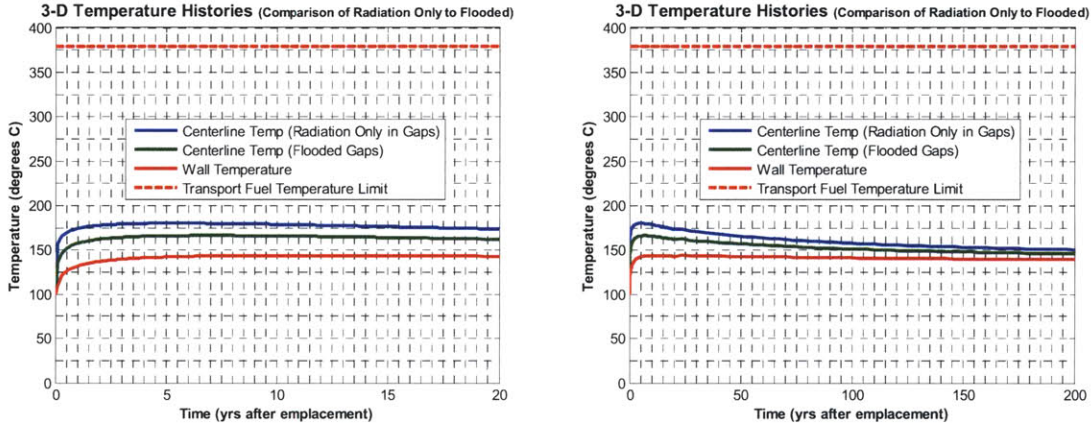
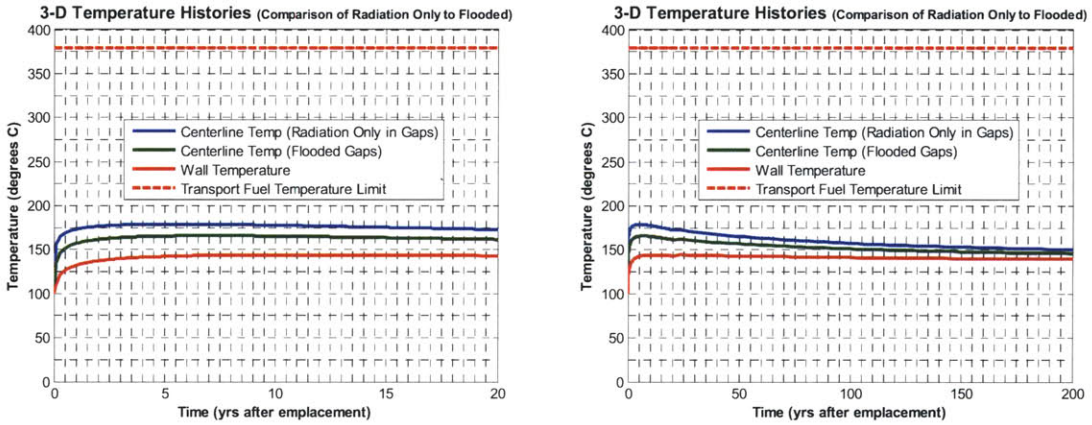


Figure 3-29: 3-D Repository Thermal Results (PWR Waste Package)

Applying the borehole wall temperature histories above to the results from Figure 3-15, the peak centerline temperatures for the PWR and BWR packages are developed and shown in Figure 3-30 and Figure 3-31, respectively.



**Figure 3-30: Centerline Temperature Results for PWR Canister
(Using 3-D Analysis Rock Wall Temperatures)**



**Figure 3-31: Centerline Temperature Results for BWR Canister
(Using 3-D Analysis Rock Wall Temperatures)**

Peak centerline temperatures of approximately 181°C for PWR waste and 179 °C for BWR waste demonstrate the feasibility of the canister and repository designs to meet thermal limits.

3.3 Mechanical Analysis of Waste Package

3.3.1 Tensile Stress

The concept loading scheme involves running an entire lateral's worth of waste packages into the borehole at one time. This produces a large tensile stress on the drill string suspending the column of waste packages, found by applying Equation [3-13]:

$$S_m = \frac{P}{A_{XS}} = \frac{W_{String} + W_{Casing} - \rho_{mud} \cdot g \cdot (V_{Casing} + V_{String})}{A_{XS}} \quad [3-13]$$

- Where :
- S_m \equiv Average Tensile Stress
 - P \equiv Axial Load
 - A_{XS} \equiv Canister Cross Sectional Area (Shell)
 - W_{String} \equiv Weight of the Total Waste String
 - W_{Casing} \equiv Weight of the Casing Above the Waste String (370m)
 - ρ_{mud} \equiv Drilling Mud Density
 - g \equiv Gravitational Constant
 - V_{Casing} \equiv Volume of Casing Above the Waste String (370m)
 - V_{String} \equiv Volume of Waste String

Per the ASME code, the maximum allowable tensile stress is:

$$S_m \leq \frac{1}{3} S_{uts} \quad \text{and} \quad S_m \leq \frac{2}{3} S_y \quad [3-14]$$

- Where :
- S_{uts} \equiv Ultimate Tensile Strength of Material
 - S_y \equiv Yield Strength of Material

As the waste column begins the kickoff (departing from vertical), the contact of the bottom canisters with the liner begins to alleviate the tensile stress on the uppermost casing segment. The most limiting case for the tensile stress therefore occurs just before the first waste canister reaches the kickoff radius. At this time, the tensile stress is 822.1 MPa for a string of PWR canisters and 819.3 MPa for a string of BWR canisters. With the ultimate tensile strength of P-110 casing steel at 861.8 MPa, and yield strength of 758.4 MPa, the maximum allowable load is 287.3 MPa or 2.9 times lower than the expected loading. While the strength of the casing at the top of the drill string could be increased, the stress at the topmost canister is likely to be nearly as high. The most

effective solution, then, is to limit the number of waste packages emplaced at a time to not exceed the weight of 690 m of PWR (138) canisters. It is conceivable that the increased presence of vitrified waste canisters would lower the weight of the stack and increase the number of canisters that may be emplaced at one time. Regardless, batch emplacement is necessary and the repository cost model should be refined to take this into account.

3.3.2 Longitudinal Buckling

The significant angle of the lateral (from vertical) will dramatically lower the crushing loads on the waste packages once emplaced. It is possible, however, for the waste string to bottom out during emplacement at which point the entire weight of the string of waste packages would be born on the bottommost canister. It is this scenario, when the bottommost canister just reaches the kickoff to start the transition to the lateral that must be analyzed for buckling. The critical buckling stress for a thin walled long cylinder with unrestrained ends is shown in Equation [3-15] (Roark, Table XVI, Formula 25)⁶⁰

$$s' = \frac{1}{\sqrt{3}} \frac{E}{\sqrt{(1-\nu^2)}} \frac{t}{r} \quad [3-15]$$

Where : s' ≡ Critical Longitudinal Buckling Stress for Thin - Shell Cylinder
 E ≡ Young's Modulus (190 GPa for Steel)
 ν ≡ Poisson's Ratio (0.26 for Steel)
 t ≡ Cylinder Wall Thickness
 r ≡ Cylinder Radius

From this critical buckling stress, a factor of safety for the repository loading may be developed using Equation [3-16] (Note: Roark explains that experimental data support designing for 40-60% of the critical buckling stress developed above).

$$F.S._{Buckling} = \frac{s' \cdot 40\% \cdot A_{XS}}{W_{Waste String} \cdot \sin(\phi)} \quad [3-16]$$

Where : $F.S._{Buckling} \equiv$ Buckling Factor of Safety
 $s' \equiv$ Critical Longitudinal Buckling
 $A_{XS} \equiv$ Canister Cross Sectional Area (Shell)
 $W_{Waste String} \equiv$ Total Waste String Weight
 $\phi \equiv$ Lateral Declination (from Horizontal)

For the repository configuration and canister material selected, the buckling factor of safety of 10.72 is achieved for canisters loaded with reconstituted PWR waste and 10.75 for canisters loaded with reconstituted BWR waste. Further, these buckling equations take no credit for the confinement of the shell wall by both the internal fill material and the lateral liner. Hence longitudinal buckling is not of concern for this design.

3.3.3 Hydrostatic & Lithostatic Crushing

One of the central advantages of lateral emplacement in very-deep boreholes is emplacement of the waste as shallow as possible while still taking full advantage of sufficient geologic isolation. Deeper emplacement produces larger pressures on the canister and increases the likelihood of the canister crushing in place.

The static uniform radial pressure load for a thin walled long cylinder with unrestrained ends is shown in Equation [3-17] (Roark, Table XVI, Formula 30)⁶¹

$$P_c = \frac{1}{4} \left(\frac{E}{1-\nu^2} \right) \left(\frac{t}{r} \right)^3 \quad [3-17]$$

Where : $P_c \equiv$ Critical External Pressure
 $E \equiv$ Young's Modulus
 $\nu \equiv$ Poisson's Ratio
 $t \equiv$ Canister Wall Thickness
 $r \equiv$ Mean Canister Radius

The resulting critical external pressure is 22.32 MPa (for the collapse of an unfilled canister) while the hydrostatic pressure on the lowest canister (at a depth of 3,007 m) is

29.4855 MPa. Thus far, no credit has been taken for the crushing resistance of the SiC particle filler material or the consolidated fuel bundle. Canadian researchers⁶² have, however, demonstrated crushing resistances of up to 10 MPa using both compacted silica sand and glass micro-beads as a filler material in CANDU disposal packages as shown in Figure 3-32.



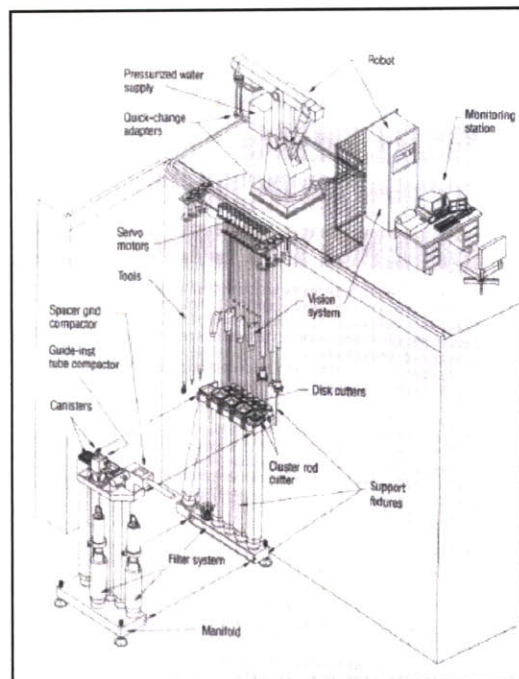
Figure 3-32: CANDU Geologic Disposal Over-pack and Canister Design
 Courtesy Canadian Nuclear FAQ⁶³

Additional research is needed to demonstrate that the SiC particle bed will provide similar crushing resistance in this design and hence will prevent radial crushing of the waste package.

4 ROD CONSOLIDATION AND PACKAGE COST

Consolidation of Light Water Reactor (LWR) Fuel was a topic for considerable research and development in the 1980s and 1990s. Significant delays in the Department of Energy's timeline to accept spent fuel for permanent disposal spurred significant industry interest in increasing the capacity of spent fuel pools. By dismantling discharged fuel assemblies, volumetric reductions of 2:1 or 3:1 of fueled components and 10:1 of non-fueled components were assessed as feasible.^{64 65}

Fuel consolidation, as studied typically, involved remote handling of assemblies and individual components while they are submerged within a spent fuel storage pool. Operators using robotic controls would remove individual assemblies from a storage site, perform several processing steps to dismantle the assembly support structure, and place individual fueled elements (typically fuel pins) back into a storage canister. The arrangement of such a handling system is shown in Figure 4-1.



The FUEL-PAC system uses a robot and remote viewing to ensure speed, reliability and flexibility.

Figure 4-1: Rod Consolidation Concept Arrangement⁶⁶

Dry (shielded) handling is also possible and is likely to achieve lower costs, as wastes would arrive at the borehole repository processing facility in dry transportation casks (cooling time was assumed to be 40 years between irradiation and emplacement in the thermal studies conducted in Chapter 3).

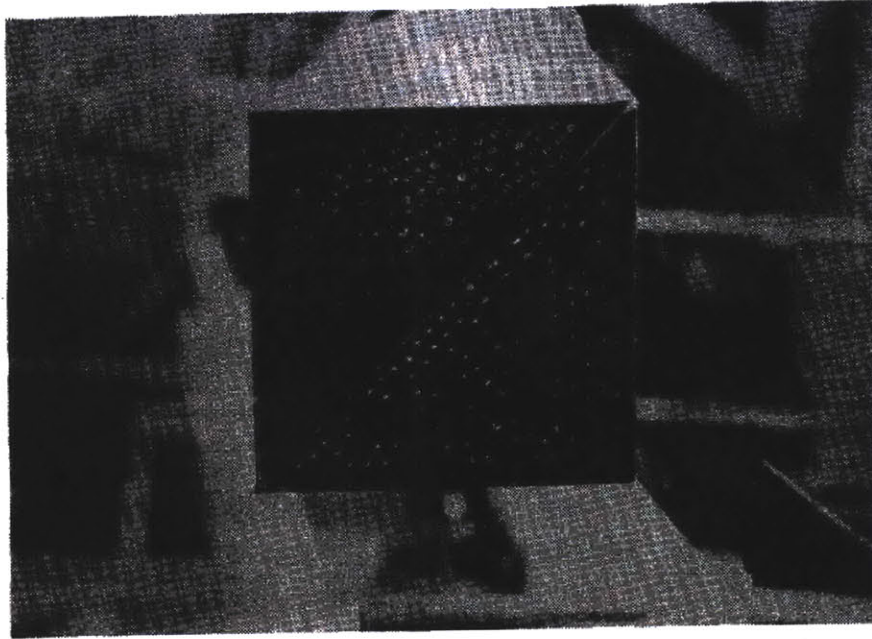


Figure 4-2: Dry Fuel Pin Consolidation at BNFP-2 Consolidated PWR Assemblies (Viewed end on)⁶⁷

Fuel assembly consolidation also typically involves compaction of the non-fuel bearing support components as shown in Figure 4-3.



Figure 4-3: Shearing of Non-Fuel Bearing Assembly Components for Compaction⁶⁸

As applied for the Very Deep Borehole, this low-level waste may be either stored in a separate facility or the shredded components may be compacted in the disposal canister along with the consolidated fuel (typical PWR assembly lengths are approximately 4.1 m in length while the package overall length is 5 m; this leaves 22,400 cm³ of room in the package for non-fuel waste).

The remainder of this chapter will estimate the anticipated consolidation and canister costs for the Very Deep Borehole Repository using a review of previous in-depth studies of fuel consolidation.

4.1 Cost Threshold for Feasibility

The lateral emplacement approach used in this project requires fuel consolidation in order to reduce the waste package diameter sufficiently to permit the use of currently deployed oil and natural gas drilling techniques. In this sense, consolidation costs are integral to the economic feasibility of such a repository. It is useful to examine under what conditions the incorporation of fuel pin consolidation becomes attractive for deep borehole disposal when it is not requisite in the design. Accordingly this section examines the impact of consolidation on a large-diameter borehole repository featuring vertical emplacement of waste packages, such as was studied by Christopher Ian Hoag (“Canister Design for Deep Borehole Disposal of Nuclear Waste,” 2006).

Hoag’s analysis produced a total repository cost of approximately \$50/kg HM. Given the geometry of Hoag’s waste package, consolidation of PWR fuel assemblies would increase the number of fuel pins from one assembly of 264 pins per canister to 955 pins per canister. This is accomplished through the

- Compaction into close packed arrangement
- Removal of unfueled ‘water rods’ from the intact assembly (these account for 26 of the 280 pin locations in the intact 17x17 Westinghouse assembly studied by Hoag)
- Use of the region between the intact assembly (square cross-section) and the canister inner wall (circular cross section)

These two configurations are shown in Figure 4-4 and Figure 4-5 below.

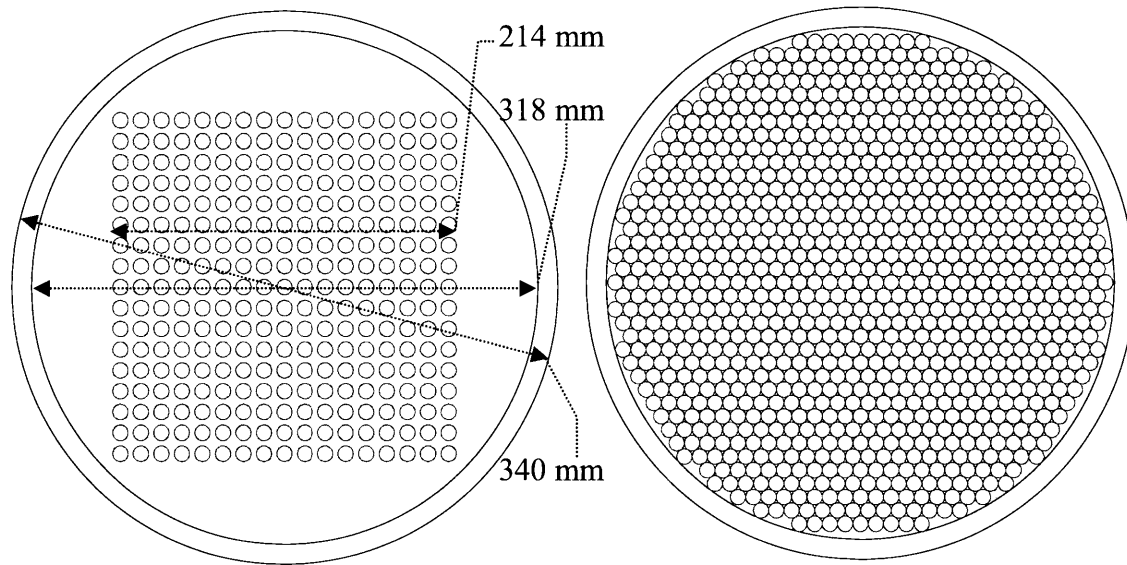


Figure 4-4: Hoag Waste Package with Intact 17 x 17 PWR Fuel Assembly

Figure 4-5: Hoag Waste Package with Consolidated PWR Fuel

This would lower the effective overall drilling costs by a factor of 3.6 or to approximately \$14/kg HM. Thus fuel consolidation must cost less than approximately \$36/kg HM for it to be an attractive aspect in borehole disposal. This analysis assumes that there are no additional costs from the increased mass of the package (i.e. the package design is still sufficient for the increased mechanical loads associated with the increased weight).

4.2 Previous Studies

Two detailed studies on rod consolidation provide thorough analyses on prospective fuel consolidation costs. The Electric Power Research Institute (1990)⁶⁹ and the Department of Energy's Prototypical Rod Consolidation Project carried out by Sciencetech (1989-1993)⁷⁰ each evaluated the full-scale infrastructure, operational and maintenance costs of a rod consolidation program. A comparison of the results from these reports is useful in bracketing expected consolidation costs for the borehole repository.

4.2.1 Electric Power Research Institute Study

Figure 4-6 shows the handling concept for the EPRI fuel consolidation process.

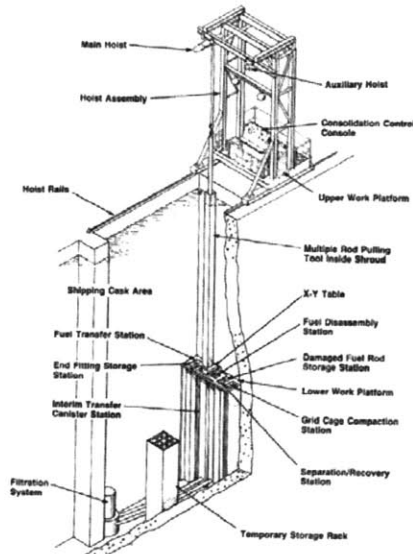


Figure 4-6: EPRI In-Pool Consolidation Handling Arrangement

Figure 4-7 shows in detail the handling steps employed in the EPRI approach to consolidate the fuel pins and compact the non-fueled components.

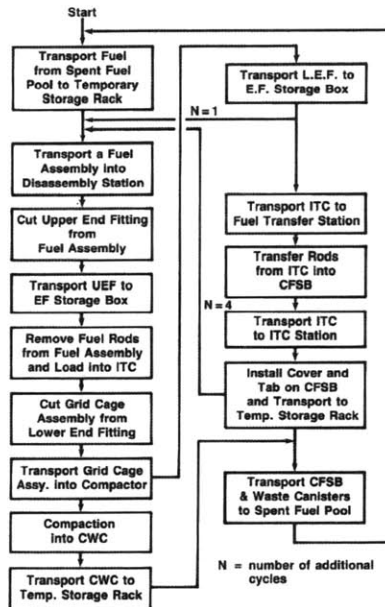


Figure 4-7: EPRI Process for Fuel Assembly Consolidation

The EPRI report estimates a total of 118-128 man-hr to consolidate two 14x14 PWR fuel assemblies into a single storage box with a total handling time of 20 hours. Thus the

capacity of the pilot operation was approximately 270 MTHM/yr (assuming two 8-hour shifts per day). EPRI further claims that the total cost to consolidate two 14 x 14 assemblies is \$11,431 – 13,043 (1990). “The Program Target for the consolidation of two assemblies was 16 hours, and [we] believe[] that this can be achieved and even improved upon by the incorporation of the equipment and procedure modifications recommended in the Cold and Hot Demonstration Reports.”⁷¹

Table 4-1 calls out the results of the EPRI rod consolidation study. Highlighted in dark gray are the canister and non-canister related costs of the study expressed in constant 2009 dollars. Taken together, these total just over \$19/kg for the consolidated fuel and canister. The light highlighting shows the canister costs per mass of steel in the canister (using the deep borehole canister design waste mass and steel mass) to identify that the canister costs are significantly conservative (the borehole model included fabricated casing costs at \$6/kg of steel; welding the package closed will not exceed the difference between \$6/kg and \$28.75/kg).

Table 4-1: EPRI Study Results Summary

EPRI Study Summary		Ref
Assembly Type	14x14 Westinghouse	
Assembly Mass	0.4687 MTHM	72
Labor Cost/2 Assy	\$5,609 (1990)	
Filter Cost/2 Assy	\$624 (1990)	
Levelized Cost (Excl. Canister)	\$12.38 /kg HM (2009)	
Canister Cost/2 Assy	\$4,636 (1990)	
Levelized Canister Cost	\$6.67 /kg HM (2009)	
Levelized Equivalent Canister Cost	\$28.75 /kg steel (2009)	
Canister Capacity	729.07 kg HM	
Canister Mass	169.11 Kg	
Labor Rate (with Overhead Factor of 1.75)	\$25.00 /hr (1990)	
Labor Escalator (1990-2001) (Union Labor)	1.480	73
Labor Escalator (2001-2009) (Manufacturing)	1.278	74
Material Escalator (1990-2009) (Gen. Purp. Machy.)	1.586	75
Material Escalator (1990-2009) (Metal Containers)	1.349	76

The cost escalators employed in updating from 1990 dollars to 2009 dollars include the Producer Price Index (PPI) for Metal Containers, PPI for General Purpose Machinery, and the Employment Cost Index and Employer Cost for Employee Compensation

furnished by the U. S. Bureau of Labor Statistics (see references in Table 4-1). The EPRI work, therefore, shows that consolidation is a promising technology for waste disposal (the total costs of \$19.05/kg are well within the feasible value of \$36/kg).

4.2.2 Sciencetech Study

The project completed by Sciencetech for the DOE was quite similar in operation to the EPRI consolidation program, the cost analysis for which is shown in Table 4-2:

Table 4-2: Sciencetech Prototypical Rod Consolidation Project Cost Summary

<u>Procurement, Fabrication, Supplies and Operating Costs (less labor)</u>		
	<u>Bare Costs</u>	<u>1989 Present Worth Costs*</u>
Direct Costs	Buyout Equipment	5,911,000
	Fabricated Equipment	\$3,206,000
Consumables	Fuel & NFBC Canisters	\$238,735,000
	Other Consumables	\$18,917,000
Spare Parts		\$2,717,850
Major Equip. Replacement		\$1,072,800
Utilities		\$1,536,000
	Total	\$145,502,440
<u>Labor Requirements</u>		
OPERATION		
	Management/Supervisory	4,160
	Operations	8,320
	Maintenance	1,900
	Support	9,504
	Total	23,884 Hr/Yr
INSTALLATION		
		1,218 Hours
TESTING		
		5,720 Hours

*Based on Present Worth Rate of 4.81%, 30 year period

The Sciencetech report summarizes these costs and the potential for future savings:⁷⁷

It is noted that of the \$145 million of procurement, fabrication, supplies, and non-labor operation costs, \$125 million is a result of the Fuel and NFBC [Non-Fuel Bearing Component] Canister costs. Assuming a labor cost of \$50 per hour, the total labor cost would be \$1.29 million per year. Using the present worth factor from Appendix I of 15.729 the present worth of the operation labor would be \$20.3 million. Adding the Installation and Testing 6928 hours at \$50 per hour results in an additional cost of the \$0.3 million for the total labor cost of about \$21 million. Therefore, for a total project cost of about \$166 million, \$125 million is for Canisters, \$21 million is for labor, and \$20 million is for all other costs. Clearly, the greatest potential for cost reduction lies with the Canister design/fabrication costs, which are 75% of the total project costs.

This highlights one of the key advantages to using a package design featuring relatively inexpensive, low-alloy steel. Table 4-3 details the results from the Sciencetech report. As in the EPRI section, the levelized unit cost for labor, the canisters, and other direct costs are highlighted in dark gray. As with the EPRI summary, the light highlighting shows the canister costs per mass of steel in the canister (using the deep borehole canister design

waste mass and steel mass). The canister cost figures show good agreement between the two studies (\$32.72/kg steel for Sciencetech, \$28.75 for EPRI) and are encouraging for our package design. The P-110 steel selected for the borehole application is both cheaper and simpler to fabricate than the high-grade stainless steels in the waste canisters used in these studies.

Table 4-3: Sciencetech PRCP Results Summary

Sciencetech Study Summary		Ref
Project Capacity	750 MTHM/yr	
Operating Lifetime	30 yr	
Direct Costs (Excluding Canisters and Labor)	\$33,360,650 (1989)	
Present Worth (PW) of Direct Costs	\$21,829,922 (1989)	
Canister Costs	\$238,735,000 (1989)	
PW of Canister Costs	\$125,163,520 (1989)	
Direct Costs (Excluding Canisters and Labor)	\$2.44 /kg HM (2009)	
Levelized Direct Costs (Excl. Canisters and Labor)	\$1.59 /kg HM (2009)	
Canister Costs	\$14.47 /kg HM (2009)	
Levelized Canister Costs	\$7.59 /kg HM (2009)	
Equivalent Canister Cost	\$62.40 /kg steel (2009)	
Levelized Equivalent Canister Cost	\$32.72 /kg steel (2009)	
Annual Labor Requirements	23,884 hr/yr	
Initial Labor Requirements	6,938 hr	
Total Labor Cost	\$36,172,900 (1990)	
PW of Labor Cost	\$19,109,070 (1990)	
Total Labor Cost	\$3.13 /kg HM (2009)	
PW of Labor Cost	\$1.65 /kg HM (2009)	
Labor Rate	\$50.00 /hr (1989)	
Labor Escalator (1989-2001) (Union Labor)	1.524	78
Labor Escalator (2001-2009) (Manufacturing)	1.278	79
Material Escalator (1989-2009) (Gen. Purp. Machy.)	1.644	80
Material Escalator (1989-2009) (Metal Containers)	1.364	81
Discount Rate	4.81%	

4.2.3 Cost Comparison

Table 4-4 compares the costs presented in the two fuel consolidation studies.

Table 4-4: EPRI and Scientech Study Cost Comparison

	EPRI	Scientech
Canister Cost (\$2009/kg HM)	6.67	7.59
Labor Cost (\$2009/kg HM)	12.38	1.65
Other Direct Costs (\$2009/kg HM)		1.59
Total Cost (\$2009/kg HM)	19.05	10.84

It is important to note that the operational scale of the two projects is significantly different (270 MT/yr for EPRI and 750 MT/yr for Scientech), and this may account for some of the difference in costs. Additionally, the canister costs per waste mass for the P-110 canister should be significantly lower than the canisters designed for the rod consolidation studies due to both material selection and the higher loading in the borehole waste package.

4.3 Cost Estimation for Waste Packaging of LWR Fuel

To permit the evaluation of a single, modular borehole repository (i.e. a single vertical shaft with 10 laterals for emplacement), a small scale consolidation plant is assumed. Based on the studies presented in section 4.2, the moderate scale of operation for a single vertical borehole repository leads to a conservative estimate for the consolidation costs of \$12.50/kg HM. This reflects the increased sunk costs per kg of infrastructure and overhead associated with a small scale and most closely resembles the consolidation at a reactor site, such as was studied in the EPRI report.

The material cost for the waste package should be close to that used in the cost model for the drill casing (\$6/kg steel, Table 2-4). Remote canister welding will increase this cost somewhat, but is not expected to exceed \$500 per waste package. These costs together equate to \$2.67/kg HM.

The package fill material, SiC particles, is commercially available⁸² (for use in abrasive applications) for \$3.12/kg. This equates to \$0.34/kg HM for this canister design. Other, less expensive fills may be examined in future work. Although the processing costs to load the fill material are not treated directly here, compaction of the fill material into the canister (such as using a vibration table) should not significantly impact the cost of the fuel package.

In Conclusion, taking together the costs for the consolidated fuel package, compaction of the spent fuel assembly, filling and sealing the canister and canister costs, the design should not exceed \$15.51/kg of HM. This is well within the DOE civilian spent nuclear fuel waste fee of 0.001 \$/kW-hr electric (which equates to roughly \$400/kg of HM). The cost is less than the incremental cost of about \$34.44/kg HM to drill a deeper borehole to accommodate unconsolidated fuel (for the Hoag design).

5 CONCLUSIONS AND FUTURE WORK

This chapter summarizes the work of this project and future work needed to further demonstrate the feasibility of lateral emplacement in very-deep borehole disposal of high level nuclear waste.

5.1 *Summary of Design and Results*

After developing a borehole drilling cost model, a trade-space study was conducted to examine what borehole configuration was most economically attractive for high level nuclear waste disposal. From over 20,000 potential repository configurations, the final design selected features were as follows:

- A 1500 meter vertical plug section for adequate isolation of the nuclear waste from the biosphere
- 10 laterals extending from each vertical borehole
- 2000 meter long lateral emplacement shafts (400 packages / lateral)
- Laterals declined 20° from horizontal
- Drill-bit schedule calling for 26” for the surface shaft, 17 ½” for the main vertical shaft, and 11 ⅝” for the laterals and radial kickoffs

The vertical shaft is lined and cemented at depths below 2100 m, above which all casings are removed to permit direct contact of the borehole plug with the exposed granite rock face. Laterals are also lined with casing but these liners are not cemented in place.

Based on the modeling in this project, drilling and emplacement costs for this repository configuration should not exceed \$47/kg HM (with a statistical confidence of 0.99).

Based on some conservative assumptions built into the model (mature drilling techniques only, equipment rental rates similar to those for a much larger diameter and deeper enhanced geothermal well) this cost estimate should be considered an upper limit on directional drilling costs for lateral emplacement. Additional costs for waste package fabrication, SiC fill, fuel pin consolidation and canister sealing are expected to not exceed \$16/kg of HM for LWR spent fuel packages. These costs are significantly lower for reprocessed or vitrified wastes as they may be packaged into the final disposal canister at

the source site. Taken together, all costs expected for a very-deep borehole amount to about \$63/kgHM, well within the DOE's waste fund fee (equivalent to ~\$400/kgHM) even when transportation costs to the repository and research and development costs are considered. The lateral emplacement configuration is therefore demonstrated to be economically feasible.

The waste package and repository design are also demonstrated to be technically feasible. Specifically, the thermal analysis shows that peak fuel temperatures and peak rock temperatures in the repository will not exceed 190 °C and 145°C respectively. These results were obtained using a three-dimensional finite element analysis of the thermal loading in the repository and validated using two-dimensional finite element and one-dimensional (infinite line source) analytical methods. Mechanical analysis also shows that the waste package design is sufficient to withstand all expected loading until after the repository is closed. Longitudinal buckling, radial crushing, and tensile failure modes were analyzed using limits based on elastic shell theory. The use of SiC particulate fill in the waste package, the modest maximum depth of the directionally drilled repository (approximately 3000 m below the surface), and the reliance on the host geology for long term isolation of the waste permit the use of an inexpensive canister material and simple design while still meeting all requirements.

5.2 Recommendations for Future Work

In order to further demonstrate the feasibility of very-deep boreholes in general and lateral emplacement in particular, further work is required in the following areas:

- Performing a total system performance assessment of borehole plugging materials
- Refining the cost model to better reflect cost dependence with depth and diameter
- Further study of radionuclide transport through crystalline rock
- Testing of fill material efficacy in improving package crushing resistance
- Evaluation of cost and efficacy of using grout / bentonite clay as fill material surrounding waste packages
- Identifying additional experiential cost data from industry for drilling model calibration

- Study of advanced drilling techniques such as air drilling and spallation drilling
- Further evaluation of cost implication of dry vice wet fuel rod consolidation
- Validation / modification of the canister design to accommodate non-vitrified defense wastes (such as spent Naval Nuclear fuel)

5.3 *Conclusions*

The small scale of the borehole concept allows for modularity and scalability of the repository. The application of currently fielded oil and gaswell drilling practices makes this approach extremely attractive for permanent and irretrievable waste disposal thereby alleviating the research and development needed for large diameter boreholes. Taking advantage of the impermeability of the crystalline formation to water/waste transport, and the down-hole environmental conditions, the material for the waste package may be selected for its strength properties and cost rather than for its performance as an engineered barrier to release of radionuclides. This project demonstrates that marrying fuel consolidation with small diameter lateral borehole disposal of high level waste produces an economically and technically feasible waste repository design.

APPENDIX A: V-DeepBoRe Code

(Very-DEEP BOREhole REpository Cost Model)

A.1 Model Script Organization

Figure A-1, below, shows the overall organization of scripts used in the organization of the drilling model and the flow of data between modules. The code for these modules is shown in section A.2.

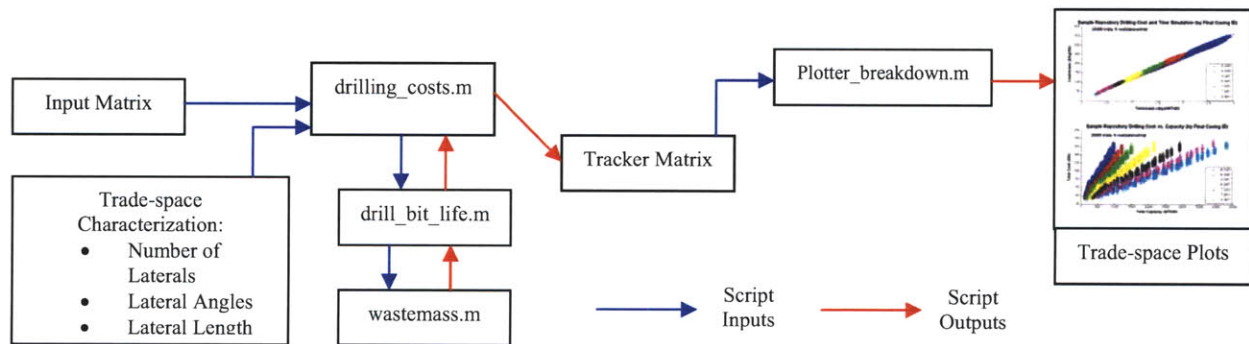


Figure A-1: Repository Cost Model Script Flowchart

A.2 Model Scripts (MATLAB)

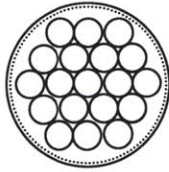
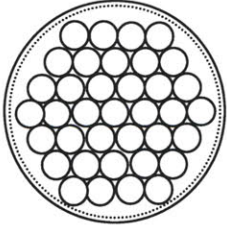
A.2.1 Waste Packing Script (wastemass.m)

```

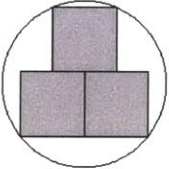
function [wasteparam]=wastemass(emplacementlength,no_laterals,...
    pipeschedule,IDs,PWR_frac,Vit_frac,vit_load)

%%%%%%%%%%%%%%%%%%%%%%%%%%%%%%%%%%%%%%%%%%%%%%%%%%%%%%%%%%%%%%%%%%%%%%%%
% This function estimates the total mass of HM stored in MTHM in the %
% repository once completely loaded %
%%%%%%%%%%%%%%%%%%%%%%%%%%%%%%%%%%%%%%%%%%%%%%%%%%%%%%%%%%%%%%%%%%%%%%%%

% Load array for hexagonal close packing circles based on the diameter of
% the hexagon
load hexarray
  
```



```
% Load array for packing squares within the diameter of a circumscribed
% Circle
```



```
load squarepacking
```

```
% Input parameters
L_BWR=.134; % Cross section dimension of BWR fuel assembly (m)
PWR_rod_diam=0.0095; % pin diameter of PWR fuel pins (reconstituted) (m)
BWR_rod_diam=0.011; % pin diameter of PWR fuel pins (reconstituted) (m)
Diam_frac=.9; % usable fraction of casing inner diameter
Pins_Assy_PWR=264; % number of pins in intact PWR assembly
m_assy_PWR=.4987; % mass of HM in 1 PWR assembly (MT)
Pins_Assy_BWR=72; % number of pins in BWR assembly
m_assy_BWR=.1917; % mass of HM in 1 BWR assembly (MT)
borosilicate=2.23; % density of borosilicate glass (MT/m^3)
heavymetal=19.1; % density of HM (MT/m^3)
```

```
% calculate the density of heavy metal in vitrified waste
rho_vit=borosilicate/((1/vit_load-1)+borosilicate/heavymetal);
```

```
% Calculate the number of canisters in repository (5 m canister length)
no_canisters=(emplacementlength/5)*no_laterals;
```

```
% Calculate the interior diameter of the waste package
% (based on inner diameter of liner and Diam_frac above)
canID=Diam_frac*IDs(pipeschedule(3))/39.37;
```

```
% Calculate the volume of the waste canister (L*pi*d^2/4)
V_can=5*(canID^2)/4*pi; % (in m^3)
```

```

% Divide up the total number of canisters by waste form
PWR_no=ceil(no_canisters*PWR_frac);
Vit_no=ceil(no_canisters*Vit_frac);
BWR_no=no_canisters-PWR_no-Vit_no;

% Calculate max number of PWR fuel pins in hex array to fit canister ID
PWR_diam=2*floor((floor(canID/PWR_rod_diam)-1)/2)+1;
no_PWR_pins=interp1(hexarray(:,1),hexarray(:,2),PWR_diam,'nearest');

% Calculate mass of fuel in a canister of PWR waste (MT)
m_PWR=no_PWR_pins/Pins_Assy_PWR*m_assy_PWR;

% Calculate mass of fuel in Vitrified waste canister
m_Vit=V_can*rho_vit;

% Calculate # of intact BWR assemblies per cannister
no_BWR_assy=floor(interp1(squarepacking(:,2),squarepacking(:,1),...
    canID/(L_BWR*2),'linear'));
no_BWR_pins=0;

% If intact BWR assy will not fit, calculate the number of BWR pins in
% waste canister and associated mass
if no_BWR_assy==0 || isnan(no_BWR_assy)
    % Calculate number of fuel pins in hexagonal array to fit canister ID
    BWR_diam=2*floor((floor(canID/BWR_rod_diam)-1)/2)+1;
    no_BWR_pins=interp1(hexarray(:,1),hexarray(:,2),BWR_diam,'nearest');
    % Calculate mass of fuel in BWR cannister
    m_BWR=no_BWR_pins/Pins_Assy_BWR*m_assy_BWR;
    BWR_reconst=true;
    no_BWR_assy=0;
else
    m_BWR=no_BWR_assy*m_assy_BWR;
    BWR_reconst=false;
end

% Tally total waste packing of repository from all three waste forms

```

```
m_HM=PWR_no*m_PWR+BWR_no*m_BWR+Vit_no*m_Vit;
```

```
% Output key results back to the drilling script for 'scoring' repository  
wasteparam=[m_HM BWR_reconst no_PWR_pins no_BWR_assy no_BWR_pins];
```

A.2.2 Drilling Cost Realization Script for Lateral Repository (drill_bit_life.m)

```

function [depthtimecosthist,drillparam,wasteparam] = drill_bit_life...
    (pluglength,emplacmentlength,declination,no_laterals,...
    pipeschedule,ODs,Holes,IDs,mu_sed,mu_gran,sd_gran,sd_sed,PWR_frac,...
    Vit_frac,rho_vit,casing_mass,bit_cost,radii)

%%%%%%%%%%%%%%%%%%%%%%%%%%%%%%%%%%%%%%%%%%%%%%%%%%%%%%%%%%%%%%%%%%%%%%%%
% This function executes a Monte Carlo simulation of drilling a single      %
% vertical shaft of a borehole repository based on the inputs from the      %
% drilling_costs.m script and outputs the simulated drilling progress in    %
% cost and time vs. depth as well as material (cement and casing) used, and %
% how the waste is accomodated (canister packing, whether reconstitution is %
% required, etc.)                                                         %
%%%%%%%%%%%%%%%%%%%%%%%%%%%%%%%%%%%%%%%%%%%%%%%%%%%%%%%%%%%%%%%%%%%%%%%%

%% Drilling Parameters

backhaul=350;                    % backhaul speed (m/hr)
surfdepth=200;                  % depth of surface hole (m)
changeoutcost=[bit_cost(pipeschedule... % additional cost associated
    (1)),bit_cost(pipeschedule(2)),... % with repair/replacement
    bit_cost(pipeschedule(3))];      % of damaged drill bit ($)
cementcost=(80*.75*1.506);       % cost for concrete poured
                                   % ($/m^3), [25% by weight
                                   % H2O, 1.506 kg/m^3 wet]

billingrate=4200;               % cost factor of time ($/hr)
emplacementbilling1=billingrate*2.5; % cost multiplier while handling
                                   % waste canisters ($/hr)
emplacementbilling2=billingrate*1.15; % cost multiplier while lowering
                                   % waste canisters ($/hr)

casingspeed=350;                % speed of lowering casing (m/hr)
casingcost=6;                   % steel casing material cost ($/kg)
lowerspeed=350;                 % speed of lowering bits (m/hr)
wastespeed1=25;                 % speed of lowering string (m/hr)
cementspeed=10;                 % cement speed (m^3/hr)
cementcure=84;                  % curetime needed for cement (hr)

```

```

overburden=500; % depth to granite formation (m)
lateraloffset=30; % required vertical spacing
                    % between lateral kickoffs (m)
kickoffdepth=(no_laterals-1)*... % calculate the depth of deepest
    lateraloffset+overburden+... % lateral start (m)
    pluglength+100;
kickcement=48; % time to cement for kickoff
latplug=72; % time to plug the lateral (hr)
boreholeplug=240; % time to plug the borehole (hr)
plugcost=1000000; % Additional plug cost
phasedelay=192; % Additional completion time at end
                    % of each phase
closeoutcosts=2000000; % Final cleanup/closure costs ($)
wastespeed2=casingspeed*.5; % Handling speed of waste once 100m
                    % into hole (no remote handling)

%% Determine the turn radius to permit 10 meter lateral liner to make bend

% minimum radius of curvature for lateral to allow casing placement (m)
turnradius=radii(pipeschedule(3)-7);

% calculate distance drilled during transition to lateral
kickoffarc=turnradius*(90-declination)*pi/180;

%% Initialize Parameters
cementtally=0; % Total volume of cement (m^3)
casingtally=0; % Total mass of casing steel (kg)
depthtimecosthist=zeros(20,3); % Time and cost history matrix
                    % (depth, time, cost)
depthtimecosthist(1,3)=changeoutcost(1);
index=2; % for indexing the hist matrix

%% Drill surface shaft
disttogo=surfdepth;

% Determine the time to drill the surface shaft
while 1==1

```



```

    surfspeed=normrnd(mu_sed(pipeschedule(1)),sd_sed(pipeschedule(1)));
    if surfspeed >= 0
        break
    end
end
while l==1
    % Determine if failure occurs during the drilling of the surface shaft
    ttf=200-lognrnd(log(100),.15);
    if ttf>(disttogo/surfspeed)
        depthtimecosthist(index,:)=[surfdepth,depthtimecosthist(index-1,...
            2)+disttogo/surfspeed,depthtimecosthist(index-1,3)+disttogo/...
            surfspeed*billingrate];
        index=index+1;
        break
    else
        disttogo=disttogo-ttf*surfspeed;
        depthtimecosthist(index,:)=[depthtimecosthist(index-1,1)+ttf*...
            surfspeed,depthtimecosthist(index-1,2)+ttf,...
            depthtimecosthist(index-1,3)+ttf*billingrate];
        index=index+1;
        depthtimecosthist(index,:)=[depthtimecosthist(index-1,1),...
            depthtimecosthist(index-1,2)+depthtimecosthist(index-1,1)...
            /backhaul+depthtimecosthist(index-1,1)/lowerspeed,...
            depthtimecosthist(index-1,3)+(depthtimecosthist(index-1,1)...
            /backhaul+depthtimecosthist(index-1,1)/lowerspeed)*...
            billingrate+changeoutcost(1)];
        index=index+1;
    end
end

end

%% Back out surface drill string

depthtimecosthist(index,:)=depthtimecosthist(index-1,:)+[0,(surfdepth/...
    backhaul),(surfdepth/backhaul*billingrate)];
index=index+1;

%% Emplace surf casing

```

```

casingmass=surfdepth*casing_mass(pipeschedule(1));
depthtimecosthist(index,:)=depthtimecosthist(index-1,:)+[0,(surfdepth/...
    casingspeed),(surfdepth/casingspeed)*billingrate+casingmass*...
    casingcost];
casingtally=casingtally+casingmass;
index=index+1;

%% Cement surf casing

% Calculate cement volume (annulus)
Vsurfcement=(Holes(pipeschedule(1))^2 - ODs(pipeschedule(1))^2)*...
    surfdepth*0.00064516/4*pi;
depthtimecosthist(index,:)=depthtimecosthist(index-1,:)+[0,(cementcure+...
    Vsurfcement/cementspeed),(cementcure+Vsurfcement/cementspeed)*...
    billingrate+cementcost*Vsurfcement];
cementtally=cementtally+Vsurfcement;
index=index+1;

%% Lower vertical drill string

depthtimecosthist(index,:)=depthtimecosthist(index-1,:)+[0,(surfdepth/...
    lowerspeed),(surfdepth/lowerspeed*billingrate)+changeoutcost(2)];
index=index+1;

%% Drill main vertical shaft

% Determine the time to drill the main shaft

% Sedimentary Overburden portion
while 1==1
    mainspeedsed=normrnd(mu_sed(pipeschedule(2)),sd_sed(pipeschedule(2)));
    if mainspeedsed >= 0
        break
    end
end
end

```

```

disttogo=overburden-surfdepth;
while l==1
    % Determine if failure occurs during the drilling of the main shaft
    ttf=200-lognrnd(log(100),.15);
    if ttf>(disttogo/mainspeedsed)
        depthtimecosthist(index,:)= [overburden,...
            depthtimecosthist(index-1,2)+disttogo/mainspeedsed,...
            depthtimecosthist(index-1,3)+disttogo/mainspeedsed*...
            billingrate];
        index=index+1;
        break
    else
        disttogo=disttogo-ttf*mainspeedsed;
        depthtimecosthist(index,:)= [depthtimecosthist(index-1,1)+ttf*...
            mainspeedsed,depthtimecosthist(index-1,2)+ttf,...
            depthtimecosthist(index-1,3)+ttf*billingrate];
        index=index+1;
        depthtimecosthist(index,:)= [depthtimecosthist(index-1,1),...
            depthtimecosthist(index-1,2)+depthtimecosthist(index-1,1)/...
            backhaul+depthtimecosthist(index-1,1)/lowerspeed,...
            depthtimecosthist(index-1,3)+(depthtimecosthist(index-1,1)/...
            backhaul+depthtimecosthist(index-1,1)/lowerspeed)*...
            billingrate+changeoutcost(2)];
        index=index+1;
    end
end

% Granite portion
while l==1
    mainspeedgran=normrnd(mu_gran(pipeschedule(2)),...
        sd_gran(pipeschedule(2)));
    if mainspeedgran >= 0
        break
    end
end

disttogo=kickoffdepth-overburden;
while l==1
    % Determine if a failure occurs during the drilling of the main shaft

```

```

tff=76-lognrnd(log(38),.1);
if tff>(disttogo/mainspeedgran)
    depthtimecosthist(index,:)= [kickoffdepth,...
        depthtimecosthist(index-1,2)+disttogo/mainspeedgran,...
        depthtimecosthist(index-1,3)+disttogo/mainspeedgran*...
        billingrate];
    index=index+1;
    break
else
    disttogo=disttogo-ttf*mainspeedgran;
    depthtimecosthist(index,:)= [depthtimecosthist(index-1,1)+ttf*...
        mainspeedgran,depthtimecosthist(index-1,2)+ttf,...
        depthtimecosthist(index-1,3)+ttf*billingrate];
    index=index+1;
    depthtimecosthist(index,:)= [depthtimecosthist(index-1,1),...
        depthtimecosthist(index-1,2)+depthtimecosthist(index-1,1)/...
        backhaul+depthtimecosthist(index-1,1)/lowerspeed,...
        depthtimecosthist(index-1,3)+(depthtimecosthist(index-1,1)/...
        backhaul+depthtimecosthist(index-1,1)/lowerspeed)*...
        billingrate+changeoutcost(2)];
    index=index+1;
end
end

%% Back out drill string

depthtimecosthist(index,:)=depthtimecosthist(index-1,:)+[0,(kickoffdepth...
    /backhaul),(kickoffdepth/backhaul*billingrate)];
index=index+1;

%% Emplace casing

casingmass=(kickoffdepth-surfdepth)*casing_mass(pipeschedule(2));
depthtimecosthist(index,:)=depthtimecosthist(index-1,:)+[0,(kickoffdepth...
    /casingspeed),(kickoffdepth/casingspeed)*billingrate+casingmass...
    *casingcost];
casingtally=casingtally+casingmass;

```

```

index=index+1;

%% Cement lower casing

% Calculate cement volume (annulus) (only portions below plug zone)
Vmaincement=(Holes(pipeschedule(2))^2 - ODs(pipeschedule(2))^2)*...
    (kickoffdepth-pluglength-surfdepth)*0.00064516/4*pi;
depthtimecosthist(index,:)=depthtimecosthist(index-1,:)+[0,(cementcure+...
    Vmaincement/cementspeed),(cementcure+Vmaincement/cementspeed)*...
    billingrate+cementcost*Vmaincement];
cementtally=cementtally+Vmaincement;
index=index+1;

%% Repeat for laterals:

for j=1:no_laterals
    %% Cement for kickoff

    depthtimecosthist(index,:)=depthtimecosthist(index-1,:)+[0,...
        (kickcement),(kickcement*billingrate)+changeoutcost(3)];
    index=index+1;

    %% Lower lateral drill string

    depthtimecosthist(index,:)=depthtimecosthist(index-1,:)+[0,...
        (kickoffdepth/lowerspeed),(kickoffdepth/lowerspeed*billingrate)];
    index=index+1;

    %% Drill through to lateral declination

    % Determine the time to drill the radial shaft
    while l==1
        latspeed=normrnd(mu_gran(pipeschedule(3)),...
            sd_gran(pipeschedule(3)));
        if latspeed >= 0
            break

```

```

    end
end
latspeed=latspeed/2;          % a factor of 2 is included to incorporate
                              % difficulty of turning radius
disttogo=kickoffarc;
while 1==1
    % Determine if a failure occurs during the drilling of the radial
    % kickoff
    ttf=76-lognrnd(log(38),.1);
    if ttf>(disttogo/latspeed)
        depthtimecosthist(index,:)=[kickoffdepth+kickoffarc,...
            depthtimecosthist(index-1,2)+disttogo/latspeed,...
            depthtimecosthist(index-1,3)+disttogo/latspeed...
            *billingrate];
        index=index+1;
        break
    else
        disttogo=disttogo-ttf*latspeed;
        depthtimecosthist(index,:)=[depthtimecosthist(index-1,1)+...
            ttf*latspeed,depthtimecosthist(index-1,2)+ttf,...
            depthtimecosthist(index-1,3)+ttf*billingrate];
        index=index+1;
        depthtimecosthist(index,:)=[depthtimecosthist(index-1,1),...
            depthtimecosthist(index-1,2)+depthtimecosthist(index-...
            1,1)/backhaul+depthtimecosthist(index-1,1)/lowerspeed,...
            depthtimecosthist(index-1,3)+(depthtimecosthist(index-...
            1,1)/backhaul+depthtimecosthist(index-1,1)/lowerspeed)...
            *billingrate+changeoutcost(3)];
        index=index+1;
    end
end

%% Drill lateral

% Determine the time to drill the remainder of the lateral shaft
latspeed=latspeed*2;          % factor of 2 removed
disttogo=emplacementlength;
while 1==1

```

```

% Determine if a failure occurs during the drilling of the lateral
ttf=76-lognrnd(log(38),.1);
if ttf>(disttogo/latspeed)
    depthtimecosthist(index,:)= [kickoffdepth+kickoffarc+...
        emplacementlength,depthtimecosthist(index-1,2)+disttogo/...
        latspeed,depthtimecosthist(index-1,3)+disttogo/latspeed*...
        billingrate];
    index=index+1;
    break
else
    disttogo=disttogo-ttf*latspeed;
    depthtimecosthist(index,:)= [depthtimecosthist(index-1,1)+ttf...
        *latspeed,depthtimecosthist(index-1,2)+ttf,...
        depthtimecosthist(index-1,3)+ttf*billingrate];
    index=index+1;
    depthtimecosthist(index,:)= [depthtimecosthist(index-1,1),...
        depthtimecosthist(index-1,2)+depthtimecosthist(index-...
        1,1)/backhaul+depthtimecosthist(index-1,1)/lowerspeed,...
        depthtimecosthist(index-1,3)+(depthtimecosthist(index-...
        1,1)/backhaul+depthtimecosthist(index-1,1)/lowerspeed)*...
        billingrate+changeoutcost(3)];
    index=index+1;
end
end

%% Back out drill string

depthtimecosthist(index,:)=depthtimecosthist(index-1,:)+[0,...
    (kickoffdepth+kickoffarc+emplacementlength)/backhaul,...
    ((kickoffdepth+kickoffarc+emplacementlength)/backhaul...
    *billingrate)];
index=index+1;

%% Emplace lateral casing
casingmass=(emplacementlength+kickoffarc)*casing_mass(pipeschedule(3));
depthtimecosthist(index,:)=depthtimecosthist(index-1,:)+[0,...
    (kickoffdepth/casingspeed+(kickoffarc+emplacementlength)/...

```

```

        (casingspeed))+phasedelay, (kickoffdepth/casingspeed+...
        ((kickofffarc+emplacementlength)/(casingspeed)+phasedelay)*...
        billingrate)+casingmass*casingcost];
casingtally=casingtally+casingmass;
index=index+1;

%% Emplace waste canisters

depthtimecosthist(index,:)=depthtimecosthist(index-1,:)+[0,...
    (emplacementlength+100)/wastespeed1+(kickoffdepth+kickofffarc-...
    100)/wastespeed2, (emplacementlength+100)/wastespeed1*...
    emplacementbilling1+(kickoffdepth+kickofffarc-100)/wastespeed2...
    *emplacementbilling2];
index=index+1;

%% Plug lateral

depthtimecosthist(index,:)=depthtimecosthist(index-1,:)+[0,latplug,...
    latplug*billingrate];
depthtimecosthist(index,1)=kickoffdepth;
index=index+1;
kickoffdepth=kickoffdepth-lateraloffset;

end

%% Back out vertical casing (above cemented region)

depthtimecosthist(index,:)=depthtimecosthist(index-1,:)+[0,...
    (pluglength+surfdepth)/backhaul, (pluglength+surfdepth)/...
    backhaul*billingrate+closeoutcosts];
depthtimecosthist(index,1)=pluglength+surfdepth;
index=index+1;

%% Plug borehole

depthtimecosthist(index,:)=depthtimecosthist(index-1,:)+[0,...
    boreholeplug,boreholeplug*billingrate+plugcost];

```



```
depthtimecosthist(index,1)=0;  
wasteparam=wastemass(emplacemlength,no_laterals,pipeschedule,IDs,...  
    PWR_frac,Vit_frac,rho_vit);  
drillparam=[casingtally cementtally];
```

A.2.3 Lateral Repository Trade Space Study Script (drilling_costs.m)

```
%%%%%%%%%%%%%%%%%%%%%%%%%%%%%%%%%%%%%%%%%%%%%%%%%%%%%%%%%%%%%%%%%%%%%%%%
% Lateral waste emplacement %
%   Drilling cost script   %
%   Jonathan S Gibbs      %
%       2009-2010         %
%%%%%%%%%%%%%%%%%%%%%%%%%%%%%%%%%%%%%%%%%%%%%%%%%%%%%%%%%%%%%%%%%%%%%%%%

clear
clc
close all
format compact

%% Parameter Initialization

load in.mat % loads parameters previously
            % imported from Excel

load radii.mat % loads minimum radii by
              % geometry of the trial

Vit_frac=.2; % fraction of canisters with
            % vitrified wasteform

PWR_frac=.64*(1-Vit_frac); % fractin of canisters with
                          % PWR waste

vit_load=.25; % waste loading of vitrified
             % waste by mass (i.e. 25% of
             % vitrified mass is waste

output=0; % determines whether trial is
         % plotted

index=1; % tracking parameter

%% Trade-space Generation

% This part of the script will bound the trade-space by plug length,
% emplacement length, declination angle of lateral, number of laterals per
% vertical hole, which combinations of pipe schedules to try, and how many
% realizations (trials) should be conducted for each combination of the
```

```

% above parameters

% Vertical plug length required (m)
min_plug_length=1500;
max_plug_length=1500;
plug_length_trials=1;
pluglength=linspace(min_plug_length,...
    max_plug_length,plug_length_trials);

% Shaft length of lateral required (m)
min_emplacement_length=1500;
max_emplacement_length=2500;
emplacement_length_trials=3;
emplacmentlength=linspace(min_emplacement_length,max_emplacement_length,...
    emplacement_length_trials);

% Declination angle of lateral emplacement (degrees from horizontal)
min_declin=20;
max_declin=50;
declin_trials=4;
declination=linspace(min_declin,max_declin,declin_trials);

% Number of lateral emplacements used per main shaft
min_laterals=10;
max_laterals=12;
no_laterals=min_laterals:1:max_laterals;

% Pipe schedule combinations to study
pipeavail=1:2;
pipeschedule=zeros(length(pipeavail),3);
% indexing matrix to determine bits and casings used
for m=1:length(pipeavail)
    pipeschedule(m,:)=pipecombos(pipeavail(m),:);
end

% Number of individual realizations for each combination
no_realizations=5;

```

```

% Total size of the trade-space
spacesize=length(no_laterals)*length(pluglength)*length(emplacemlength)...
    *length(declination)*size(pipeschedule,1)*no_realizations;
% Initialize the tracker matrix
tracker=zeros(spacesize,16);           % output matrix for key results
                                       % from each trial

%% Trade-space study

if output==1
    figure('Position',[100 100 750 900])
end
% For each trial in the trade-space (for each realization) calculate the
% results from the drill_bit_life.m and wastemass.m scripts
for i=1:length(no_laterals)
    for j=1:length(pluglength)
        for k=1:length(emplacemlength)
            for l=1:length(declination)
                for m=1:size(pipeschedule,1)
                    for n=1:no_realizations
                        [depthtimecosthist,drillparam,wasteparam]=...
                            drill_bit_life(pluglength(j),...
                                emplacemlength(k),declination(l),...
                                no_laterals(i),pipeschedule(m,:),ODs,Holes,...
                                IDs,mu_sed,mu_gran,sd_gran,sd_sed,PWR_frac,...
                                Vit_frac,vit_load,casing_mass,bit_cost,radii);
                        time=depthtimecosthist(size(depthtimecosthist,1)...
                            ,2)/24/wasteparam(1);
                        cost=depthtimecosthist(size(depthtimecosthist,1)...
                            ,3)/wasteparam(1);
                        tracker(index,:)=[time,cost,drillparam,wasteparam...
                            ,pluglength(j),emplacemlength(k),...
                            declination(l),no_laterals(i),...
                            Holes(pipeschedule(m,1)),...
                            Holes(pipeschedule(m,2)),...
                            Holes(pipeschedule(m,3))];
                    end
                end
            end
        end
    end
end
%% Output
% If plotting is desired, plot the history of depth

```

```

% vs. time and cost for the most recent trial
if output==1
    depthtimecosthist(:,2)=depthtimecosthist(:,2)...
        /24;
    subplot(3,1,1)
    figure(1)
    hold on
    plot(depthtimecosthist(:,2),-...
        depthtimecosthist(:,1),'LineWidth',2)
    xlabel('\fontsize{10}\bfTime (days)')
    ylabel(['\fontsize{10}\bfTotal Pathlength'...
        ' Hole Depth (m)'])
    grid on
    title(['\fontsize{14}\bfSample Repository'...
        ' Drilling Cost and Time Simulation'])
    subplot(3,1,2)
    hold on
    plot(depthtimecosthist(:,3)/1e6,...
        -depthtimecosthist(:,1),'LineWidth',2)
    xlabel('\fontsize{10}\bfCost ($M)')
    ylabel(['\fontsize{10}\bfTotal Pathlength'...
        ' Hole Depth (m)'])
    grid on
    subplot(3,1,3)
    hold on
    plot(depthtimecosthist(:,2),...
        depthtimecosthist(:,3)/wasteparam(1)/...
        1e3,'LineWidth',2)
    xlabel('\fontsize{10}\bfTime (days)')
    ylabel('\fontsize{10}\bfCost ($/kgHM)')
    grid on
end
index=index+1;
end
end
(index-1)/spacesize*100
% outputs to the screen a progress indication
end

```

```
        end
    end
end

% save all results for use in plotting later
save final.mat tracker spacesize no_realizations declin_trials...
    declination emplacement_length_trials emplacementlength no_laterals
```

A.2.4 Drilling Cost Realization Script for EGS Borehole (drill_egs.m)

```
function [depthtimecosthist,drillparam] =
drill_egs(ODs,Holes,mu_sed,mu_gran,sd_gran,sd_sed,casing_mass,bit_cost)

%%%%%%%%%%%%%%%%%%%%%%%%%%%%%%%%%%%%%%%%%%%%%%%%%%%%%%%%%%%%%%%%%%%%%%%%
% This function executes a Monte Carlo simulation of drilling a single      %
% vertical shaft EGS borehole based on the inputs from the                 %
% drilling_costs_egs.m script and outputs the simulated drilling progress  %
% in cost and time vs. depth                                             %
%%%%%%%%%%%%%%%%%%%%%%%%%%%%%%%%%%%%%%%%%%%%%%%%%%%%%%%%%%%%%%%%%%%%%%%%

%% Drilling Parameters

backhaul=350; % backhaul speed (m/hr)
conductordepth=15.24; % depth of conductor hole (m)
surfdepth=152.4; % depth of surface hole (m)
intdepth=1524; % depth of intermediate hole (m)
prod1depth=3048; % depth of production hole 1 (m)
prod2depth=5181.6; % depth of production hole 2 (m)
prod3depth=6096; % depth of production hole 3 (m)
changeout=0; % delay time lost on the surface after
backhauling a drill bit
pipeschedule=[15 16 1 4 8 12]; % calls out the pipes to be used in the EGS
% comparison hole
changeoutcost=[bit_cost(... % additional cost associated with repair/
pipeschedule(1)),... %replacement of damaged drill bit ($)
bit_cost(pipeschedule(2)),...
bit_cost(pipeschedule(3)),...
bit_cost(pipeschedule(4)),...
bit_cost(pipeschedule(5)),...
bit_cost(pipeschedule(6))];
cementcost=(80*.75*1.506); % cost for concrete poured ($/m^3)
% [25% by weight H2O, 1.506 kg/m^3 wet]
billingrate=4200; % cost multiplier of time ($/hr)
casingspeed=350; % speed of lowering casing (m/hr)
```

```

casingcost=6; % steel casing material cost ($/kg)
lowerspeed=350; % speed of lowering drill bits (m/hr)
cementspeed=10; % pumping speed of cement (m^3/hr)
cementcure=48; % curetime required for cementing (hr)
overburden=500; % depth to granite formation (m)
cementtally=0; % Total volume of cement (m^3)
casingtally=0; % Total mass of casing used (kg)
phasedelay=192; % Additional delay time at end of each phase
closeoutcosts=2000000; % Final cleanup and closure costs ($M)
depthtimecosthist=zeros(20,3); % preallocates the time and cost history
% matrix (depth, time, cost)

depthtimecosthist(1,3)=...
    changeoutcost(1);
index=2; % this parameter will index the hist matrix

%% Drill Conductor shaft

disttogo=conductordepth;
% Determine the time to drill the conductor shaft
while l==1
    condspeed=normrnd(mu_sed(pipeschedule(1)),sd_sed(pipeschedule(1)));
    if condspeed >= 0
        break
    end
end
while l==1
    % Determine if a failure occurs during the drilling of the conductor
shaft
    ttf=200-lognrnd(log(100),.15);
    if ttf>(disttogo/condspeed)
        depthtimecosthist(index,:)=[conductordepth,...
            depthtimecosthist(index-1,2)+disttogo/condspeed,...
            depthtimecosthist(index-1,3)+disttogo/condspeed*billingrate];
        index=index+1;
        break
    else
        disttogo=disttogo-ttf*condspeed;
        depthtimecosthist(index,:)=[depthtimecosthist(index-1,1)+ttf*...

```



```

        condspeed,depthtimecosthist(index-1,2)+ttf,...
        depthtimecosthist(index-1,3)+ttf*billingrate];
    index=index+1;
    depthtimecosthist(index,:)=depthtimecosthist(index-1,1),...
        depthtimecosthist(index-1,2)+depthtimecosthist(index-1,1)/...
        backhaul+depthtimecosthist(index-1,1)/lowerspeed+changeout,...
        depthtimecosthist(index-1,3)+(changeout+depthtimecosthist(...
        index-1,1)/backhaul+depthtimecosthist(index-1,1)/lowerspeed)...
        *billingrate+changeoutcost(1)];
    index=index+1;
end
end

%% Back out drill string

depthtimecosthist(index,:)=depthtimecosthist(index-1,:)+[0,...
    (conductordepth/backhaul),(conductordepth/backhaul*billingrate)];
index=index+1;

%% Emplace conductor casing

casingmass=conductordepth*casing_mass(pipeschedule(1));
depthtimecosthist(index,:)=depthtimecosthist(index-1,:)+[0,...
    (conductordepth/casingspeed),(conductordepth/casingspeed)*...
    billingrate+casingmass*casingcost];
casingtally=casingtally+casingmass;
index=index+1;

%% Cement conductor casing

% Calculate cement volume (annulus)
Vcondcement=(Holes(pipeschedule(1))^2 - ODs(pipeschedule(1))^2)*...
    conductordepth*0.00064516/4*pi;
depthtimecosthist(index,:)=depthtimecosthist(index-1,:)+[0,...
    (cementcure+Vcondcement/cementspeed),(cementcure+Vcondcement/...
    cementspeed)*billingrate+cementcost*Vcondcement];
cementtally=cementtally+Vcondcement;

```

```

index=index+1;

%% Lower vertical drill string

depthtimecosthist(index,:)=depthtimecosthist(index-1,:)+[0,...
    conductordepth/lowerspeed, (conductordepth/lowerspeed*...
    billingrate)+changeoutcost(2)];
index=index+1;

%% Drill Surf shaft

disttogo=surfdepth-conductordepth;
% Determine the time to drill the surface shaft
while 1==1
    surfspeed=normrnd(mu_sed(pipeschedule(2)),sd_sed(pipeschedule(2)));
    if surfspeed >= 0
        break
    end
end
while 1==1
    % Determine if a failure occurs during the drilling of the surface shaft
    ttf=200-lognrnd(log(100),.15);
    if ttf>(disttogo/surfspeed)
        depthtimecosthist(index,:)=[surfdepth,depthtimecosthist(index-...
            1,2)+disttogo/surfspeed,depthtimecosthist(index-1,3)+...
            disttogo/surfspeed*billingrate];
        index=index+1;
        break
    else
        disttogo=disttogo-ttf*surfspeed;
        depthtimecosthist(index,:)=[depthtimecosthist(index-1,1)+ttf*...
            surfspeed,depthtimecosthist(index-1,2)+ttf,depthtimecosthist(...
            index-1,3)+ttf*billingrate];
        index=index+1;
        depthtimecosthist(index,:)=[depthtimecosthist(index-1,1),...
            depthtimecosthist(index-1,2)+depthtimecosthist(index-1,1)/...
            backhaul+depthtimecosthist(index-1,1)/lowerspeed+changeout,...

```

```

        depthtimecosthist(index-1,3)+(changeout+depthtimecosthist(...
        index-1,1)/backhaul+depthtimecosthist(index-1,1)/lowerspeed)*...
        billingrate+changeoutcost(1)];
    index=index+1;
end
end

%% Back out drill string

depthtimecosthist(index,:)=depthtimecosthist(index-1,:)+[0,(surfdepth/...
    backhaul),(surfdepth/backhaul*billingrate)];
index=index+1;

%% Emplace surf casing

casingmass=surfdepth*casing_mass(pipeschedule(2));
depthtimecosthist(index,:)=depthtimecosthist(index-1,:)+[0,(surfdepth/...
    casingspeed),(surfdepth/casingspeed)*billingrate+casingmass*casingcost];
casingtally=casingtally+casingmass;
index=index+1;

%% Cement surf casing

% Calculate cement volume (annulus)
Vsurfcement=(Holes(pipeschedule(2))^2 - ODs(pipeschedule(2))^2)*...
    surfdepth*0.00064516/4*pi;
depthtimecosthist(index,:)=depthtimecosthist(index-1,:)+[0,(cementcure+...
    Vsurfcement/cementspeed),(cementcure+Vsurfcement/cementspeed)*...
    billingrate+cementcost*Vsurfcement];
cementtally=cementtally+Vsurfcement;
index=index+1;

%% Lower vertical drill string

depthtimecosthist(index,:)=depthtimecosthist(index-1,:)+[0,(surfdepth/...
    lowerspeed),(surfdepth/lowerspeed*billingrate)+changeoutcost(3)];

```

```

index=index+1;

%% Drill Intermediate shaft

% Determine the time to drill the intermediate shaft

% Overburden portion
while l==1
    intspeedsed=normrnd(mu_sed(pipeschedule(3)),sd_sed(pipeschedule(3)));
    if intspeedsed >= 0
        break
    end
end
disttogo=overburden-surfdepth;
while l==1
    % Determine if a failure occurs during the drilling of the surface shaft
    ttf=200-lognrnd(log(100),.15);
    if ttf>(disttogo/intspeedsed)
        depthtimecosthist(index,:)= [overburden,depthtimecosthist(index-1,...
            2)+disttogo/intspeedsed,depthtimecosthist(index-1,3)+disttogo/...
            intspeedsed*billingrate];
        index=index+1;
        break
    else
        disttogo=disttogo-ttf*prodl speedsed;
        depthtimecosthist(index,:)= [depthtimecosthist(index-1,1)+ttf*...
            intspeedsed,depthtimecosthist(index-1,2)+ttf,...
            depthtimecosthist(index-1,3)+ttf*billingrate];
        index=index+1;
        depthtimecosthist(index,:)= [depthtimecosthist(index-1,1),...
            depthtimecosthist(index-1,2)+depthtimecosthist(index-1,1)/...
            backhaul+depthtimecosthist(index-1,1)/lowerspeed+changeout,...
            depthtimecosthist(index-1,3)+(depthtimecosthist(index-1,1)/...
            backhaul+depthtimecosthist(index-1,1)/lowerspeed+changeout)*...
            billingrate+changeoutcost(3)];
        index=index+1;
    end
end

```

```

end

% Granite portion
while l==1
    intspeedgran=normrnd(mu_gran(pipeschedule(3)),sd_gran(pipeschedule(3)));
    if intspeedgran >= 0
        break
    end
end
disttogo=intdepth-overburden;
while l==1
    % Determine if failure occurs when drilling of the intermediate shaft
    ttf=76-lognrnd(log(38),.1);
    if ttf>(disttogo/intspeedgran)
        depthtimecosthist(index,:)=[intdepth,depthtimecosthist(index-...
            1,2)+disttogo/intspeedgran,depthtimecosthist(index-1,3)+...
            disttogo/intspeedgran*billingrate];
        index=index+1;
        break
    else
        disttogo=disttogo-ttf*intspeedgran;
        depthtimecosthist(index,:)=[depthtimecosthist(index-1,1)+ttf*...
            intspeedgran,depthtimecosthist(index-1,2)+ttf,...
            depthtimecosthist(index-1,3)+ttf*billingrate];
        index=index+1;
        depthtimecosthist(index,:)=[depthtimecosthist(index-1,1),...
            depthtimecosthist(index-1,2)+depthtimecosthist(index-1,1)/...
            backhaul+depthtimecosthist(index-1,1)/lowerspeed+changeout,...
            depthtimecosthist(index-1,3)+(depthtimecosthist(index-1,1)/...
            backhaul+depthtimecosthist(index-1,1)/lowerspeed+changeout)...
            *billingrate+changeoutcost(3)];
        index=index+1;
    end
end

end

%% Back out drill string

```

```

depthtimecosthist(index,:)=depthtimecosthist(index-1,:)+[0,(intdepth/...
    backhaul),(intdepth/backhaul*billingrate)];
index=index+1;

%% Emplace casing

casingmass=intdepth*casing_mass(pipeschedule(3));
depthtimecosthist(index,:)=depthtimecosthist(index-1,:)+[0,(intdepth/...
    casingspeed),(intdepth/casingspeed)*billingrate+casingmass*casingcost];
index=index+1;
depthtimecosthist(index,:)=depthtimecosthist(index-1,:)+[0,phasedelay,...
    phasedelay*billingrate];
casingtally=casingtally+casingmass;
index=index+1;

%% Cement casing

% Calculate cement volume (annulus)
Vintcement=(Holes(pipeschedule(3))^2 - ODs(pipeschedule(3))^2)*intdepth*...
    0.00064516/4*pi;
depthtimecosthist(index,:)=depthtimecosthist(index-1,:)+[0,(cementcure+...
    Vintcement/cementspeed),(cementcure+Vintcement/cementspeed)*...
    billingrate+cementcost*Vintcement];
cementtally=cementtally+Vintcement;
index=index+1;

%% Lower vertical drill string

depthtimecosthist(index,:)=depthtimecosthist(index-1,:)+[0,(intdepth/...
    lowerspeed),(intdepth/lowerspeed*billingrate)+changeoutcost(4)];
index=index+1;

%% Drill production shaft 1

% Determine the time to drill the production shaft 1
while l==1

```

```

    prodlspeedgran=normrnd(mu_gran(pipeschedule(4)),sd_gran(...
        pipeschedule(4)));
    if prodlspeedgran >= 0
        break
    end
end
disttogo=prodldepth-intdepth;
while l==1
    % Determine if failure occurs during the drilling of production shaft 1
    ttf=76-lognrnd(log(38),.1);
    if ttf>(disttogo/prodlspeedgran)
        depthtimecosthist(index,:)=[prodldepth,depthtimecosthist(index-...
            1,2)+disttogo/prodlspeedgran,depthtimecosthist(index-1,3)+...
            disttogo/prodlspeedgran*billingrate];
        index=index+1;
        break
    else
        disttogo=disttogo-ttf*prodlspeedgran;
        depthtimecosthist(index,:)=[depthtimecosthist(index-1,1)+ttf*...
            prodlspeedgran,depthtimecosthist(index-1,2)+ttf,...
            depthtimecosthist(index-1,3)+ttf*billingrate];
        index=index+1;
        depthtimecosthist(index,:)=[depthtimecosthist(index-1,1),...
            depthtimecosthist(index-1,2)+depthtimecosthist(index-1,1)/...
            backhaul+depthtimecosthist(index-1,1)/lowerspeed+changeout,...
            depthtimecosthist(index-1,3)+(depthtimecosthist(index-1,1)/...
            backhaul+depthtimecosthist(index-1,1)/lowerspeed+changeout)...
            *billingrate+changeoutcost(4)];
        index=index+1;
    end
end

%% Back out drill string

depthtimecosthist(index,:)=depthtimecosthist(index-1,:)+[0,(prodldepth/...
    backhaul),(prodldepth/backhaul*billingrate)];
index=index+1;

```

```

%% Emplace casing

casingmass=prodldepth*casing_mass(pipeschedule(4));
depthtimecosthist(index,:)=depthtimecosthist(index-1,:)+[0,(prodldepth/...
    casingspeed),(prodldepth/casingspeed)*billingrate+casingmass*...
    casingcost];
casingtally=casingtally+casingmass;
index=index+1;

%% Cement casing

% Calculate cement volume (annulus)
Vprodlcement=(Holes(pipeschedule(4))^2 - ODs(pipeschedule(4))^2)*...
    prodldepth*0.00064516/4*pi;
depthtimecosthist(index,:)=depthtimecosthist(index-1,:)+[0,(cementcure+...
    Vprodlcement/cementspeed),(cementcure+Vprodlcement/cementspeed)*...
    billingrate+cementcost*Vprodlcement];
index=index+1;
depthtimecosthist(index,:)=depthtimecosthist(index-1,:)+[0,phasedelay,...
    phasedelay*billingrate];
cementtally=cementtally+Vprodlcement;
index=index+1;

%% Lower vertical drill string

depthtimecosthist(index,:)=depthtimecosthist(index-1,:)+[0,(prodldepth/...
    lowerspeed),(prodldepth/lowerspeed*billingrate)+changeoutcost(5)];
index=index+1;

%% Drill production shaft 2

% Determine the time to drill the production shaft 2

while l==1

```



```

prod2speedgran=normrnd(mu_gran(pipeschedule(5)),sd_gran(pipeschedule(5)));
    if prod2speedgran >= 0
        break
    end
end
disttogo=prod2depth-prod1depth;
while 1==1
    % Determine if a failure occurs during the drilling of the main shaft
    ttf=76-lognrnd(log(38),.1);
    if ttf>(disttogo/prod2speedgran)
        depthtimecosthist(index,:)=[prod2depth,depthtimecosthist(index-...
            1,2)+disttogo/prod2speedgran,depthtimecosthist(index-1,3)+...
            disttogo/prod2speedgran*billingrate];
        index=index+1;
        break
    else
        disttogo=disttogo-ttf*prod2speedgran;
        depthtimecosthist(index,:)=[depthtimecosthist(index-1,1)+ttf*...
            prod2speedgran,depthtimecosthist(index-1,2)+ttf,...
            depthtimecosthist(index-1,3)+ttf*billingrate];
        index=index+1;
        depthtimecosthist(index,:)=[depthtimecosthist(index-1,1),...
            depthtimecosthist(index-1,2)+depthtimecosthist(index-1,1)/...
            backhaul+depthtimecosthist(index-1,1)/lowerspeed+changeout,...
            depthtimecosthist(index-1,3)+(depthtimecosthist(index-1,1)/...
            backhaul+depthtimecosthist(index-1,1)/lowerspeed+changeout)...
            *billingrate+changeoutcost(5)];
        index=index+1;
    end
end

%% Back out drill string

depthtimecosthist(index,:)=depthtimecosthist(index-1,:)+[0,(prod2depth/...
    backhaul),(prod2depth/backhaul*billingrate)];
index=index+1;

```

```

%% Emplace casing

casingmass=(prod2depth-prod1depth)*casing_mass(pipeschedule(5));
depthtimecosthist(index,:)=depthtimecosthist(index-1,:)+[0,(prod2depth/...
    casingspeed),(prod2depth/casingspeed)*billingrate+casingmass*casingcost];
casingtally=casingtally+casingmass;index=index+1;

%% Cement casing

% Calculate cement volume (annulus)
Vprod2cement=(Holes(pipeschedule(5))^2 - ODs(pipeschedule(5))^2)*...
    (prod2depth-prod1depth)*0.00064516/4*pi;
depthtimecosthist(index,:)=depthtimecosthist(index-1,:)+[0,(cementcure+...
    Vprod2cement/cementspeed),(cementcure+Vprod2cement/cementspeed)*...
    billingrate+cementcost*Vprod2cement];
index=index+1;
depthtimecosthist(index,:)=depthtimecosthist(index-1,:)+[0,phasedelay,...
    phasedelay*billingrate];
cementtally=cementtally+Vprod2cement;
index=index+1;

%% Lower vertical drill string

depthtimecosthist(index,:)=depthtimecosthist(index-1,:)+[0,(prod2depth/...
    lowerspeed),(prod2depth/lowerspeed*billingrate)+changeoutcost(6)];
index=index+1;

%% Drill production shaft 3

% Determine the time to drill the production shaft 3
while 1==1
    prod3speedgran=normrnd(mu_gran(pipeschedule(6)),sd_gran(...
        pipeschedule(6)));
    if prod3speedgran >= 0
        break
    end
end

```

```

end
end
disttogo=prod3depth-prod2depth;
while l==1
    % Determine if a failure occurs during the drilling of the main shaft
    ttf=76-lognrnd(log(38),.1);
    if ttf>(disttogo/prod3speedgran)
        depthtimecosthist(index,:)= [prod3depth,depthtimecosthist(index-...
            1,2)+disttogo/prod3speedgran,depthtimecosthist(index-1,3)+...
            disttogo/prod3speedgran*billingrate];
        index=index+1;
        break
    else
        disttogo=disttogo-ttf*prod3speedgran;
        depthtimecosthist(index,:)= [depthtimecosthist(index-1,1)+ttf*...
            prod3speedgran,depthtimecosthist(index-1,2)+ttf,...
            depthtimecosthist(index-1,3)+ttf*billingrate];
        index=index+1;
        depthtimecosthist(index,:)= [depthtimecosthist(index-1,1),...
            depthtimecosthist(index-1,2)+depthtimecosthist(index-1,1)/...
            backhaul+depthtimecosthist(index-1,1)/lowerspeed+changeout,...
            depthtimecosthist(index-1,3)+(depthtimecosthist(index-1,1)/...
            backhaul+depthtimecosthist(index-1,1)/lowerspeed+changeout)*...
            billingrate+changeoutcost(6)];
        index=index+1;
    end
end

%% Back out drill string

depthtimecosthist(index,:)=depthtimecosthist(index-1,:)+[0,(prod3depth/...
    backhaul),(prod3depth/backhaul*billingrate)];
index=index+1;

%% Emplace casing

casingmass=(prod3depth-prod2depth)*casing_mass(pipeschedule(6));

```

```

depthtimecosthist(index,:)=depthtimecosthist(index-1,:)+[0,(prod3depth/...
    casingspeed),(prod3depth/casingspeed)*billingrate+casingmass*casingcost];
casingtally=casingtally+casingmass;
index=index+1;

%% Cement casing

% Calculate cement volume (annulus)
Vprod3cement=(Holes(pipeschedule(6))^2 - ODs(pipeschedule(6))^2)*(...
    prod3depth-prod2depth)*0.00064516/4*pi;
depthtimecosthist(index,:)=depthtimecosthist(index-1,:)+[0,(cementcure+...
    Vprod3cement/cementspeed),(cementcure+Vprod3cement/cementspeed)*...
    billingrate+cementcost*Vprod3cement];
index=index+1;
depthtimecosthist(index,:)=depthtimecosthist(index-1,:)+[0,phasedelay,...
    phasedelay*billingrate+closeoutcosts];
cementtally=cementtally+Vprod3cement;
drillparam=[casingtally cementtally];

```

A.2.5 EGS Borehole Trial Script (drilling_costs_egs.m)

```
%%%%%%%%%%%%%%%%%%%%%%%%%%%%%%%%%%%%%%%%%%%%%%%%%%%%%%%%%%%%%%%%%%%%%%%%
%           EGS Comparison           %
%   Drilling cost script             %
%   Jonathan S Gibbs                 %
%           2009-2010                 %
%%%%%%%%%%%%%%%%%%%%%%%%%%%%%%%%%%%%%%%%%%%%%%%%%%%%%%%%%%%%%%%%%%%%%%%%

% This script runs the overall cost model for the specific case of the EGS
% nominal borehole (20,000 ft deep well) presented in Sandia National
% Laboratories report SAND2008-7866, December 2008 and then plots 10 trials
% of these results against those from Sandia's report

%% Parameter Initialization
clear
clc
close all
format compact
load in.mat          % loads parameters previously imported from Excel
no_realizations=10;
output=1;
index=1;
tracker=zeros(no_realizations,4);
trackerheader=['time ', ' cost', ' casing_mass', ' cement_volume'];
if output==1
    figure('Position',[100 100 750 900])
end
for i=1:no_realizations
    [depthtimecosthist,drillparam]=drill_egs(ODs,Holes,mu_sed,mu_gran,...
        sd_gran,sd_sed,casing_mass,bit_cost);
    time=depthtimecosthist(size(depthtimecosthist,1),2)/24;
    cost=depthtimecosthist(size(depthtimecosthist,1),3);
    tracker(index,:)=time,cost,drillparam;
    %% Output
    if output==1
        depthtimecosthist(:,2)=depthtimecosthist(:,2)/24;
```

```

subplot(3,1,1)
figure(1)
hold on
plot(EGSdepthtimecost(:,2),-EGSdepthtimecost(:,1),'r--',...
     'LineWidth',2)
plot(depthtimecosthist(:,2),-depthtimecosthist(:,1),'LineWidth',1)
xlabel('\fontsize{10}\bfTime (days)')
ylabel('\fontsize{10}\bfTotal Hole Depth (m)')
grid on
title(['\fontsize{14}\bfEGS Reference Simulation Cost and Time'...
      ' Simulation'])
legend(['20,000 ft EGS Well','Borehole Drilling Cost'...
      ' Simulations'],'Location','SouthWest')
subplot(3,1,2)
hold on
plot(EGSdepthtimecost(:,3)/1e3,-EGSdepthtimecost(:,1),'r--',...
     'LineWidth',2)
plot(depthtimecosthist(:,3)/1e6,-depthtimecosthist(:,1),...
     'LineWidth',1)
xlabel('\fontsize{10}\bfCost ($M)')
ylabel('\fontsize{10}\bfTotal Hole Depth (m)')
grid on
legend('20,000 ft EGS Well','Borehole Drilling Cost Simulations',...
      'Location','SouthWest')
subplot(3,1,3)
hold on
plot(EGSdepthtimecost(:,2),EGSdepthtimecost(:,3)/1e3,'r--',...
     'LineWidth',2)
plot(depthtimecosthist(:,2),depthtimecosthist(:,3)/1e6,...
     'LineWidth',1)
xlabel('\fontsize{10}\bfTime (days)')
ylabel('\fontsize{10}\bfCost ($M)')
grid on
legend('20,000 ft EGS Well','Borehole Drilling Cost Simulations'...
      , 'Location','NorthWest')
end
index=index+1;
end

```

A.3 Drilling Sample Problem

To evaluate a small trade space, the following repository features are examined:

- Emplacement Length 2000m or 2500m
- Lateral Declinations 20° or 40°
- Number of Laterals 3, 4, or 5
- Pipe Schedule 26", 17 ½", 11 5/8"

With a single realization per trial, a total of 24 realizations are run.

The inputs (as produced from an excel dataset shown in Figure 2-6) are:

Drill Bit Diameters	Liner Inner Diameter	Liner Outer Diameter
Lookup (inches)	Lookup (inches)	Lookup (inches)
>> Holes	>> IDs	>> ODs
Holes =	IDs =	ODs =
26	19.25	20
24	17.25	18
20	15.25	16
17.5	13.25	14
17	12	12.75
15.5	11	11.75
14.5	10.02	10.75
12.25	8.941	9.625
11.625	7.981	8.625
10.75	7.023	7.625
9	6.065	6.625
8.75	5.047	5.563
7.875	4.506	5
6.25	4.026	4.5
48	39.125	40
36	29.125	30

**Drill Bit Replacement
Cost Lookup (\$)**

>> bit_cost

bit_cost =

72024
64774
50568
41890
40173
35058
31679
24167
22103
19229
13537
12730
9917.9
4745.5
1.583e+005
1.0976e+005

**Casing Mass Lookup
(kg/m)**

>> casing_mass

casing_mass =

116.97
105.05
92.98
81.209
73.753
67.801
60.241
50.464
42.487
35.031
28.23
21.757
18.662
16.057
275.1
205.57

**Kickoff Radius of
Curvature Lookup (m)**

>> radii

radii =

270.69
242.41
234.51
305.65
230.59
250.31
392.05

Allowable			2	5	12		5	9	13
Combinations of Pipe			1	6	12		1	4	14
Diameters			2	6	12		1	5	14
>> pipecombos			1	7	12		2	5	14
			2	7	12		1	6	14
pipecombos =			3	7	12		2	6	14
			1	8	12		1	7	14
1	4	8	2	8	12		2	7	14
1	4	9	3	8	12		3	7	14
1	5	9	4	8	12		1	8	14
2	5	9	1	4	13		2	8	14
1	4	10	1	5	13		3	8	14
1	5	10	2	5	13		4	8	14
2	5	10	1	6	13		1	9	14
1	6	10	2	6	13		2	9	14
2	6	10	1	7	13		3	9	14
1	4	11	2	7	13		4	9	14
1	5	11	3	7	13		5	9	14
2	5	11	1	8	13		1	10	14
1	6	11	2	8	13		2	10	14
2	6	11	3	8	13		3	10	14
1	7	11	4	8	13		4	10	14
2	7	11	1	9	13		5	10	14
3	7	11	2	9	13		6	10	14
1	4	12	3	9	13				
1	5	12	4	9	13				

Figure A-2 shows the trace of each trial in this sample (depth, time and cost history)

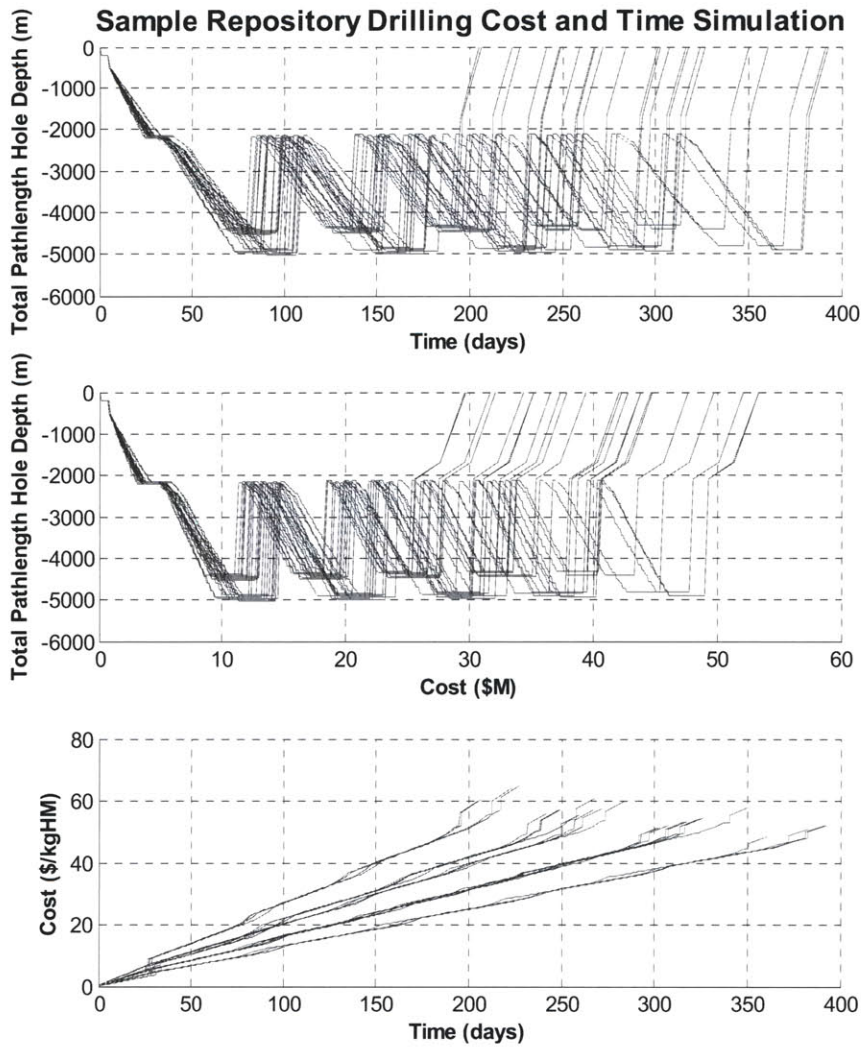


Figure A-2: Sample Problem Output

Table A-1 lists the output (tracker) from these 24 trials.

Table A-1: Drilling Script Output

Trial	1	2	3	4	5	6	7	8	9	10	11	12
Time (Days/MTHM)	0.4613	0.4186	0.4034	0.4043	0.4520	0.4161	0.4350	0.3922	0.4325	0.4134	0.3741	0.3673
Cost (\$/MTHM)	65145	60261	57103	57121	64163	60176	60705	55721	59937	57686	52159	51266
Casing Mass (kg)	475235	464450	538965	528180	475235	464450	538965	528180	575228	560848	660202	645822
Cement Volume (m ³)	53.67	53.67	53.67	53.67	53.67	53.67	53.67	53.67	55.34	55.34	55.34	55.34
Repository Capacity (MTHM)	492.52	492.52	615.60	615.60	492.52	492.52	615.60	615.60	656.69	656.69	820.80	820.80
BWR Reconstitution	1	1	1	1	1	1	1	1	1	1	1	1
PWR Pins	271	271	271	271	271	271	271	271	271	271	271	271
BWR Assemblies	0	0	0	0	0	0	0	0	0	0	0	0
BWR Pins	169	169	169	169	169	169	169	169	169	169	169	169
Plug Length	1500	1500	1500	1500	1500	1500	1500	1500	1500	1500	1500	1500
Lateral Length	2000	2000	2500	2500	2000	2000	2500	2500	2000	2000	2500	2500
Declination	20	40	20	40	20	40	20	40	20	40	20	40
Number of Laterals	3	3	3	3	3	3	3	3	4	4	4	4
Bit Size 1	26	26	26	26	26	26	26	26	26	26	26	26
Bit Size 2	17.5	17.5	17.5	17.5	17.5	17.5	17.5	17.5	17.5	17.5	17.5	17.5
Bit Size 3	11.625	11.625	11.625	11.625	11.625	11.625	11.625	11.625	11.625	11.625	11.625	11.625

Trial	13	14	15	16	17	18	19	20	21	22	23	24
Time (Days/MTHM)	0.4064	0.3952	0.3687	0.3854	0.4268	0.3977	0.3813	0.3725	0.3945	0.3868	0.3826	0.3515
Cost (\$/MTHM)	56914	55616	51534	53369	58074	54583	51965	50802	54391	53450	51995	48492
Casing Mass (kg)	575228	560848	660202	645822	675221	657246	781439	763464	675221	657246	781439	763464
Cement Volume (m ³)	55.34	55.34	55.34	55.34	57.02	57.02	57.02	57.02	57.02	57.02	57.02	57.02
Repository Capacity (MTHM)	656.69	656.69	820.80	820.80	820.80	820.80	1026.00	1026.00	820.80	820.80	1026.00	1026.00
BWR Reconstitution	1	1	1	1	1	1	1	1	1	1	1	1
PWR Pins	271	271	271	271	271	271	271	271	271	271	271	271
BWR Assemblies	0	0	0	0	0	0	0	0	0	0	0	0
BWR Pins	169	169	169	169	169	169	169	169	169	169	169	169
Plug Length	1500	1500	1500	1500	1500	1500	1500	1500	1500	1500	1500	1500
Lateral Length	2000	2000	2500	2500	2000	2000	2500	2500	2000	2000	2500	2500
Declination	20	40	20	40	20	40	20	40	20	40	20	40
Number of Laterals	4	4	4	4	5	5	5	5	5	5	5	5
Bit Size 1	26	26	26	26	26	26	26	26	26	26	26	26
Bit Size 2	17.5	17.5	17.5	17.5	17.5	17.5	17.5	17.5	17.5	17.5	17.5	17.5
Bit Size 3	11.625	11.625	11.625	11.625	11.625	11.625	11.625	11.625	11.625	11.625	11.625	11.625

This matrix of values are then plotted to evaluate any trends in the cost and completion time of the repositories to identify the most feasible repository configuration. Figures A-3 through A-6 show the small trade-space study.

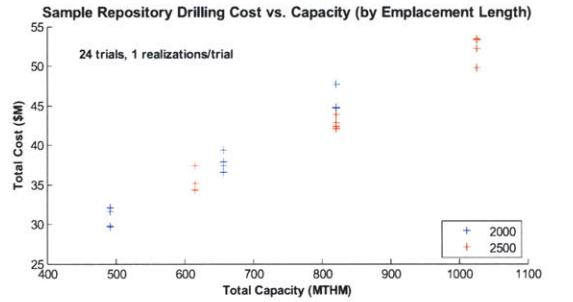
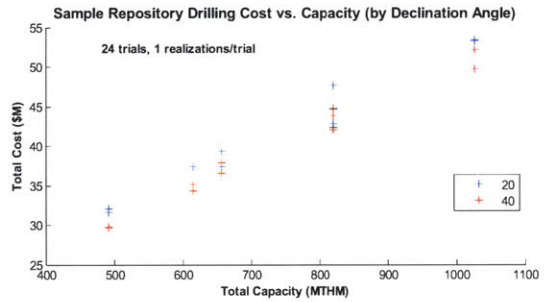
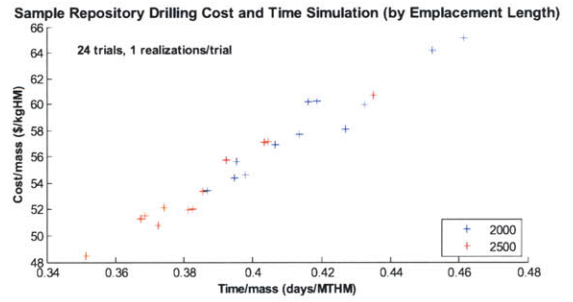
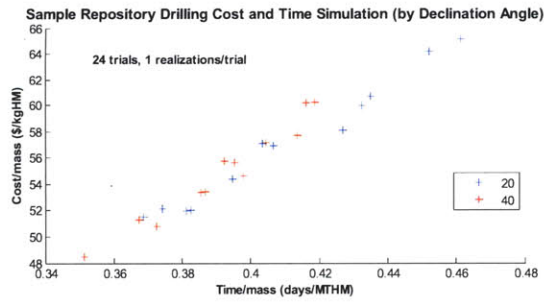


Figure A-3: Trade-space by Declination Angle (°)

Figure A-4: Trade-space by Emplacement Length (m)

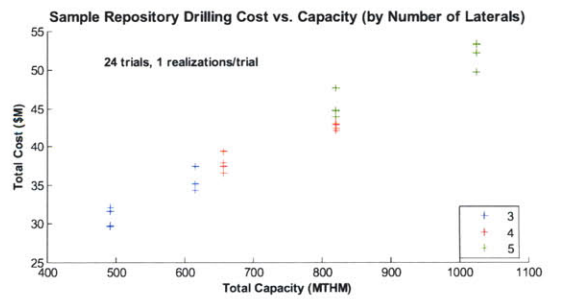
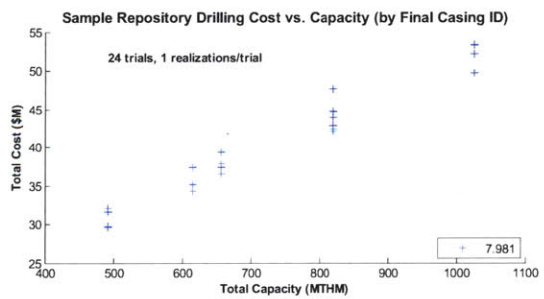
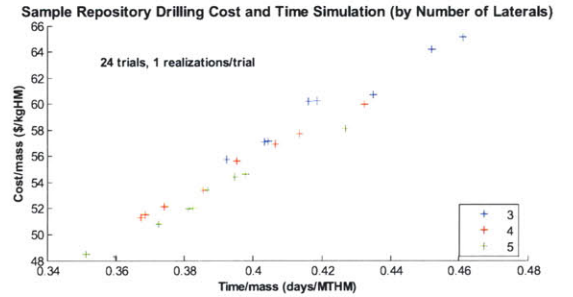
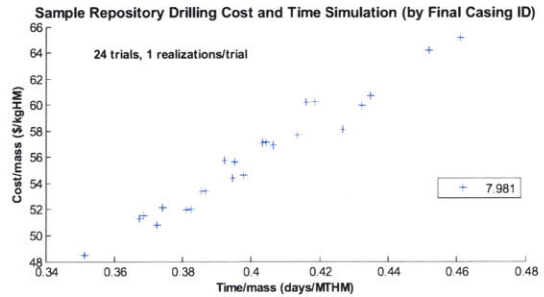


Figure A-5: Trade-space by Lateral Inner Diameter (in)

Figure A-6: Trade-space by Number of Laterals

APPENDIX B: THERMAL ANALYSIS CALCULATIONS

B.1 Decay Heat Modeling

Decay Heat Generation Estimation: Comparison of Malbrain, Lester, Deutch to ANS Standard

Parameters from notional PWR Reactor

Thermal Rating of Reactor	$Q_{Tot} := 3411 \text{ MW}$
Total Number of Assemblies in Reactor	$N_{assy} := 193$
Number of Fuelled Pins/Assembly	$N_{pins} := 264$
Fuel Pin Total Length	$L_{assy_PWR} := 4.1 \text{ m}$
Full Power Pin Thermal Rating	$Q_{pin_fullpower} := \frac{Q_{Tot}}{N_{assy} \cdot N_{pins}}$
PWR Fuel Assembly mass	$m_{assy} := 0.4987 \text{ tonne}$

Fuel Parameters

Time of cooling	$t_c := 40 \text{ yr}$	$L_{assy_BWR} := 4.2 \text{ m}$
Time of operation (for ANS Std)	$t_s := 3.53 \text{ yr}$	

Decay Power Relations

ANS Standard (from Kazimi and Todreas):

$$Q_{pin}(t) := Q_{pin_fullpower}^{0.066} \cdot \left[\left(t \cdot \frac{yr}{sec} + \frac{t_c}{sec} \right)^{-0.2} - \left(t \cdot \frac{yr}{sec} + \frac{t_c}{sec} + \frac{t_s}{sec} \right)^{-0.2} \right]$$

$$N_{pins_can} :=$$

- 61
- 91
- 127
- 175
- 217
- 301
- 367

From Malbrain, Lester, Deutch:

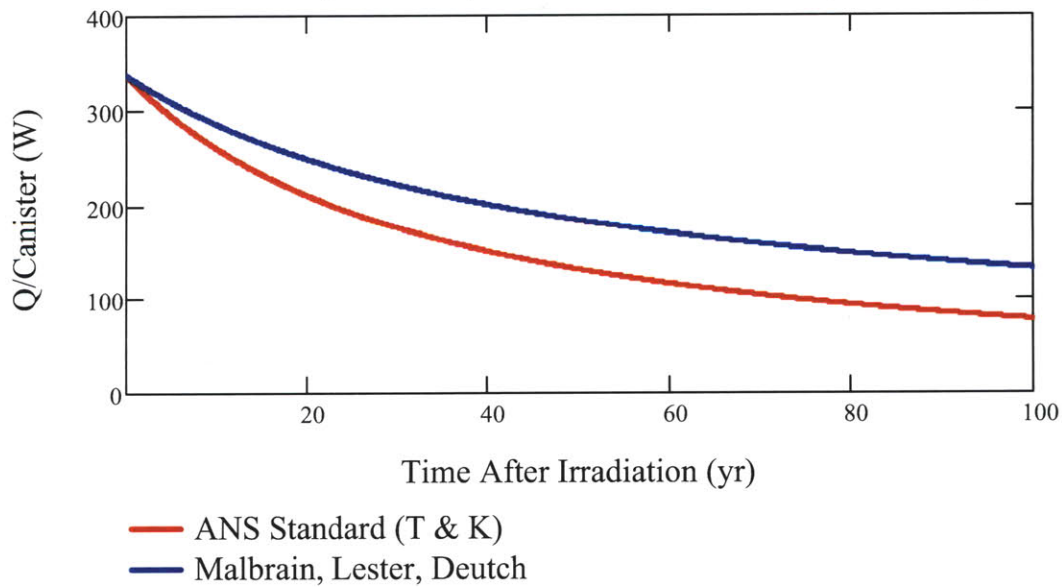
$$C_1 := 550 \quad C_2 := 0.223 \quad C_3 := 0.117$$

$$\beta := 0.749 \quad D_1 := 9.41 \cdot 10^3$$

$$Q_{assy}(t) := \begin{cases} m_{assy} \cdot C_1 \cdot \left[\exp \left[\left[C_2 + C_3 \cdot \left(t + \frac{t_c}{yr} \right)^{-1} \right] \right] \cdot \frac{W}{tonne} \right. & \text{if } t + \frac{t_c}{yr} < 31.4824 \\ m_{assy} \cdot \left[D_1 \cdot \left(t + \frac{t_c}{yr} \right)^{-\beta} \right] \cdot \frac{W}{tonne} & \text{otherwise} \end{cases}$$

$$Q_{pin2}(t) := \frac{Q_{assy}(t)}{N_{pins}}$$

PWR Decay Power (301 Pins / Canister, 40 yr Cooling)



ANS Standard

Immediately After Irradiation:

$$\frac{Q_{\text{pin}}(0) \cdot N_{\text{pins_can } 5}}{L_{\text{assy_PWR}}} = 82.3 \frac{\text{W}}{\text{m}}$$

Immediately After Emplacement

$$\frac{Q_{\text{pin}}\left(\frac{t_c}{\text{yr}}\right) \cdot N_{\text{pins_can } 5}}{L_{\text{assy_PWR}}} = 36.732 \frac{\text{W}}{\text{m}}$$

Malbrain, Lester, Deutch

Immediately After Irradiation:

$$\frac{Q_{\text{pin2}}(0) \cdot N_{\text{pins_can } 5}}{L_{\text{assy_PWR}}} = 82.35 \frac{\text{W}}{\text{m}}$$

Immediately After Emplacement

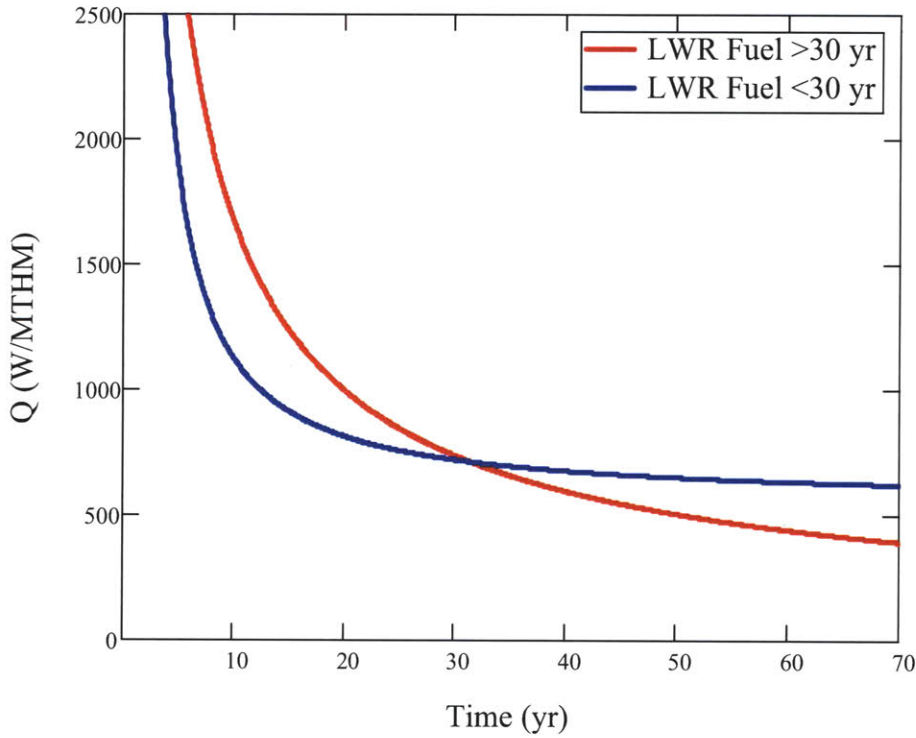
$$\frac{Q_{\text{pin2}}\left(\frac{t_c}{\text{yr}}\right) \cdot N_{\text{pins_can } 5}}{L_{\text{assy_PWR}}} = 49 \frac{\text{W}}{\text{m}}$$

$$m_{\text{assybwr}} := 0.1947 \text{ tonne} \quad N_{\text{pinsbwr}} := 72$$

$$Q_{\text{assybwr}}(t) := \begin{cases} m_{\text{assybwr}} \cdot C_1 \cdot \exp\left[\left[C_2 + C_3 \cdot \left(t + \frac{t_c}{\text{yr}}\right)^{-1}\right]\right] \cdot \frac{\text{W}}{\text{tonne}} & \text{if } t + \frac{t_c}{\text{yr}} < 31.4824 \\ m_{\text{assybwr}} \cdot \left[D_1 \cdot \left(t + \frac{t_c}{\text{yr}}\right)^{-\beta}\right] \cdot \frac{\text{W}}{\text{tonne}} & \text{otherwise} \end{cases}$$

$$Q_{\text{pinbwr}}(t) := \frac{Q_{\text{assybwr}}(t)}{N_{\text{pinsbwr}}} \cdot \frac{Q_{\text{pinbwr}}\left(\frac{t_c}{\text{yr}}\right) \cdot (N_{\text{pins_can } 4} - 6)}{L_{\text{assy_BWR}}} = 48 \frac{\text{W}}{\text{m}}$$

Decay Heat Correlation for LWR Uranium Fuel



$$\kappa := 2.7 \frac{\text{W}}{\text{m} \cdot \Delta^\circ\text{C}} \quad \alpha := 40 \frac{\text{m}^2}{\text{yr}}$$

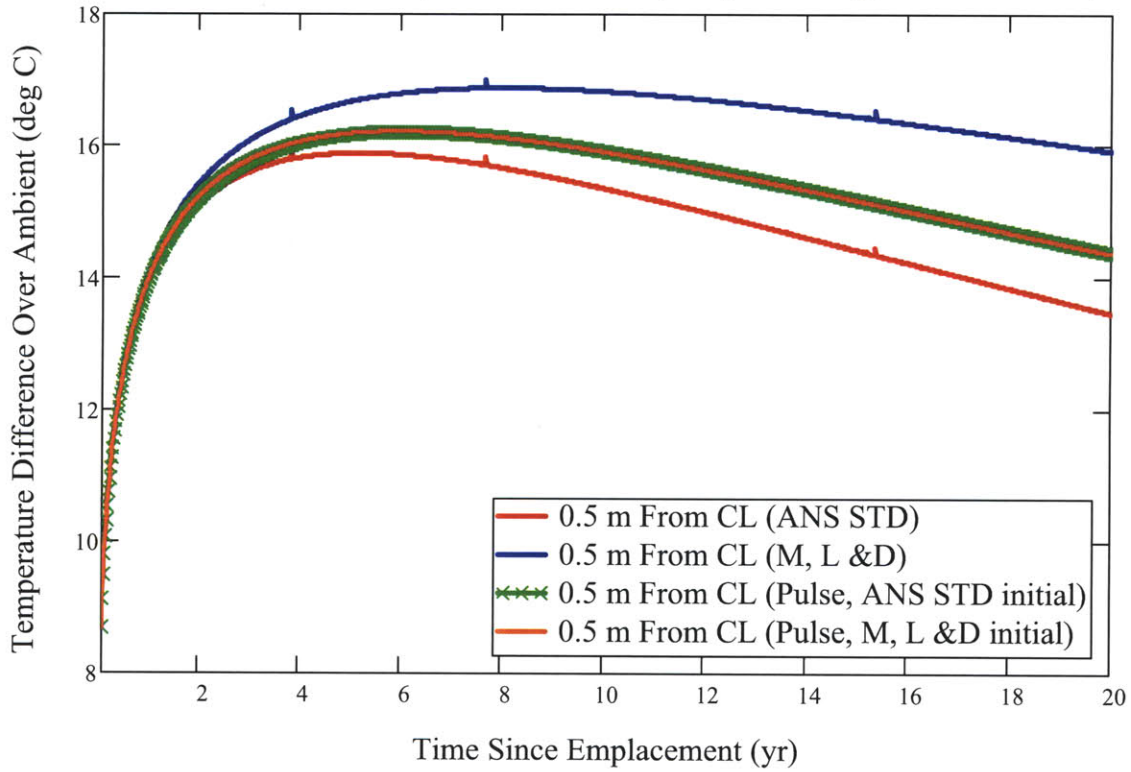
$$\text{Temp1}(r, t) := \frac{\int_0^{t \cdot \text{yr}} \frac{Q_{\text{pin}}(t) \cdot N_{\text{pins_can}_5}}{L_{\text{assy_PWR}} \cdot 4 \cdot \pi \cdot \kappa} \cdot \frac{\exp\left[-\frac{(r \cdot \text{m})^2}{4\alpha \cdot (t \cdot \text{yr} - \tau)}\right]}{t \cdot \text{yr} - \tau} d\tau}{\Delta^\circ\text{C}} \quad r \text{ in m, } t \text{ in yr}$$

$$\text{Temp2}(r, t) := \frac{\int_0^{t \cdot \text{yr}} \frac{Q_{\text{pin2}}(t) \cdot N_{\text{pins_can}_5}}{L_{\text{assy_PWR}} \cdot 4 \cdot \pi \cdot \kappa} \cdot \frac{\exp\left[-\frac{(r \cdot \text{m})^2}{4\alpha \cdot (t \cdot \text{yr} - \tau)}\right]}{t \cdot \text{yr} - \tau} d\tau}{\Delta^\circ\text{C}} \quad r \text{ in m, } t \text{ in yr}$$

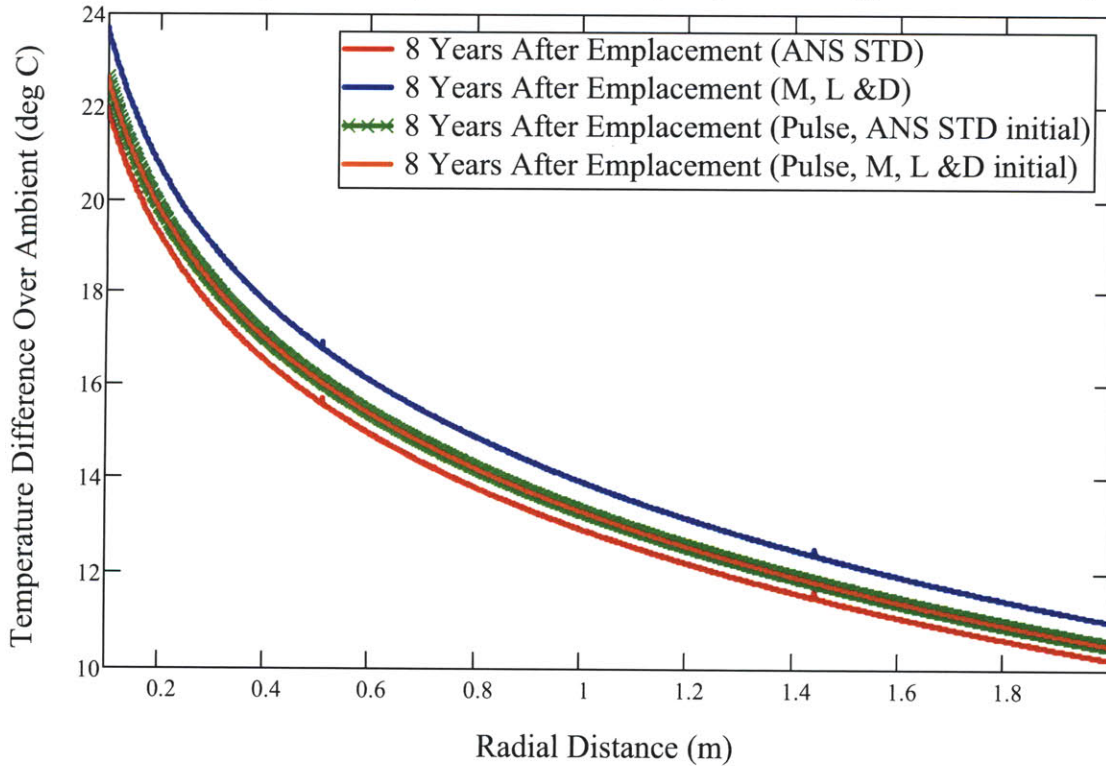
$$\text{Temp3}(r, t) := \frac{Q_{\text{pin}}(0) \cdot N_{\text{pins_can}_5} \cdot \frac{t_c}{t \cdot \text{yr} + t_c} \cdot \left[\ln\left[\frac{4 \cdot \alpha \cdot t \cdot \text{yr}}{(r \cdot \text{m})^2} \right] - 0.5772 \right]}{\Delta^\circ\text{C}} \quad r \text{ in m, } t \text{ in yr}$$

$$\text{Temp4}(r, t) := \frac{Q_{\text{pin2}}(0) \cdot N_{\text{pins_can}_5} \cdot \frac{t_c}{t \cdot \text{yr} + t_c} \cdot \left[\ln\left[\frac{4 \cdot \alpha \cdot t \cdot \text{yr}}{(r \cdot \text{m})^2} \right] - 0.5772 \right]}{\Delta^\circ\text{C}} \quad r \text{ in m, } t \text{ in yr}$$

1-D Time Histories (Inf Line Source, 40 yr cooling, 301 Pins/Can)



1-D Temp Profiles (Inf Line Source, 40 yr cooling, 301 Pins/Can)



B.2 Scaling Validation Test Results

In order to validate the 3-Dimensional scaling performed for the Finite Element Analysis used in Section 3.2.3, a simplified scaled problem was modeled in *Solidworks*. In this test, a full scale 10m x 10m x 2m slab with a 4m diameter curved surface (with a heat source) was also modeled at 1/10th small scale. Identical fixed temperature boundary conditions at the top and bottom to both cases and the material density and the heat flux on the curved surface are scaled according to Table blah (the same scaling methodology as in section 3.2.3.). It is demonstrated that the temperatures and times of the problem are preserved in the scaled model and that the methodology is valid.

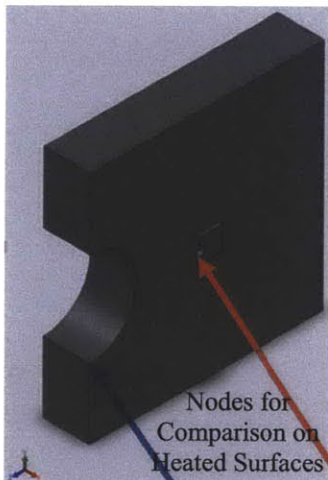


Figure B-1: Full and Small Scale Geometry

Table B-1: Scaling Parameters for Test

	Small Scale Block	Large Scale Block
Height (m)	1	10
Width (m)	1	10
Thickness (m)	0.2	2
Hole Diameter (m)	0.4	4
k (W/m·K)	16	16
ρ (kg/m ³)	800000	8000
Cp (J/kg·K)	500	500
q" (W/m ² ·K)		
(Decay Curve Multiplier)	100	10
Upper Temp (°C)	25	25
Lower Temp (°C)	109	109

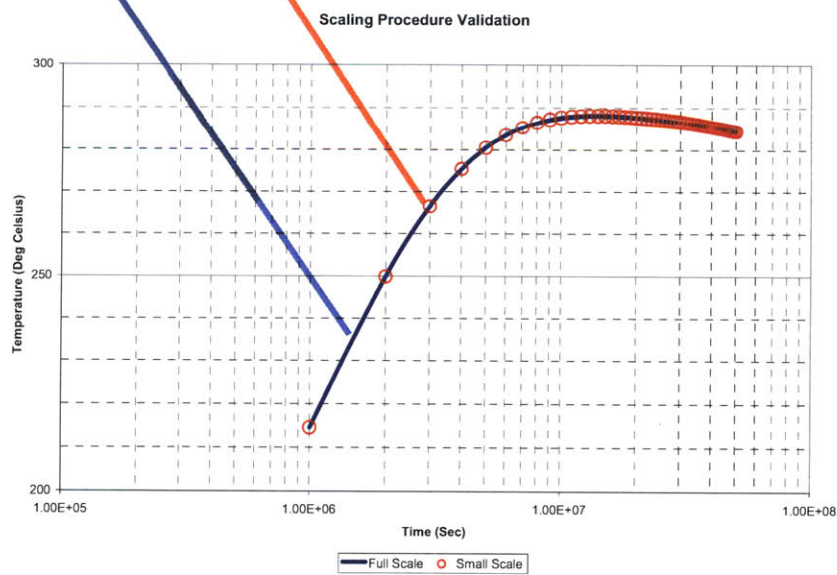


Figure B-2: Temperature History Comparison of Scaled and Unscaled Geometries

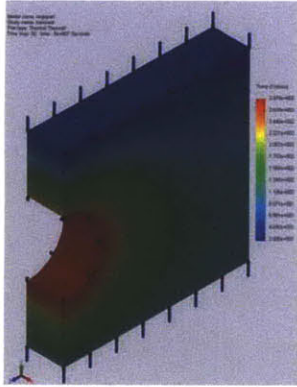


Figure B-3: Full Scale Final Temperature

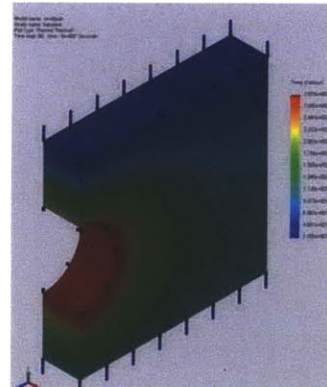


Figure B-4: Small Scale Final Temperature

APPENDIX C: MECHANICAL STRESS CALCULATIONS

Borehole Canister Stress Analysis

$$r_{in} := \frac{7 + \frac{1}{8}}{2} \cdot in \quad r_{in} = 90.4875 \text{ mm} \quad E_{steel} := 190000 \text{ MPa}$$

$$r_{out} := \frac{7 + \frac{11}{16}}{2} \cdot in \quad r_{out} = 97.63125 \text{ mm} \quad \nu := 0.26$$

$$l_w := 5 \text{ m}$$

Critical stress for localized buckling (Roark EQN 25 of Table XVI):

$$s_{prime} := \frac{E_{steel}}{\sqrt{3} \cdot \sqrt{1 - \nu^2}} \cdot \frac{r_{out} - r_{in}}{r_{out}} \quad s_{prime} = 8.3124537 \times 10^9 \text{ Pa}$$

Canister Mass:

Casing Mass

$$V_{steel} := \pi \left(r_{out}^2 - r_{in}^2 \right) \cdot l + 2 \cdot r_{in}^2 \cdot \pi \cdot (r_{out} - r_{in}) \quad V_{steel} = 2.1477035 \times 10^7 \text{ mm}^3$$

$$\rho_{steel} := 7874 \frac{\text{kg}}{\text{m}^3} \quad m_{steel} := V_{steel} \cdot \rho_{steel} \quad m_{steel} = 169.1101713 \text{ kg}$$

Waste Mass

$$N_{pins_PWR} := 301 \quad N_{pins_BWR} := 211 \quad l_{assy_PWR} := 4.2 \text{ m} \quad l_{assy_BWR} := 4.1 \text{ m}$$

$$m_{assy_PWR} := 700 \text{ kg} \quad N_{pins_assy_PWR} := 289 \quad m_{pin_PWR} := \frac{m_{assy_PWR}}{N_{pins_assy_PWR}}$$

$$m_{pin_PWR} = 2.4221453 \text{ kg} \quad m_{PWR_waste} := N_{pins_PWR} \cdot m_{pin_PWR} \quad m_{PWR_waste} = 729.0657439 \text{ kg}$$

$$m_{assy_BWR} := 273 \text{ kg} \quad N_{pins_assy_BWR} := 81 \quad m_{pin_BWR} := \frac{m_{assy_BWR}}{N_{pins_assy_BWR}}$$

$$m_{pin_BWR} = 3.3703704 \text{ kg} \quad m_{BWR_waste} := N_{pins_BWR} \cdot m_{pin_BWR} \quad m_{BWR_waste} = 711.1481481 \text{ kg}$$

SiC Fill Mass

$$V_{\text{fill_PWR}} := \left[1 - 2 \cdot (r_{\text{out}} - r_{\text{in}}) \right] \cdot (r_{\text{in}}^2) \cdot \pi - N_{\text{pins_PWR}} \cdot \left[\pi \cdot \frac{(9.5\text{mm})^2}{4} \right] \cdot l_{\text{assy_PWR}}$$

$$V_{\text{fill_PWR}} = 3.863983 \times 10^7 \text{ mm}^3 \quad \rho_{\text{fill}} := 3.1 \frac{\text{gm}}{\text{cm}^3} \quad \text{Packing_Factor} := 0.65$$

$$m_{\text{fill_PWR}} := V_{\text{fill_PWR}} \cdot \rho_{\text{fill}} \cdot \text{Packing_Factor} \quad m_{\text{fill_PWR}} = 77.8592576 \text{ kg}$$

$$V_{\text{fill_BWR}} := \left[1 - 2 \cdot (r_{\text{out}} - r_{\text{in}}) \right] \cdot (r_{\text{in}}^2) \cdot \pi - N_{\text{pins_BWR}} \cdot \left[\pi \cdot \frac{(11\text{mm})^2}{4} \right] \cdot l_{\text{assy_BWR}}$$

$$V_{\text{fill_BWR}} = 4.6035885 \times 10^7 \text{ mm}^3$$

$$m_{\text{fill_BWR}} := V_{\text{fill_BWR}} \cdot \rho_{\text{fill}} \cdot \text{Packing_Factor} \quad m_{\text{fill_BWR}} = 92.7623089 \text{ kg}$$

Total Canister Mass

$$m_{\text{Canister_PWR}} := m_{\text{steel}} + m_{\text{PWR_waste}} + m_{\text{fill_PWR}} \quad m_{\text{Canister_PWR}} = 976.0351728 \text{ kg}$$

$$m_{\text{Canister_BWR}} := m_{\text{steel}} + m_{\text{BWR_waste}} + m_{\text{fill_BWR}} \quad m_{\text{Canister_BWR}} = 973.0206283 \text{ kg}$$

Total Weight of Waste String

$$W_{\text{string_PWR}} := \frac{2000 \text{ m}}{1} \cdot m_{\text{Canister_PWR}} \cdot g \quad W_{\text{string_PWR}} = 3.8286541 \times 10^6 \text{ N}$$

$$W_{\text{string_BWR}} := \frac{2000 \text{ m}}{1} \cdot m_{\text{Canister_BWR}} \cdot g \quad W_{\text{string_BWR}} = 3.8168291 \times 10^6 \text{ N}$$

Tensile Stress in Canister Wall

$$A_{\text{Cross_Section}} := \pi \cdot (r_{\text{out}}^2 - r_{\text{in}}^2) \quad A_{\text{Cross_Section}} = 4.2219026 \times 10^3 \text{ mm}^2 \quad \rho_{\text{mud}} := 1000 \frac{\text{kg}}{\text{m}^3}$$

$$\sigma_{\text{Top_of_String_PWR}} := \frac{W_{\text{string_PWR}} - \rho_{\text{mud}} \cdot 2000 \text{ m} \cdot \pi \cdot (r_{\text{out}}^2) \cdot g}{A_{\text{Cross_Section}}}$$

$$\sigma_{\text{Top_of_String_PWR}} = 7.6774142 \times 10^8 \text{ Pa}$$

$$\sigma_{\text{Top_of_String_BWR}} := \frac{W_{\text{string_BWR}} - \rho_{\text{mud}} \cdot 2000 \text{ m} \cdot \pi \cdot (r_{\text{out}}^2) \cdot g}{A_{\text{Cross_Section}}}$$

$$\sigma_{\text{Top_of_String_BWR}} = 7.6494054 \times 10^8 \text{ Pa}$$

At the time the lowest canister of waste begins kickoff radius

$$\text{String_Above_Waste} := 370 \text{ m} \quad \rho_{\text{casing}} := 42.49 \frac{\text{lbf}}{\text{ft}}$$

$$W_{\text{string_above}} := \text{String_Above_Waste} \cdot \rho_{\text{casing}} \quad W_{\text{string_above}} = 2.2943513 \times 10^5 \text{ N}$$

$$\sigma_{\text{Top_of_Hole_PWR}} := \frac{W_{\text{string_PWR}} + W_{\text{string_above}} - \rho_{\text{mud}} \cdot 2000 \text{ m} \cdot \pi \cdot (r_{\text{out}})^2 \cdot g}{A_{\text{Cross_Section}}}$$

$$\sigma_{\text{Top_of_Hole_BWR}} := \frac{W_{\text{string_BWR}} + W_{\text{string_above}} - \rho_{\text{mud}} \cdot 2000 \text{ m} \cdot \pi \cdot (r_{\text{out}})^2 \cdot g}{A_{\text{Cross_Section}}}$$

$$\sigma_{\text{Top_of_Hole_PWR}} = 8.2208543 \times 10^8 \text{ Pa} \quad \sigma_{\text{Top_of_Hole_BWR}} = 8.1928456 \times 10^8 \text{ Pa}$$

$$\sigma_{\text{tensile_limit_P110}} := 125000 \text{ psi} \quad \sigma_{\text{tensile_limit_P110}} = 8.6184466 \times 10^8 \text{ Pa}$$

$$FS_{\text{tens_PWR}} := \frac{\sigma_{\text{tensile_limit_P110}}}{\sigma_{\text{Top_of_Hole_PWR}}} \quad FS_{\text{tens_BWR}} := \frac{\sigma_{\text{tensile_limit_P110}}}{\sigma_{\text{Top_of_Hole_BWR}}}$$

$$FS_{\text{tens_PWR}} = 1.0483639 \quad FS_{\text{tens_BWR}} = 1.0519479$$

Local Buckling limit at the bottom of the hole:

$$FS_{\text{buck_PWR}} := \frac{s_{\text{prime}} \cdot 4 \cdot A_{\text{Cross_Section}}}{W_{\text{string_PWR}} \cdot \sin(20 \text{ deg})} \quad FS_{\text{buck_BWR}} := \frac{s_{\text{prime}} \cdot 4 \cdot A_{\text{Cross_Section}}}{W_{\text{string_BWR}} \cdot \sin(20 \text{ deg})}$$

$$FS_{\text{buck_PWR}} = 10.7201192 \quad FS_{\text{buck_BWR}} = 10.7533315$$

Lithostatic / Hydrostatic crushing:

Critical Pressure for Radial Crushing (Roark EQN 30 of Table XVI):

$$P_c := \frac{1}{4} \cdot \left(\frac{E_{\text{steel}}}{1 - \nu^2} \right) \cdot \left(\frac{r_{\text{out}} - r_{\text{in}}}{\frac{r_{\text{out}} + r_{\text{in}}}{2}} \right)^3 \quad P_c = 22.3184393 \text{ MPa}$$

$$P_{\text{hyd}}(d) := \left(1 \cdot \frac{\text{gm}}{\text{cm}^3} \right) \cdot d \cdot g \quad P_{\text{hyd}}(3006.686 \text{ m}) = 29.4855173 \text{ MPa}$$

$$P_{\text{lith}}(d) := \frac{78 \text{ MPa}}{3 \text{ km}} \cdot d \quad P_{\text{lith}}(3006.686 \text{ m}) = 78.173836 \text{ MPa}$$

REFERENCES

- ¹ Christopher Ian Hoag, “Canister Design for Deep Borehole Disposal of Nuclear Waste,” SM Thesis, MIT Dept. of Nuclear Science and Engineering, September 2004.
- ² “Light-Water Reactor Fuel,” Nuclear Fuel Industries, 2010, Accessed 7 May 2010 at <http://www.nfi.co.jp/e/product/prod02.html>.
- ³ Hoag.
- ⁴ C. G. Sizer, C. I. Hoag, S. Shaikh, M. J. Driscoll, “Partitioning and Internment of Selected High Level Wastes,” *Transactions of the American Nuclear Society*, Vol. 96, June 2007.
- ⁵ Patrick V. Brady, Bill W. Arnold, Geoff A. Freeze, Peter N. Swift, Stephen J. Bauer, Joseph L. Kanney, Robert P. Rechar, and Joshua S. Stein, “Deep Borehole Disposal of High-Level Radioactive Waste,” Sandia National Laboratories, Report SAND2009-4401, Albuquerque, New Mexico, August 2009.
- ⁶ F. G. F. Gibb, N. A. McTaggart, K. P. Travis, D. Burley, K. W. Hesketh, “High-Density Support Matrices: Key to the Deep Borehole Disposal of Spent Nuclear Fuel,” *Journal of Nuclear Materials*, Vol. 374, 2008, pgs. 370-377.
- ⁷ Massachusetts Institute of Technology, “The Future of Geothermal Energy: Impact of Enhanced Geothermal Systems (EGS) on the United States in the 21st Century,” Idaho Falls: Idaho National Laboratory, Geothermal Program in the Renewable Energy and Power Department, 2006.
- ⁸ Hunt, C. B., *Natural Regions of the United States and Canada*, San Francisco: W.H. Freeman and Company, 1967.
- ⁹ U.S. Census, “Population Density for Counties and Puerto Rico Municipios: July 1, 2009,” 2009, Accessed 7 May 2010 at http://www.census.gov/popest/gallery/maps/PopDensity_09.pdf.
- ¹⁰ U.S. Department of Energy, Office of Civilian Radioactive Waste Management, “A National Map of Current Waste Locations,” Accessed 7 May 2010 at http://ocrwm.doe.gov/info_library/newsroom/photos/photos_graphics.shtml.
- ¹¹ Title 42 of the United States Code, Chapter 108, Subchapter 1, Part E, § 10172a(c), Accessed 7 May 2010 at http://www.law.cornell.edu/uscode/html/uscode42/usc_sec_42_00010172---a000-.html.
- ¹² Mary P. Anderson, “Introducing Ground Water Physics,” *Physics Today*, Vol. 60, No. 5, May 2007.
- ¹³ P. Hölttä, M. Hakanen, M. Siitari-Kauppi, and A. Hautojärvi, “Radionuclide Retardation in Crystalline Rock Fractures,” Scientific Basis for Nuclear Waste Management XVIII, Edited by Takahashi Murakami and Rodney C. Ewing, Materials Research Society Symposium Proceedings, Vol. 353, 1995.
- ¹⁴ P. Hölttä, M. Siitari-Kauppi, M. Kelokaski, and V. Tukiainen, “Radionuclide Retardation in Granitic Rocks by Matrix Diffusion and Sorption,” Scientific Basis for Nuclear Waste Management XXXI, Edited by William E. Lee, John W. Roberts, Neil C. Hyatt, and Robin W. Grimes, Materials Research Society Symposium Proceedings, Vol. 1107, 2008.
- ¹⁵ Anonymous, “Permeable UK Granite is Good News for Geothermal Energy,” *Power*, Vol. 154, No. 4, pg. 12.

-
- ¹⁶ A. D. Hill, Ding Zhu, and Michael J. Economides, Multilateral Wells, Society of Petroleum Engineers, Richardson Texas, 2008.
- ¹⁷ Hoag.
- ¹⁸ John T. Finger, Sandia National Laboratory, Email to the Author, 14 November, 2009.
- ¹⁹ Ibid.
- ²⁰ Ibid.
- ²¹ Ibid.
- ²² Yarom Polsky, Louis Capuano Jr., John Finger, Michael Huh, Steve Knudsen, A.J. Chip Mansure, David Raymond and Robert Swanson, "Enhanced Geothermal Systems (EGS) Well Construction Technology Evaluation Report," Sandia National Laboratory, SAND2008-7866, December 2008, Accessed 15 September, 2009 at http://www1.eere.energy.gov/geothermal/pdfs/egs_well_construction.pdf.
- ²³ Finger.
- ²⁴ Alibaba Building Supply Exchange Website, 2009, Accessed 12 October, 2009 at <http://www.alibaba.com/showroom/cement-price-per-bag.html>.
- ²⁵ Drilling Rigs Website, 2009, Accessed 29 September, 2009 at http://www.sunmachinery.com/drill_pipe.htm.
- ²⁶ Polsky, et al.
- ²⁷ Ibid.
- ²⁸ "Fuel Design Data", *Nuclear Engineering International*, Vol. 54, 3 September, 2009, pg. 36.
- ²⁹ Ibid.
- ³⁰ Ibid.
- ³¹ Ibid.
- ³² Ibid.
- ³³ Ibid.
- ³⁴ Ibid.
- ³⁵ Ibid.
- ³⁶ WoodCo USA Website, 2009, Accessed September 19, 2009 at <http://www.woodcousa.com/>.
- ³⁷ Finger.
- ³⁸ Ibid.
- ³⁹ Erich Friedman, "Erich's Packing Center," 2009, Accessed August 29, 2009 at <http://www2.stetson.edu/~efriedma/packing.html>.
- ⁴⁰ Polsky, et al.
- ⁴¹ "Conduction," The Physics Hypertextbook, 1998-2010, Accessed April 11, 2010 at <http://physics.info/conduction/>.
- ⁴² "Densities of Various Solids," The Engineering Toolbox, 2005, Accessed April 11, 2010 at http://www.engineeringtoolbox.com/density-solids-d_1265.html.
- ⁴³ "Emissivity of Specific Materials," Cole-Parmer Technical Library, 2010, Accessed April 11, 2010 at <http://www.coleparmer.com/techinfo/techinfo.asp?htmlfile=Emissivity.htm&ID=254>.
- ⁴⁴ "Solids- Specific Heat Capacities," The Engineering Toolbox, 2005, Accessed April 11, 2010 at http://www.engineeringtoolbox.com/specific-heat-solids-d_154.html
- ⁴⁵ Ailsa Allaby and Michael Allaby, "Geothermal Gradient," A Dictionary of Earth Sciences, 1999, Encyclopedia.com, Accessed April 11, 2010 at <http://www.encyclopedia.com/doc/1O13-geothermalgradient.html>

-
- ⁴⁶ “Thermal Conductivity,” Hyperphysics Website, Accessed April 11, 2010 at <http://hyperphysics.phy-astr.gsu.edu/Hbase/Tables/thrcn.html>
- ⁴⁷ “Emissivity Coefficients of Some Common Materials,” The Engineering Toolbox, 2005, Accessed April 11, 2010 at http://www.engineeringtoolbox.com/emissivity-coefficients-d_447.html
- ⁴⁸ Hoag, pg. 96.
- ⁴⁹ “Silicon Carbide, SiC, Engineering Properties,” Accuratus, 2002, Accessed April 11, 2010 at <http://www accuratus.com/silicar.html>.
- ⁵⁰ Hoag, pg. 101.
- ⁵¹ Hoag, pg. 102.
- ⁵² “Conduction – Cylindrical Coordinates – Heat Transfer,” Engineering Edge, LLC, 2010, Accessed April 11, 2010 at http://www.engineersedge.com/heat_transfer/conduction_cylindrical_coor.htm.
- ⁵³ Neil E. Todreas and Mujid Kazimi, Nuclear Systems Volume I: Thermal Hydraulic Fundamentals, 2nd Edition, Taylor and Francis, 1993, pg. 66.
- ⁵⁴ Carl M. Malbrain, Richard K. Lester, and John M. Deutch, “Analytical Approximations for the Long Term Decay Behavior of Spent Fuel and High Level Waste,” *Nuclear Technology*, Vol. 57, May 1982, pgs. 292-305.
- ⁵⁵ Young Joo Kwon, “Finite Analysis of Transient Heat Transfer in and Around a Deep Geological Repository for Spent Nuclear Fuel Disposal Canister and the Heat Generation of the Spent Nuclear Fuel,” *Nuclear Science and Engineering*, Vol. 164, 2010, pgs. 264-286.
- ⁵⁶ H. S. Carslaw and J. C. Jaeger, Conduction of Heat in Solids- 2nd Edition, Oxford University Press Inc., New York, 1959, pg. 204.
- ⁵⁷ “Conduction – Cylindrical Coordinates – Heat Transfer,” (See Ref 52).
- ⁵⁸ M. N. Ozisik, Basic Heat Transfer, McGraw-Hill, 1977.
- ⁵⁹ R. D. Manteufel and N. E. Todreas, “Effective Thermal Conductivity and Edge Conductance Model for a Spent-Fuel Assembly,” *Nuclear Technology*, Vol. 105, March 1994, pgs. 421-440.
- ⁶⁰ Raymond J. Roark, Formulas for Stress and Strain, 4th Edition, McGraw-Hill, New York, 1965, pg. 352.
- ⁶¹ Ibid, pg. 354.
- ⁶² Charles W. Forsberg, “Description of the Canadian Particulate-Fill Waste-Package (WP) System for Spent-Nuclear Fuel (SNF) and its Applicability to Lightwater Reactor SNF WPS with Depleted Uranium-Dioxide Fill,” Oak Ridge National Laboratory Report TM-13502, October 20, 1997.
- ⁶³ Jeremy Whitlock, Canadian Nuclear FAQ, 2010, Accessed 26 April, 2010 at <http://www.nuclearfaq.ca/index.html>
- ⁶⁴ “Fuel Rod Consolidation- a Key Process in Spent Fuel-Storage Systems,” *Transactions of the American Nuclear Society*, Vol. 40, 1982, pgs. 149-150.
- ⁶⁵ “Interim Spent Fuel Storage Using Rod Consolidation,” *Transactions of the American Nuclear Society*, Vol. 46, 1984, pg. 105.
- ⁶⁶ “Simplifying Fuel Rod Consolidation,” *Nuclear Engineering International*, Vol. 34, September 1989, pgs. 24-25.

-
- ⁶⁷ G. A. Townes, "Dry Spent Fuel Consolidation Demonstration at the Barnwell Nuclear Fuel Plant (BNFP)," American Nuclear Society Symposium, Savannah Georgia, 1982.
- ⁶⁸ "Putting Fuel Master Rod Consolidation to the Test," *Nuclear Engineering International*, Vol. 35, December 1990, pgs. 20-25.
- ⁶⁹ "Fuel Consolidation Demonstration Program: Final Report," U. S. Department of Energy, Office of Civilian Radioactive Waste Management and Electric Power Research Institute, EPRI NP-6892, June 1990.
- ⁷⁰ "DOE Prototypical Rod Consolidation Report," Prepared for the U. S. Department of Energy by Sciencetech, June 1993.
- ⁷¹ "Fuel Consolidation Demonstration Program: Final Report," pg. 2-32, (See Ref 69).
- ⁷² "Fuel Design Data," 2009 (See Ref 28).
- ⁷³ "Employer Costs for Employee Compensation Historical Listing (Annual), 1986-2001," Bureau of Labor Statistics, June 19, 2002, Accessed 4 May 2010 at <ftp://ftp.bls.gov/pub/special.requests/ocwc/ect/ecechist.pdf>.
- ⁷⁴ "Employment Cost Index Historical Listing, Current-dollar, March 2001 – March 2010," April 30, 2010, Accessed 4 May 2010 at <http://www.bls.gov/web/eci/echistrynaics.pdf>.
- ⁷⁵ "PPI: General Purpose Machinery and Equipment, Non-Seasonally Adjusted" Economagic Website, 2010, Accessed 4 May 2010 at <http://www.economagic.com/em-cgi/data.exe/blswp/wpu114>
- ⁷⁶ "PPI: Metal Containers, Non-Seasonally Adjusted," Economagic Website, 2010, Accessed 4 May 2010 at <http://www.economagic.com/em-cgi/data.exe/blswp/wpu103>.
- ⁷⁷ "DOE Prototypical Rod Consolidation Report," pg. 1.
- ⁷⁸ "Employer Costs for Employee Compensation Historical Listing (Annual), 1986-2001."
- ⁷⁹ "Employment Cost Index Historical Listing, Current-dollar, March 2001 – March 2010."
- ⁸⁰ "PPI: General Purpose Machinery and Equipment."
- ⁸¹ "PPI: Metal Containers."
- ⁸² Sandblasting Abrasives Website, 2010, Accessed on 13 April 2010 at <http://sandblastingabrasives.com/silicon-carbides-10/rock-tumbling-13/black-silicon-carbide-rock-tumbling-grit-pick-a-grade-25lb-box-or-more-778.html>.